THE ALLENDE – PIEDRAS NEGRAS TRANSBOUNDARY AQUIFER: AN INITIAL MODELING ASSESSMENT

A Thesis

by

LAURA MARCELA RODRIGUEZ LOZADA

Submitted to the Office of Graduate and Professional Studies of

Texas A&M University

in partial fulfillment of the requirements for the degree of

MASTER OF SCIENCE

Chair of Committee,	Hongbin Zhan
Co-Chair of Committee,	Rosario Sanchez
Committee Member,	Peter Knappett
Head of Department,	John R. Giardino

December 2018

Major Subject: Water Management and Hydrological Science

ABSTRACT

The Allende-Piedras Negras (APN) aquifer is located between the state of Texas (USA) and the state of Coahuila (Mexico). The Rio Grande/Rio Bravo crosses the aquifer acting as a natural and political divide between both countries. Besides, the area had a gap identified by previous studies where the absence of an aquifer assignment was notorious; also, these studies were developed at the local level but not covering the entire gap. The main purpose of this work is generating a hydrogeological model to perform a detailed analysis of the APN aquifer.

To generate a hydrogeological model, geological information was collected to correlate the geological units on both sides of the border and define the physical dimensions of the aquifer. Precipitation, river discharge, and evapotranspiration data were assembled from field data and remote sensors; hydraulic parameters such as permeability, hydraulic conductivity and specific storage were obtained from previous studies performed in the area. For the Texas side, water well information was downloaded from the Texas Water Development Board website. For the Mexican side, water well information was provided by the Public Registry of Water Rights (Registro Publico de Derechos del Agua), Lesser and Associates and the United States Environmental Protection Agency (EPA). The software Visual MODFLOW was used to develop the hydrogeological model, which verified the hydraulic connections of the transboundary aquifer system. At last, a water budget analysis was performed to determine the groundwater amounts coming from both countries into the Rio Grande/Rio Bravo system.

The hydrogeological model quantified an accumulated drawdown of 0.76 m in 17 years. Also, the flow convergence zone located below the Rio Grande/Rio Bravo, shifted mainly to USA due to the high pumping rates of the wells near the river. This shifting allows the categorization of the APN aquifer as a “transboundary groundwater flow” system, which would influence water management decisions across the USA-Mexico border. Lastly, most of the groundwater discharged into the Rio Grande/Rio Bravo comes from the Mexican side due to steeper terrain slopes south of the border.

The methodology followed in this study to perform a detailed analysis of the Allende-Piedras Negras aquifer could also be applied in other aquifers that straddle the border. The expected impact of this study is that it will motivate future modeling studies on other poorly studied aquifers along the border between USA-Mexico and provide the first assessments for potential joint aquifer management in the region.

ACKNOWLEDGEMENTS

I would like to thank my committee chair, Dr. Hongbin Zhan, and my committee members, Dr. Rosario Sanchez, and Dr. Peter Knappett, for their guidance and support throughout the course of this research.

I would like to thank Dr. Alfonso Rivera for his recommendations on the development of the hydrogeological model and Dr. Quanrong Wang for his suggestions regarding Visual MODFLOW.

Thanks also to my friends and colleagues who helped on my research and their support which are so important to my study. Finally, thanks to my mother and father for their encouragement.

CONTRIBUTORS AND FUNDING SOURCES

Contributors

This work was supervised by a thesis committee consisting of Dr. Hongbin Zhan and Dr. Peter Knappett of the Department of Geology & Geophysics and Dr. Rosario Sanchez of the Texas Water Resources Institute (TWRI).

All other work conducted for the thesis was completed by the student.

Funding Sources

This work was made possible by the funding from the TAAP program through the Texas Water Resources Institute (TWRI).

Graduate study was partly supported by scholarships awarded by the Department of Water Management and Hydrological Science.

NOMENCLATURE

APN	Allende-Piedras Negras
CN	Curve number
CONAGUA	National Commission of Water (Comision Nacional del Agua in Spanish)
DEM	Digital Elevation Model
EPA	United States Environmental Protection Agency
ET	Evapotranspiration
Fm.	Formation
GLDAS	NASA Global Land Data Assimilation System
Gr.	Group
ISARM	Internationally Shared Aquifer Resources Management
K	Hydraulic Conductivity
Q	Discharge
PEST	Parameter Estimation Simulation
REPDA	Public registry of water rights (Registro Público de Derechos del Agua in spanish)
RG	Rio Grande
SGM	Mexico Geological Service (Servicio Geologico Mexicano in Spanish)
SCS	Soil Conservation Service
Ss	Specific Storage

Sy	Specific Yield
TMPA	TRMM Multi Satellite Precipitation Analysis
TWDB	Texas Water Development Board
VMF	Visual MODFLOW

TABLE OF CONTENTS

Page

LIST OF FIGURES

Page

LIST OF TABLES

Page

1. INTRODUCTION

1.1 Background

Recently, a total of 36 potential transboundary aquifers have been identified in the Mexican-U.S border (Sanchez et al., 2016). Sixteen aquifers were identified and characterized as transboundary with a reasonable level of confidence; however, only 11 aquifers have been recognized officially as transboundary by Mexico and the United States. The Allende-Piedras Negras (APN) aquifer between Texas (USA) and the state of Coahuila (Mexico), has been identified as transboundary with a reasonable level of confidence (Sanchez et al., 2016, Sanchez et al., 2018); however, it has not been recognized officially by both countries or at the international level (Internationally Shared Aquifer Resources Management - ISARM). The only available studies focused merely on the central portion of the aquifer located in the Mexico side (Aguilar, 2013, Boghici, 2002, Castillo Aguiñaga, 2000, CONAGUA, 2014, Grupo Modelo, 2003).These studies excluded the northern portion located in Texas and the southern portion located in Mexico as well (Figure 1).

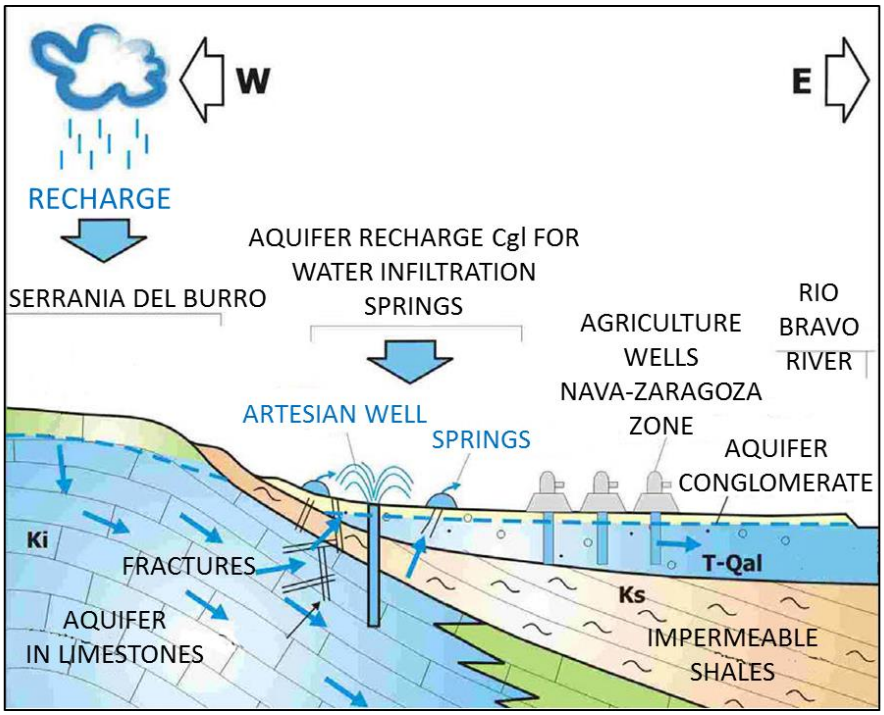

Figure 1. Hydrogeological conceptual model of the APN aquifer, Mexico side. (Modified from Grupo Modelo, 2003)

Because of its location on the political border, the depletion of the APN aquifer water table has the potential of decreasing the volumetric flux of streams into the Rio Grande/Rio Bravo River system, affecting the water allocation set in the bi-national 1944 water treaty (Colorado-Rio Grande, 1944).

In addition, the APN aquifer supplies 85% of the water needs in the region, and expected socioeconomic development activities would potentially be affected by water scarcity, as well as a high risk for extraction to overtake the natural recharge of the aquifer (CONAGUA, 2014, DOF, 2011).

As of 2011, the APN aquifer was not overexploited, with a positive difference between the recharge and the extraction water volumes of 31.8 m^3/year (DOF, 2011); however, the aquifer is located in an arid to semi-arid region where most of the rainfall

water evaporates, reducing the runoff and infiltration in the area of interest. Due to the limitations by climatic conditions imposed on the aquifer, the establishment of water restrictions was recommended by CONAGUA (DOF, 2011). More recently, restrictions on the water extraction were established for the APN aquifer due to the high risk of overexploitation and the low recharge rates induced by the climate conditions in the area (DOF, 2013)

The APN aquifer in the Texas side resides within Kinney and Maverick counties, and it is managed by the Kinney Groundwater District as “the local Austin Chalk Management Zone and Uvalde gravel”. A management zone is the term assigned to every aquifer in the area which corresponds to published groundwater flow models developed by the Texas Water Development Board (TWDB) (Kinney County Groundwater Conservation District, 2013). Every management zone will have certain drought stage levels (withdrawal levels measured on selected observation wells) used as indicators to set pumping regulations or minimum distances between wells; the purpose of this regulation is minimizing the cone of depression or interference with the boundaries of affected areas in the management zones; however, these measurements have not been implemented yet (Kinney County Groundwater Conservation District, 2013). In contrast, since Maverick County does not have a groundwater conservation district, the rule of capture still prevails for the aquifers in this area (Potter, 2004, TWDB, 2017b).

The development of a numerical model of the APN aquifer using the software Visual MODFLOW will allow the visualization and evaluation of water flows moving across the political border, the water moving across the Rio Grande/Rio Bravo River system and

variations in flow patterns due to the effect of pumping wells or extreme weather events in the region.

Under pre-development conditions, the flow pathways within the aquifer converged into the Rio Grande/Rio Bravo River, but it is expected that pumping wells in the surrounding areas of the river will cause the flow convergence zone to shift towards the wells with higher extraction rates. According to Rivera (2015), this type of aquifer where the river acts as a political border may have little transboundary flow unless the extraction of groundwater impacts baseflow to the river through changing hydraulic heads, which modify the system into a transboundary groundwater flow.

1.2 Problem statement

Due to the strategic location on the international border, changes in the water table within the APN disturb the surface water flows to the Rio Grande/Rio Bravo river system, affecting the water allocation agreed by USA and Mexico in the bi-national 1944 water treaty (Colorado-Rio Grande, 1944). In addition, this aquifer is a shared resource between two countries, but it has not been considered for binational detailed studies. Therefore, the changing flow pathways within the APN aquifer under the influence of pumping on both sides of the border should be assessed in a more precise research with the aim of achieving a better understanding of the water resources in the region.

The APN aquifer is considered an unconfined aquifer, and is comprised of alluvial material with a thickness of no more than 40 m. The aquifer is recharged by precipitation and consequent infiltration from Rio Escondido (Castillo Aguiñaga, 2000). The groundwater is likely to move across the border in areas adjacent to the Rio Grande/Rio Bravo River, where variable flow paths and strong surface water-

groundwater interactions are expected, while in regions of the aquifer from distant from river, the flow paths are expected to be more stable. Also, due to its unconfined nature, it is expected that the water table would be very sensitive to extreme weather events and high pumping rates.

One of the limitations encountered in this study was the lack of publicly available information in the Mexican side on virtual platforms and, in some cases, gaps in hydrologic data source over long periods. In several occasions, methodological differences on both sides of the border to calculate parameters and run the hydrogeological model was a constraint, because it was necessary to homogenize the parameters to do the input into the groundwater numerical model.

Sometimes, it was not possible to use rain gages due to large spatial or temporal gaps. This was solved by using remote sensing data when possible (Tropical Rainfall Measurement Mission or TRMM, satellite products for precipitation). However, in few cases, a comparison between the rain gages with the TRMM products was performed to know if the datasets from remote sensors were similar compared to the direct measurements in the field; Evapotranspiration was also obtained from GLDAS (NASA Global Land Data Assimilation System), but it was not possible to perform a comparison due to the absence of land data sets in the area of interest

1.3 Objectives

The main objective of this work is to demonstrate the hydrogeological linkages of the APN aquifer at the transboundary level and better understand the system, to support its identification, recognition and future joint management at the international

level. This was primarily achieved through the development of a hydrogeological model using the software Visual MODFLOW.

The specific objectives of this study are:

Objective 1. To include Texas and southern portions of the aquifer to better understand the transboundary nature of the system.

Objective 2. To update the aquifer model developed by Boghici (2002) and Grupo Modelo (2011) with recent information from both sides of the USA/Mexico border (water wells, precipitation and evapotranspiration from remote sensing data).

Objective 3. To understand how groundwater flows across the border region of the aquifer and determine significant variables affecting volumetric discharge and flow paths.

Objective 4. To analyze the water budget and estimate the groundwater amounts flowing from and into Rio Grande/Rio Bravo River, the Texas region and the Coahuila region.

2. SETTINGS

2.1 Allende Piedras Negras (APN) Aquifer location

The Allende-Piedras Negras aquifer is located in the southeast state of Texas (Figure 2 (a)), USA and at the north of the state of Coahuila, Mexico. The total area covered by this aquifer is 7023.8 km^2, with 5426.8 km^2 lying in Mexico and the remaining 1597 km^2 in the USA (Figure 2 (b)). The aquifer boundaries were delineated to follow the distribution of late Neogene and Quaternary deposits on the lower flatlands of the region. These are surrounded by older Paleogene and Cretaceous hard rocks placed as mountain chains and small hills at the Northwest of the APN aquifer (Aguilar, 2013).

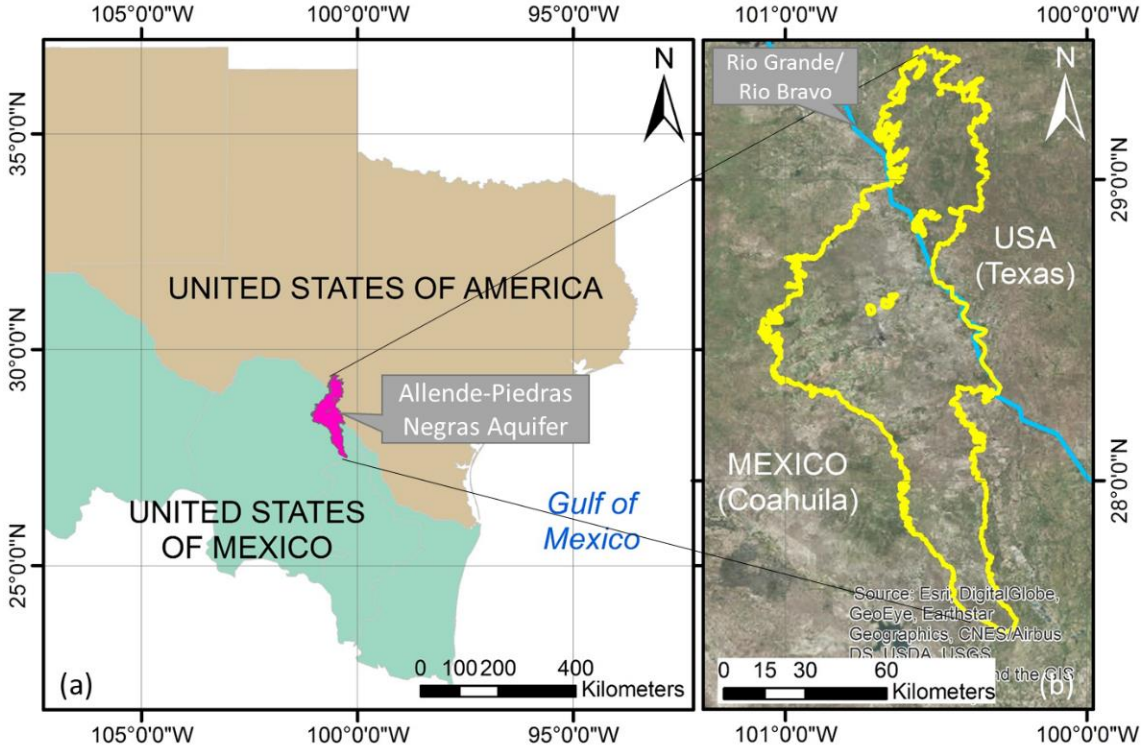

Figure 2. Allende-Piedras Negras aquifer location

2.2 Topography and Drainage

The study area is located between two physiographic provinces: the Eastern Sierra Madre comprise the western portion, and the Great Plains of North America comprise the central and eastern portions. The aquifer is bordered by mountain chains known as Serrania del Burro, Lomerio Peyotes and Anacacho Mountains (Figure 3). In this region Cretaceous rock outcrops are separated by flat, elongated valleys which reflect the calcareous nature of the area; the Cretaceous rocks were covered by alluvial sediments during the late Neogene and Quaternary, creating the present-day plains in the region (Castillo Aguiñaga, 2000).

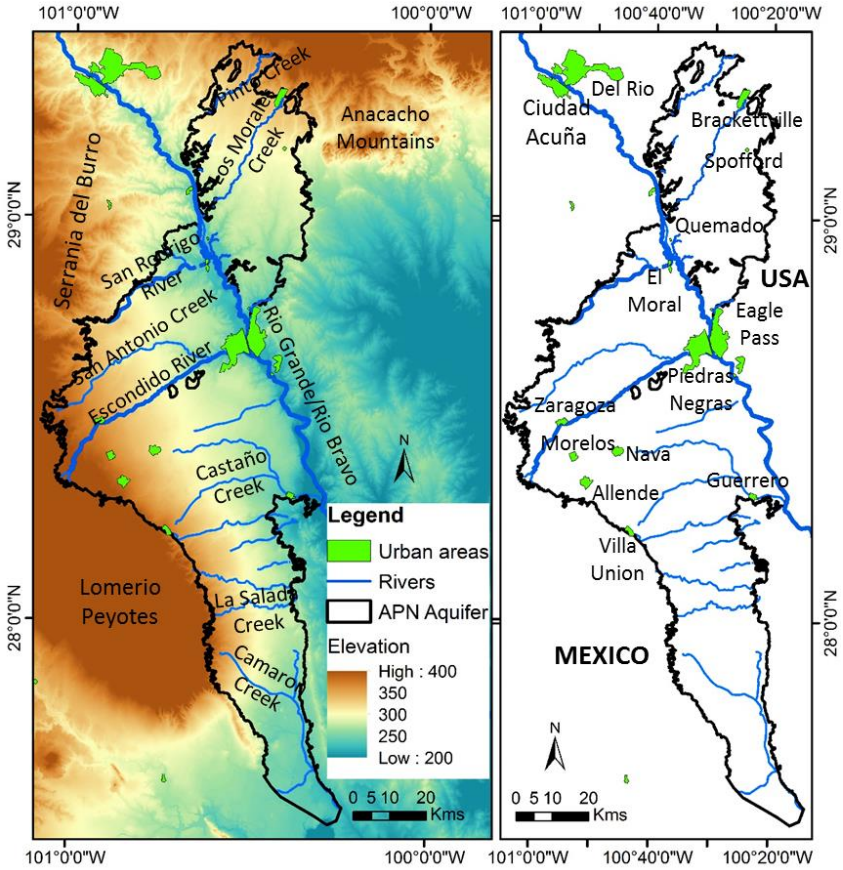

Figure 3. Main topographic features, drainages and urban areas in the APN Aquifer.

The main drainages in the area are San Antonio, San Rodrigo and Escondido Rivers, flowing from Serrania del Burro in Mexico, into the Rio Grande/Rio Bravo. Los Morales creek flows through Maverick County in Texas, running into the Rio Grande/Rio Bravo River, which functions as a natural boundary in the region. The flow for these drainage systems is intermittent, forming ponds along their courses or even drying completely during summer. Only Escondido River and Castaño Creek have perennial flows with average discharges of 4 m^3/s and 2 m^3/s (Aguilar 2013) (Figure 3).

2.3 Climate and precipitation

In the Piedras Negras (Mexico)/Eagle Pass (USA) region, the climate is arid to semi-arid and most of the precipitation occurs as sporadic thunderstorms. According to precipitation records for the period 1960-2007, an average of 446 mm rain falls each year, with the heaviest rainfall occurring from May through September (Aguilar, 2013). The average temperature of the region is 21.2°C, ranging from an averaged minimum of 14.5°C to an averaged maximum of 28°C (Boghici, 2002).

In the surrounding areas of Allende, Guerrero, Morelos, Nava, Piedras Negras, Villa Union, and Zaragoza (Mexico), the average annual temperature ranges from 20°C to 22°C, whereas in the highlands of Serrania del Burro it is 18°C. (Aguilar, 2013). The predominant climate in the study area is semi-dry to semi-arid (Boghici, 2002). The maximum monthly precipitation occurs during September while the maximum monthly temperature of 30°C is recorded during July and August (Aguilar, 2013).

2.4 Evapotranspiration

Evapotranspiration is the water transfer from the soil into the atmosphere and was estimated for the APN aquifer in 433.2 mm/year by CONAGUA (2014) using the

Coutagne empiric equation (Coutagne, 1954), which uses antecedent precipitation and current temperature to perform the calculation. There are no direct, ground-based measurements of evapotranspiration in the area of the study. The potential evapotranspiration ranges from an annual average of 1746 mm in the city of Allende, to an annual average of 1816 mm in the city of Piedras Negras (CONAGUA, 2014).

2.5 Geology

The following section describes the geological features of the formations identified and correlated between Mexico and Texas in the area of interest. They are identified starting with the name given in Mexico, followed by the name given in the USA. There are formations that were reported in either side of the border therefore not crossing the boundary; these formations are identified as Formation (USA) or Formation (MEX), which means they were rocks identified only on one side of the border. The following description only addresses those formations that are located along the border between Northern Coahuila State and Southern Texas, not considering those formations beyond the study area. Furthermore, the lithologic formations of interest in the APN aquifer are identified as “primary” and the surrounding formations are identified with the word “secondary” to differentiate the geology description (Figure 4 and Table 1).

Most of the mountains surrounding the APN aquifer are comprised of Lower Cretaceous age deposited in a reef barrier marine environment with secondary porosity comprised of fractures and dissolution cavities. These rocks are overlain by upper Cretaceous rocks deposited as fine sediment layers. These impermeable rocks locally confine the underlying aquifers. The flat lands surrounding the APN aquifer are formed by discordant Paleogene and Neogene deposits of continental and transitional origin.

Lastly, the Quaternary fluvial deposits unconformably overly the Cretaceous and Paleogene rocks. Table 1 shows in bold the geological units that were grouped to comprise the APN aquifer.

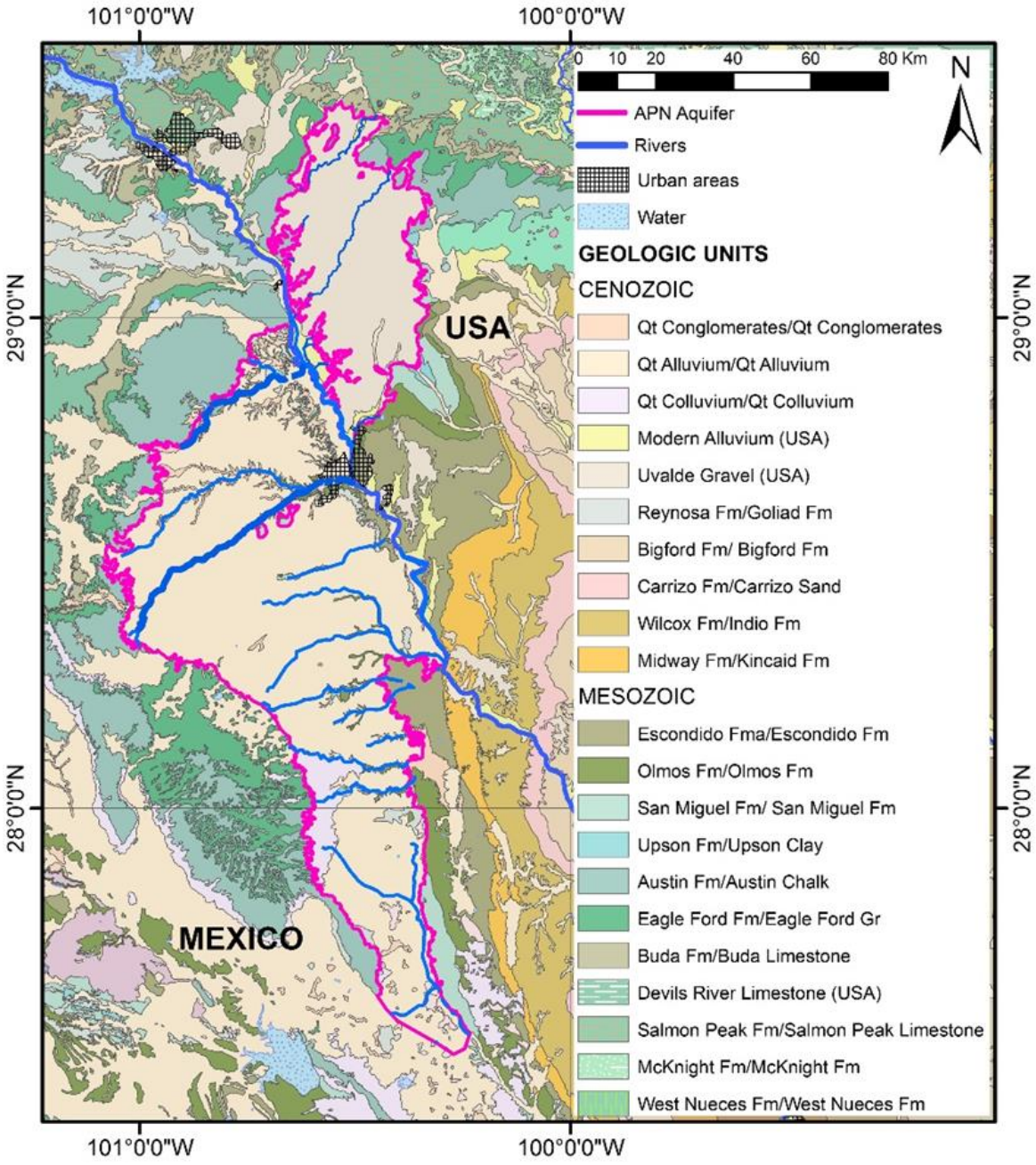

Figure 4. Geology of the area surrounding the APN aquifer.

Table 1. Stratigraphic column describing sediments and rocks on both sides of the Mexico-USA border (modified from Hamlin (1988) and Smith (1970)).

<table>
<tr><th>ERA</th><th>PERIOD</th><th>EPOCH</th><th>AGE</th><th colspan="2">MEX</th><th colspan="2">USA</th></tr>
<tr><td rowspan="15">Cenozoic</td><td rowspan="3">Quaternary</td><td>Holocene</td><td></td><td rowspan="2">Qt Conglomerates / Qt Conglomerates (Mex and USA)</td><td rowspan="2">Qt Alluvium/ Qt Alluvium (Mex and USA)</td><td rowspan="2">Qt Colluvium/ Qt Colluvium (Mex and USA)</td><td>Modern Alluvium</td></tr>
<tr><td>Pleistocene</td><td></td><td rowspan="2">Uvalde Gravel</td></tr>
<tr><td rowspan="2">Neogene</td><td>Pliocene</td><td></td><td colspan="2" rowspan="2">Reynosa Fm</td><td rowspan="2">Goliad Fm</td></tr>
<tr><td>Miocene</td><td></td></tr>
<tr><td rowspan="5">Paleogene</td><td rowspan="3">Eocene</td><td>Lutetian</td><td colspan="2" rowspan="2">Bigford Fm</td><td colspan="2" rowspan="2">Bigford Fm</td></tr>
<tr><td rowspan="3">Ypresian</td></tr>
<tr><td colspan="2">Carrizo Fm</td><td colspan="2">Carrizo Sand</td></tr>
<tr><td rowspan="2">Paleocene</td><td colspan="2" rowspan="2">Wilcox Fm</td><td colspan="2" rowspan="2">Indio Fm</td></tr>
<tr><td>Thanetian</td></tr>
<tr><td>Danian</td><td colspan="2">Midway Fm</td><td colspan="2">Kincaid Fm</td></tr>
<tr><td rowspan="14">Mesozoic</td><td rowspan="14">Cretaceous</td><td rowspan="10">Upper</td><td rowspan="2">Maastrichtian</td><td colspan="2">Escondido Fm</td><td colspan="2">Escondido Fm</td></tr>
<tr><td colspan="2">Olmos Fm</td><td colspan="2">Olmos Fm</td></tr>
<tr><td rowspan="2">Campanian</td><td colspan="2" rowspan="2">San Miguel Fm</td><td colspan="2" rowspan="2">San Miguel Fm</td></tr>
<tr><td rowspan="2"></td></tr>
<tr><td>Santonian</td><td colspan="2" rowspan="2">Austin Fm</td><td colspan="2" rowspan="2">Austin Chalk</td></tr>
<tr><td>Coniacian</td></tr>
<tr><td>Turonian</td><td colspan="2" rowspan="2">Eagle Ford Fm</td><td colspan="2" rowspan="2">Eagle Ford Gr</td></tr>
<tr><td rowspan="2">Cenomanian</td></tr>
<tr><td colspan="2">Buda Fm</td><td colspan="2">Buda Limestone</td></tr>
<tr><td rowspan="4">Lower</td><td rowspan="4">Albian</td><td colspan="2" rowspan="2">Salmon Peak Fm</td><td rowspan="2">Salmon Peak Limestone</td><td rowspan="4">Devils River Limestone</td></tr>
<tr><td rowspan="3"></td></tr>
<tr><td colspan="2">McKnight Fm</td><td>McKnight Fm</td></tr>
<tr><td colspan="2">West Nueces Fm</td><td>West Nueces Fm</td></tr>
</table>

2.5.1 Mesozoic

WEST NUECES FORMATION (Middle Albian) (Secondary): This formation is known as West Nueces Formation/West Nueces Formation. This formation is comprised of shales with lesser amounts of limestone. The thickness ranges from 40 m to 60 m. The Mexico part of West Nueces formation also correlates to the Devils River Limestone near Del Rio, Texas and the Fort Terret member of the Edwards Formation in Texas. According to (CONAGUA, 2015b), at greater depths the West Nueces Formation located in Serrania del Burro, Coahuila, can have the potential of an aquifer with confined to semi-confined conditions. In south central Texas, the upper portion of West Nueces formation in Edwards Plateau Area, is considered moderately permeable, while the lower portion is impermeable and performs more as an aquitard (Barker et al., 1994).

MCKNIGHT FORMATION (Albian) (Secondary): Referred to as the McKnight Fm./McKnight Fm. This unit outcrops in Valverde County in Texas and is comprised of gray, thin-bedded limestones in the lower portion. The middle portion is comprised of brown to black, thin bedded clay to calcareous mudstone, and the upper portion are mainly comprised of breccia layers separated by thin layers of mudstones. In Mexico, this unit is comprised of brown clayey mudstones with interbedded claystones and anhydrites. The estimated thickness ranges from 30 to 152 m. This formation has been reported to have low permeability and has been classified as an aquitard by Clark and Small (1997).

SALMON PEAK FORMATION (Albian) (Secondary): This formation is known as the Salmon Peak Fm./Salmon Peak Limestone. In Texas, this formation is comprised of

gray to green limestone with interbedded flint nodules. In North Coahuila and part of Chihuahua (Mexico), the unit is mainly comprised of massive gray limestones and fractures filled with calcite. The thickness ranges from 94 m to 195 m. The lower portion of the formation has low porosity and low permeability values, but water is extracted from fractured areas (Clark and Small, 1997); while the upper portion is porous, permeable and water is considered to be fresh to saline (Boghici, 2002).

DEVILS RIVER LIMESTONE (Albian-Cenomanian) (Secondary): This formation is known as the Devils River Limestone (USA). This term was used to describe the outcropping limestones in South Texas. The unit is comprised of fossiliferous wackestones locally dolomitized and rudist layers. The estimated thickness is around 210 m. In Mexico, the Devils River formation is considered part of Santa Elena Formation. The porosity and permeability of this formation appears much greater within the upper portion of the formation, and is a product of primary porosity and secondary porosity by rock dissolution. Vertical fractures near the top of the unit provide paths for effective recharge of the aquifer providing the most efficient portion of the formation for water extraction (Clark and Small, 1997). The middle part of the formation has secondary porosity produced by evaporite dissolution increasing its permeability, but not as high as the upper Devils River portion (Clark and Small, 1997). The lower portion has porosity values up to 15% but low permeability (Clark and Small, 1997). The Devils River Limestone yields fresh to saline water to wells in Kinney, Val Verde and Uvalde counties in Texas (Boghici, 2002).

BUDA LIMESTONE (Cenomanian) (Secondary): This formation is known as the Buda-Del Rio Fm./Buda Limestone-Del Rio Clay. This formation is comprised of

limestone with massive layers that vary in consistency and hardness. The color of this limestone is white, yellow and orange. The Buda limestone has been identified in South Texas, and in Big Bend National Park. In Mexico, the formation is mainly comprised of brown and gray mudstones, and has calcite veins and small ferruginous nodules. The reported thickness is 30 m. According to CONAGUA (2015d), the Buda Limestone would constitute an aquifer in the region of Chihuahua with confined to semi-confined conditions due to the presence of mudstones; however, this is a deep aquifer that has not been explored yet. Castillo Aguiñaga (2000) clarifies that the porosity of this formation is secondary due to fracturing with absence of primary porosity, and classifies this unit as semi-permeable. Reeves and Small (1973) report little extraction of fresh water from wells in ValVerde and Kinney counties, but in some cases the water is unacceptable for human consumption due to a sulphate taste (Fallin, 1990).

EAGLE FORD GROUP (Cenomanian-Turonian) (Secondary): This formation is known as the Eagle Ford Fm./Eagle Ford Gr. This formation is mainly comprised of dark shales, interbedded with argillaceous limestones in thin layers. The lower part is laminated siltstone and fine-grained sandstone. The thickness ranges from 20 to 178 m. The Eagle Ford Group functions locally as a confining geological unit for the western portion of Edwards Aquifer and also is one of the units separating the Edwards aquifer from the Cenozoic deposits in Southwest Texas (Boghici, 2002). This formation is only a productive aquifer in areas where it is fractured and outcropping in Southeast Texas (Bennett and Sayre, 1962).

AUSTIN CHALK (Coniacian-Santonian) (Secondary): This formation is known as Austin Fm./Austin Chalk. This formation is comprised of blue to beige fossiliferous

limestones, outcropping in Southeast Texas. In Mexico, this unit is comprised of shales and limestones interbedded with argillaceous limestones. The shales are light gray in color, and the argillaceous limestones are distributed as dark gray thin layers, sometimes with presence of coal. The thickness varies from 90 m to 500 m. This formation is a good water producer and Boghici (2002) has reported large pumping rates from shallow wells near Uvalde, Texas. However, Clark and Small (1997) consider this formation as the upper confining unit for Edwards aquifer.

UPSON CLAY (Campanian) (Secondary): This formation is known as the Upson Fm./Upson Clay. This formation is present in Medina and Maverick counties, Texas, and is comprised of gray to green calcareous shale. In northeast Mexico this unit is comprised of shales and siltstones, with sporadic calcareous sandstones interbedded. The thicknesses varies from 42 m to 622 m. Due to the predominance of terrigenous material, this geological unit is considered an aquitard by Boghici (2002).

SAN MIGUEL FORMATION (Campanian-Maastrichtian) (Secondary): Known as the San Miguel Fm./San Miguel Fm, this formation was identified in Texas as sandstone deposits distributed in thin and thick layers, separated by claystone bands and glauconitic material with several fossils; there is predominance of thick claystone layers near the top of the formation. In Northeast Coahuila, this formation was described as interbedded fossiliferous and calcareous sandstones, in some cases muddy sandstones can also be found with conglomeratic layers. The thickness of this formation varies from 22 m to 277 m. According to Boghici (2002), the small amounts of water pumped from San Miguel formation in Texas are highly mineralized thus are used for livestock supply.

OLMOS FORMATION (Maastrichtian) (Secondary): Olmos formation is known as Olmos Fm./Olmos Fm. This formation outcrops in Southern Texas and Northern Mexico. It is predominantly constituted by coal shales and calcareous shales, with some interbedded marl, coquina, mudstone, and coal layers. The thickness varies from 10 m to 378 m. This formation is not considered an optimal aquifer because of its limited water transmissivity reported in Texas. Some sandstone beds have been mapped in Kinney county, but the lack of connection between the sandstone beds probably inhibits the groundwater flow (Boghici, 2002).

ESCONDIDO FORMATION (Maastrichtian) (Secondary): This formation is referred as Escondido Fm./Escondido Fm. This formation is described as mudstone and dark marl, interbedded with sandstone layers, limestone and fossiliferous banks at the North of Piedras Negras. In Texas, this formation has a thickness ranging from 229 m to 792 m. The permeability of this unit is generally low; however, there are livestock wells in Maverick County that pump groundwater from this formation (Boghici, 2002). Close to Allende and Villa Union in Coahuila, the water pumped has high sulfate and calcium contents, with TDS varying from 1000 to 2500 ppm.

2.5.2 Cenozoic

MIDWAY FORMATION (Paleocene) (Secondary): This formation is identified as Midway Fm./Kincaid Fm, in Mexico the formation is dark gray green shale, with calcareous to sandy composition, occurrence of ferruginous concretions and quartz sandstones in layers up to 10 m thick. In South Texas, the formation is characterized by glauconitic sandstones, gypsiferous claystones and some limestone lentils. The sandstone layers are fine grained and strong cemented with calcite, the porosity is from

medium to poor. The unit thickness varies from 400 m to 1000 m. The geologic nomenclature in Texas refers to this unit as Kincaid Formation from Midway Group; however, in Mexico it is recognized as Midway Formation. According to Boghici (2002), Midway Formation is a confining unit located on the bottom of Carrizo-Wilcox Aquifer.

WILCOX GROUP (Paleocene-Eocene) (Secondary): Identified as Wilcox Fm./Indio Fm, this formation is described as interbedded thin layers of shales and clay sandstones, with occasionally thick red clay layers. Gypsum and lignite layers can also be identified in the middle of the formation. The thickness ranges from 5 m to 427 m. Hamlin (1988) assigns the name of Indio Formation to this unit in the Texas side. According to Ashworth and Hopkins (1995) this formation has been also recognized as part of the Carrizo – Wilcox aquifer due to the connectivity between both geological units.

CARRIZO FORMATION (Eocene) (Secondary): In Figure 4 this unit is refereed as Carrizo Fm./Carrizo Sand, it is constituted by a sequence of gray colored fine to coarse-grained sandstones. Due to its iron content, the weathered color is from yellow to red. It is common to find hematite nodules which are linked to erosion surfaces. The thickness vary from 5 m to 100 m. As it has been mentioned, this geological formation is considered part of the Carrizo – Wilcox aquifer by Ashworth and Hopkins (1995), allowed by the similarity of their hydrogeological features and their geographical proximity.

BIGFORD FORMATION (Eocene)(Secondary): This formation is identified as Bigford Fm./Bigford Fm, in Webb County, Texas, this formation is configured by gray – green sandstone with 0.5 m thick lignite layers. This formation has been described as a

sandstone, mudstone, shale and coal sequence in Nuevo Leon and Tamaulipas, Mexico. The thickness measured varies from 8 m to 280 m. According to the aquifer classification made by CONAGUA (2006) based on aquifer potential and water quality, Bigford formation is considered Unit I type of aquifer with poor to very poor potential conditions and very low quality of groundwater.

REYNOSA FORMATION/GOLIAD FORMATION (Miocene-Pliocene) (Primary): This formation is known as Reynosa Fm./Goliad Fm. Trownbridge (1923) mentions that the formation is a mixture of cemented gravels with carbonated silt, non-cemented gravels, limestones with pebbles, limestones with very low quantities of gravel and sand and low quantities of clay. According to Barnes (1974), this formation includes pink to gray claystones, gray mid to coarse grained sandstones, marl, caliche and conglomerates in Texas. Previously, the upper deposits were recognized as Uvalde Gravel by Deussen (1914), but in 1924 he modified the name to Reynosa Formation. Recently, the U. S. Geological Survey (2017) changed the name from Reynosa Formation to Goliad Formation, and named both Goliad Formation and Uvalde Gravel as independent units. Goliad Formation is then correlated to Reynosa Formation in Mexico (López-Ramos, 1979). The thickness varies depending on the author: Trownbridge (1923) reports a total thickness of 45 m. Lately, the reports vary from 5-10 m (Ramirez-Gutierrez et al., 2003), 10 to 35 m (Herrera-Monreal et al., 2003) and 20 m (Loaeza-García et al., 2004). CONAGUA (2015e) estimates a thickness between 60 m to 150 m in North Tamaulipas (Mexico).

In Texas, this formation is considered part of the Evangeline Aquifer within the Gulf Coast Aquifer according to Ashworth and Hopkins (1995), with a corresponding average

water level change of 0.4 m (Boghici, 2011). The average values of hydraulic conductivity and transmissivity are 1.5 m/d and 22 m^2/d (TWDB, 2017a). In the classification made by CONAGUA (2006) this formation is considered as Unit II type of aquifer, with regular aquifer potential and good to regular groundwater quality.

UVALDE GRAVEL (Pliocene-Pleistocene) (Primary): This formation is referred as Uvalde Gravel (USA). The term was used first by Hill (1891) to describe the gravel deposits located in highlands from Central and South Texas. Sellard et al. (1966) described gravel deposits with rounded flint, calcite and quartz pebbles, in a calcareous loam and caliche matrix with cross stratification in some areas. According to Barnes (1977), the thickness measured in south Texas is 10 m. Montiel Escobar et al. (2005) homologates the unit in Mexico as Reynosa Formation which is recognized by Boghici (2002) and CONAGUA (2006); however, the Mexico Geological Service (SGM) refers to this formation as Quaternary Alluvium. Therefore, Uvalde Gravel and Quaternary alluvium will be treated as separate units for the purpose of this research.

In Piedras Negras, Mexico, the Quaternary Alluvium is the main exploitable aquifer, recognized by Boghici (2002) and CONAGUA (2014) as the Allende – Piedras Negras aquifer, though the reported aquifer boundaries from both sides do not coincide. Boghici (2002) describes this aquifer as highly permeable with fresh to slightly saline water and transmissivity values between 0.0005 m^2/s and 0.005 m^2/s (CONAGUA, 2014). In Figure 4, the APN aquifer is identified in Coahuila (Mexico) as Quaternary Alluvium deposits, the Quaternary Conglomerates and the Uvalde Gravel in Texas (USA), all grouped as the whole aquifer.

MODERN ALLUVIUM (Holocene) (Secondary): According to Page et al. (2009), the modern alluvium is described as recent terrace deposits of gravel, sand, silt, clay and occasionally organic material. The thickness varies between 2 and 10 m (Page et al., 2009).

QUATERNARY DEPOSITS (Pleistocene-Holocene) (Primary): According to Estavillo and Aguayo (1985), the quaternary deposits are described according to its precedence. In Mexico, these deposits are identified as mud and clay, finely laminated, with some ancient channels buried and filled with fine sand. Specifically, the main composition of lacustrine deposits (shown in Figure 4 as Qt Lacustrine/Qt Lacustrine) is silt, clay, organic matter and some salt and gypsum disseminations. The colluvium deposits (identified in Figure 4 as Qt Colluvium/Qt Colluvium) are poorly selected conglomerates and sands located in creeks and chain mountain flanks (Santiago and Escalante, 2006).

The quaternary deposits, specifically the alluvial deposits (shown in Figure 4 as Qt Alluvium/Qt Alluvium), are distributed along the Rio Grande/Rio Bravo River, and in some cases have optimal hydrogeological properties according to CONAGUA (CONAGUA, 2015b, CONAGUA, 2015d). It is common; however, that alluvial deposits cover other geological units creating small deposits randomly located, working as small aquitards. Even if there are alluvial deposits located close to Rio Grande with aquifer potential, they could be limited to local water supply due to the reduced size of the deposit. In some areas, hydraulic parameters of these alluvial deposits were measured in the field. Other small quaternary deposits along the Rio Grande in Serrania del Burro and Presa La Amistad regions have been identified by CONAGUA (CONAGUA, 2015a,

CONAGUA, 2015b) but there is limited data on the hydrogeological properties or water quality conditions in this region. However, given the lithological similarities, CONAGUA (2014) makes an association of hydrogeological properties of the Allende – Piedras Negras aquifer with these quaternary deposits. The recharge processes of the quaternary alluviums are the underflow from upstream, infiltration from the Rio Grande and its tributaries, and underflow from adjacent deposits (Groat, 1972).

In the Piedras Negras region, Mexico, the main exploitable aquifer is recognized by Boghici (2002) and CONAGUA (2014) as the Allende – Piedras Negras aquifer. In Texas, this aquifer is formed by the Uvalde Gravel, described above. CONAGUA (2014) describes this aquifer as highly permeable with transmissivity values between 0,0005 m^2/s and 0.005 m^2/s. In Figure 4, the Allende – Piedras Negras aquifer is identified in Mexico as Quaternary Alluvial deposits and Quaternary Conglomerates. It is necessary to clarify that Boghici (2002) classifies the Mexico portion of the aquifer as the Reynosa Formation. However, CONAGUA (2014) and Servicio Geológico Mexicano (2008b) identify the formation as Quaternary Alluvial deposits. For the purpose of this research, the nomenclature taken as reference for the APN aquifer is from Servicio Geológico Mexicano (SGM).

QUATERNARY CONGLOMERATES (Pleistocene – Holocene) (Primary): This formation is referred as Qt Conglomerates/Qt conglomerates. The quaternary deposits are mainly conglomerates from the Rio Grande/Rio Bravo River, and are located along the river covering Mesozoic and Cenozoic rocks. The deposits are formed by angular clasts of igneous rocks, limestones, sandstones and shales and a silt to sandy matrix (CONAGUA, 2015c). According to Ashworth and Hopkins (1995) and CONAGUA (2015c), these

quaternary deposits are common in the upper part of the Bolson aquifers located between Texas and Chihuahua, and some small deposits on the APN Aquifer in Coahuila as shown in Figure 4.

2.6 Socio economic considerations and importance of the aquifer

The principal cities of interest in the region are Zaragoza, Morelos, Allende, Villa Union, Nava, El Moral, Guerrero and Piedras Negras on the Mexico side. The USA side has Quemado, Spofford, Brackettville and Eagle Pass as its principle cities. Piedras Negras and Eagle Pass stand as the biggest urban centers in the area with a total population of 272410. (Table 2).

Table 2. Urban centers and population on the APN aquifer region, being the most important cities Piedras Negras (Mexico and Eagle Pass (USA), which also are the greatest border towns in the area of interest. Retrieved from *www.census.gov* and *www.inegi.org.mx*.

COUNTRY	URBAN CENTER	POPULATION	%
Mexico	Allende	20153	6.0
	El Moral	390	0.1
	Guerrero	959	0.3
	Morelos	1516	0.4
	Nava	22132	6.6
	Piedras Negras	245155	72.7
	Villa Union	6138	1.8
	Zaragoza	12411	3.7
USA	Eagle Pass	26255	7.8
	Brackettville	1876	0.6
	Quemado	230	0.1
	Spofford	94	0.0
Total		337309	100.0

Both the USA and Mexico cite agriculture and cattle raising as their main economic activities in the region. However, coal mining and other industries such as beer production are limited to the Mexico side. Several companies including firearms fabrication are manufactured on the USA side.

The APN aquifer is essential to maintain several of the economic activities in the region, as well as the water supply for the population allocated in the area. The APN aquifer supplies 85% of the total water needs in the region. From this percentage of groundwater use, 69.2% is used for agriculture, 17.3% industrial, 4.9% public supply, and the remaining 8.9% is used by rural household (CONAGUA, 2014).

Recently, the development of “Maquiladoras”, or assembly, processing or manufacturing industries, has increased the population growth by 3.7% in the surrounding Mexican areas of the Mexico – USA border (Terry, 2017). This has added enormous pressure on the natural resources (such as sand and gravel unconsolidated deposits) which are extracted from San Rodrigo River and used as construction material (Olivera et al., 2018). The activities of building material extraction over the course of San Rodrigo River are permitted through concessions from CONAGUA but there also illegal extraction. Overall, the riparian zones have suffered deforestation and water quality degradation in the area (Olivera et al., 2018).

The Escondido River crosses the APN aquifer from West to East on the Mexico side, and receives baseflow from the APN aquifer (Figure 3). The groundwater pumping for irrigation and mining activities between the cities of Allende and Piedras Negras has modified the potentiometric surface which has the potential of affecting the baseflow to the Escondido River (FUMEC, 1999).

The APN aquifer has been previously recognized as transboundary by Boghici (2002), Sanchez et al. (2016) and Sanchez et al. (2018) but it has not been recognized officially by both countries or at an international level. The USA-Mexico transboundary aquifer assessment program (TAAP) reflects the aquifer assessment priorities located along the USA-Mexico border, enacted by the *United States-Mexico Transboundary Aquifer Assessment Act* as public law 109-449 in 2006. This law paved the way to binational negotiations which motivated the 2009 signing of the *Joint Report of the Principal Engineers Regarding the Joint Cooperative Process United States-Mexico for the Transboundary Aquifer Assessment Program.* This document as signed by the principal managers involved in the International Boundary and Water Commission (IBWC), establishing the jurisdiction and structure under which personnel from USA and Mexico would collectively study shared aquifers. Under this act, the TAAP has been authorized to implement methodologies required to develop conservation policies between both countries to set “sustainable development in a cooperative framework” (Milanes Murcia, 2017).

3. METHODS

Following the order of the objectives previously described on section 1.3, it was necessary to construct a hydrogeological model. This section approaches the data preparation and parameters selection to generate the model with the aim of knowing the water paths underneath the hyporheic zone (the upper few centimeters of sediments below a surface water body (Sophocleous, 2002)), the water table evolution during the seventeen- year simulation and the amounts of water coming from different regions into the Rio Grande/Rio Bravo system.

3.1 Area selection

At first, the information review was crucial to define the scope of the project where the study made by Sanchez et al. (2016) gave a first assessment on the transboundary aquifers between the U.S. and Mexico border; and a gap was also identified between East Texas (USA) and Coahuila (Mex), where the area did not have any aquifer assignation at the moment.

Boghici (2002) made an assessment in the area identifying the Allende-Piedras Negras transboundary aquifer, generating a hydrogeological model on the Mexico side. Other authors such as Castillo Aguiñaga (2000) and CONAGUA (2014) have generated also the hydrogeological conceptual model limited to the Mexico side.

3.2 Boundary definition

Next, the physical boundaries for the aquifer were defined. The boundary definition was made by downloading the geologic maps at 1:250000 scale from Instituto Nacional de Estadistica y Geografia (INEGI) (Servicio Geológico Mexicano, 2008b,

Servicio Geológico Mexicano, 2008a), as well as the Texas geologic map (U. S. Geological Survey, 2007).

The map used to correlate the geological units in both sides of the border was the *Preliminary geologic map of the Laredo, Crystal City-Eagle Pass, San Antonio, and Del Rio 1 degree x 2 degree quadrangles, Texas, and the Nuevo Laredo, Ciudad Acuna, Piedras Negras, and Nueva Rosita 1 degree x 2 degree quadrangles, Mexico.* (Page et al., 2009). This map was preferred because it contains the lithological formations with Texas nomenclature, making it possible to follow them continuously across the border. In conjunction with the geologic maps from SGM, other assignments included the equivalent lithological formation with Mexican nomenclature to extend the correlation to areas not covered by the initial geological map. In some cases, it was necessary to use the lithological descriptions and correlations to find the equivalent formation in both sides of the border (Figure 4).

For the APN aquifer model input, the physical boundaries rely on the lithologic differences between the Neogene-Quaternary deposits (Uvalde Gravel, Reynosa Formation and Quaternary deposits) and the surrounding Cretaceous and Paleogene formations as previously shown in Figure 4.

3.3 Isopachs

After the delineation of surface geologic units, the drilling reports were used on the Texas side, downloaded from the public database on the Texas Water Development Board webpage (TWDB, 2017b). Using the lithology descriptions for Uvalde Gravel and Quaternary deposits in the area from drilling reports, an aquifer thickness was estimated, taking in account the lithologic descriptions given in the drilling reports and

matching them with the geologic descriptions from literature. The thickness estimates were converted from feet to meters when necessary.

There was no drilling information available for Coahuila; however, there were 4 oil wells with available lithological information provided by private Mexican companies (Galaxia-1, Coconal-1, Omega-1, Allende-1); in this case, the thickness of the quaternary deposits was extracted from the oil well drilling reports. Furthermore, a cross section provided by the same private company was used to infer the thickness of quaternary deposits near the towns of Nava, Zaragoza and Piedras Negras (Coahuila). As there were some areas without available lithological information, water wells were used separating them into clusters depending on the well depth; the dominant trend that emerged from this analysis was that the deeper wells were on the periphery of the APN aquifer where its expected thickness was less than 1 m. These wells were assumed to be pumping from deeper formations and not screened within the quaternary deposits. Another parameter used to filter the wells was an ID given in the databases, where the wells with alluvial ID codes were filtered and used to generate the isopach map of the Quaternary and Neogene deposits.

As seen in the isopach map in Figure 5, the aquifer thickness ranges from 1 m to 40 m, which was the greatest thickness used in the Visual MODFLOW input (VMF). The greatest thickness predominates in the center of the basin in the region of Coahuila, where also most of the pumping wells are located. In the Rio Grande/Rio Bravo area, the thickness of the aquifer ranges from 10 to 25 m with no dissection of the aquifer by river erosion; an important assumption is that the Quaternary and Neogene deposits are forming the deposits below the hyporheic zone, isolating the river system from older

underlying rocks (Cretaceous and Paleogene deposits). In the southern area there was not enough information available to generate a proper interpolation; however, according to the available information the approximate thickness ranges from 1 to 30 m.

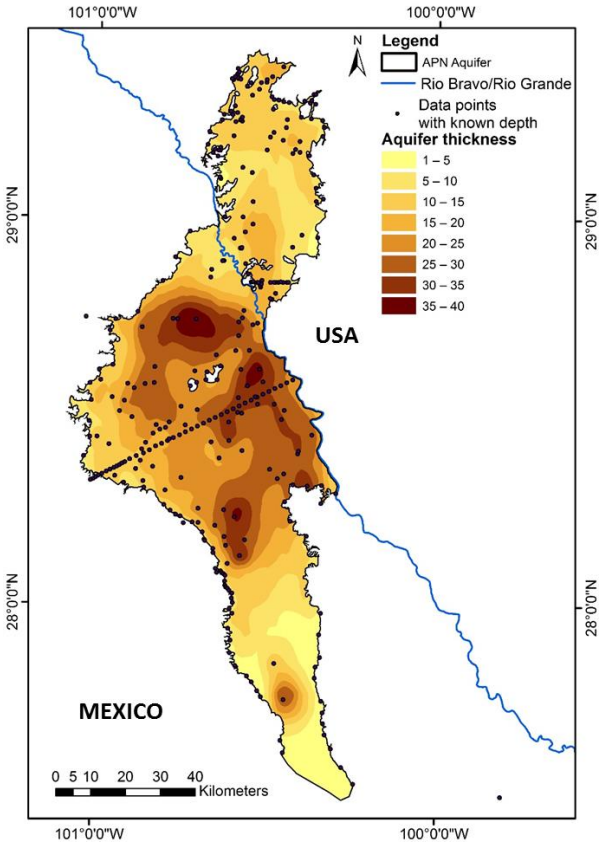

Figure 5. Isopachs APN aquifer. Map generated from drilling information and cross section estimates.

The isopach map was used to generate a database of points with interpolated top and bottom elevations of the aquifer extracted from combining the isopach map with DEM (Digital Elevation Model) models using ArcGIS software. It was necessary to generate txt files to do the input in VMF including the categories of coordinates, top elevation and bottom elevation of the aquifer. Some points were assigned outside the

aquifer boundary where elevation of the top had the same value as the elevation of the bottom layer to simulate the absence of the aquifer in these regions. Also, the status setting of areas outside the aquifer perimeter as inactive cells was necessary to avoid the inclusion of these areas into VMF calculations.

3.4 Evapotranspiration

The evapotranspiration (ET) was obtained from the NASA Global Land Data Assimilation System (GLDAS), where the monthly average evapotranspiration is available for the area of interest. It is not possible to obtain ET directly from remote sensing products, but GLDAS evapotranspiration models calculate ET from a water-energy balance (Rodell et al., 2004), with a temporal resolution ranging from 3 hours to a monthly basis; for this study, the time range used was from January 2000 to December 2017 (Figure 6). Ground-based observations were not used to validate ET from GLDAS due to the absence of ET stations in the area of study.

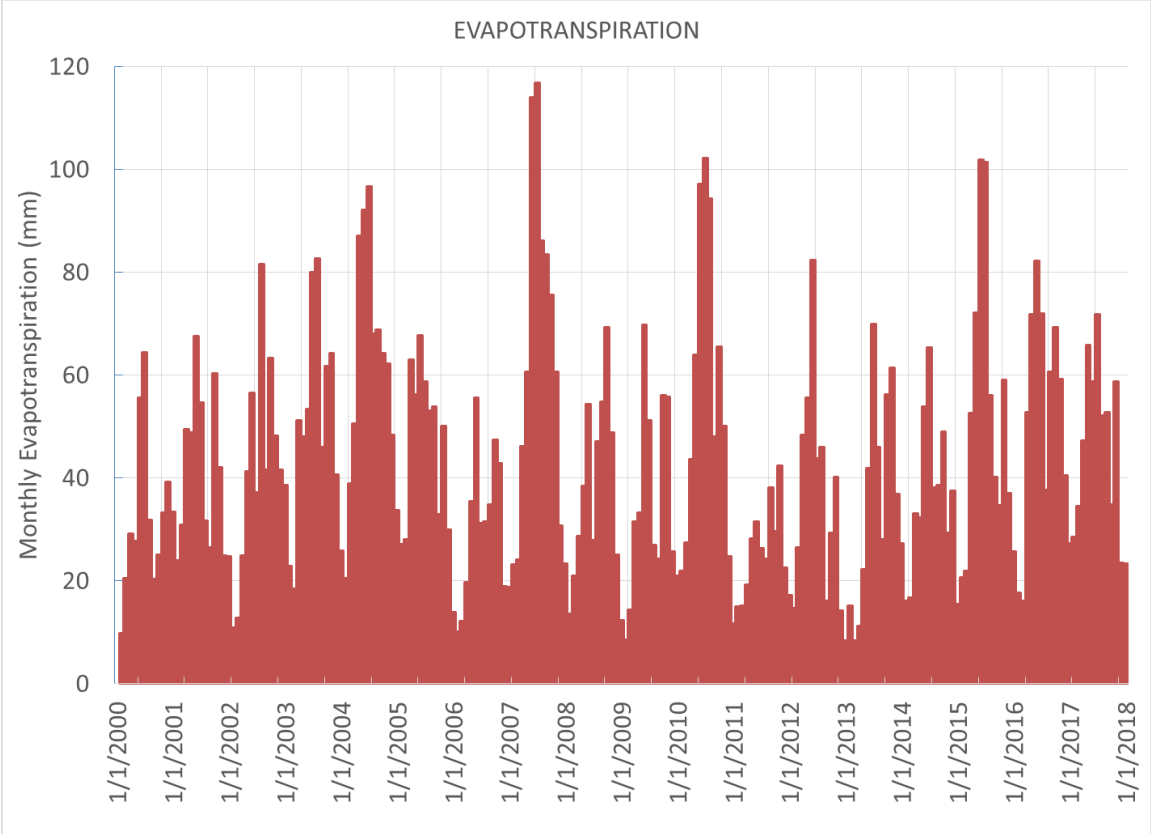

Figure 6. Averaged monthly evapotranspiration for the APN aquifer outcropping area. The data was obtained from monthly GLDAS evapotranspiration models.

Extraction of evapotranspiration values from NASA GLDAS images on a monthly basis gave an estimate of 512 mm/year for the period of interest with the highest evapotranspiration occurring between June and November, a maximum of 744.9 mm/year for 2004 and a minimum of 309.8 mm/year for 2011 (Table 3). Also, the same value of ET was assumed for the entire area in order of simplifying the numerical model.

Table 3. Averaged monthly evapotranspiration (mm/month) on the APN aquifer area. The red value is the lowest annual ET, reported on 2011 and the highest annual ET was obtained for 2007. The monthly data was obtained from GLDAS models

YEAR	Jan	Feb	Mar	Apr	May	Jun	Jul	Aug	Sep	Oct	Nov	Dec	Annual ET (mm)
2000	33	9.8	20.5	29.1	27.7	55.6	64.4	31.9	20.3	25.1	33.3	39.3	390.6
2001	25	24	30.9	49.4	48.8	67.6	54.6	31.7	26.5	60.4	42.1	24.9	485.7
2002	39	11	12.8	24.9	41.3	56.6	37.3	81.5	41.7	63.4	48.3	41.7	499.1
2003	26	23	18.5	51.2	48.1	53.4	80	82.7	46.1	61.8	64.2	40.7	595.6
2004	34	21	38.9	50.6	87.1	92.1	96.7	68	68.8	64.2	62.2	48.5	731.3
2005	14	27	28.1	63	56.2	67.8	58.8	53	53.8	32.9	50	29.9	534.7
2006	19	10	12.2	19.7	35.5	55.6	31.3	31.5	34.9	47.5	42.9	18.9	358.9
2007	23	23	24.1	46.3	60.6	114	117	86.1	83.5	75.6	60.6	30.7	744.9
2008	12	14	20.9	28.7	38.5	54.4	27.9	47.1	54.8	69.4	48.8	25.1	441.6
2009	21	8.6	14.4	31.5	33.3	69.8	51.2	26.9	24.3	56	55.8	25.7	418.5
2010	12	22	27.5	43.7	64	97.1	102	94.3	48.1	65.6	50	24.7	651.0
2011	17	15	15.2	19.3	28.3	31.5	26.3	24.3	38.1	29.7	42.5	22.5	309.8
2012	8.4	15	26.5	48.5	55.6	82.3	43.9	46.1	16.2	29.3	40.3	14.2	425.9
2013	27	15	8.37	11.2	22.3	41.9	70	46.1	28.1	56.2	61.4	36.9	424.9
2014	16	16	16.7	33.1	32.3	53.8	65.4	38.1	38.7	49	29.3	37.5	425.7
2015	26	21	21.9	52.6	72.2	102	101	56	40.3	34.7	59	37.1	623.7
2016	27	18	16.2	52.8	71.8	82.1	72	37.7	60.6	69.4	59.2	40.5	607.3
2017	23	29	34.5	47.3	65.8	58.8	71.8	52.2	52.8	34.9	58.8	23.5	552.3
AVG	22	18	21.6	39.1	49.4	68.7	65.1	52	43.2	51.4	50.5	31.2	**512.3**

The Extinction Depth is defined as the depth where ET from the water table ceases (McDonald and Harbaugh, 1988) and it is a necessary term to input in VMF for calculations related to water loss in the model. The extinction depth used in the VMF ET input was 1.5 m, as recommended by Shah et al. (2007) for sandy loam with bare soil and grass land covers. A txt file was used to do the VMF input with start day, end day, ET value and extinction depth for the entire project.

3.5 Precipitation and Recharge

The precipitation data was obtained from the Tropical Rainfall Measurement Mission (TRMM) as TMPA 3B43 Version 7, satellite images were downloaded from NASA for the period January 2000-December 2017 in a monthly basis and spatial resolution of 0.25° X 0.25°. The TRMM rainfall estimates are acquired from infrared data with available products on different temporal resolutions, ranging from 3 hours to a monthly basis (Huffman and Bolvin, 2013) (Figure 7). The monthly value obtained was assumed to be representative of the entire area to simplify this initial numerical model assessment; however, refined spatial data would give accurate results on the numerical model, mostly on water budget calculations.

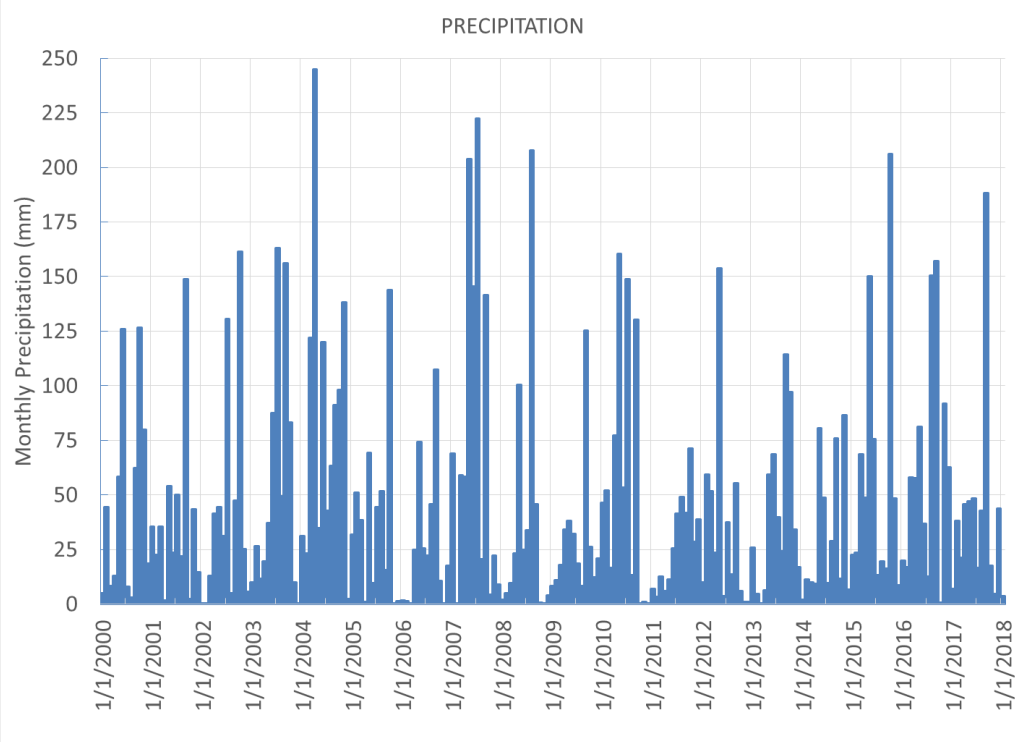

Figure 7. Monthly precipitation obtained from TRMM rainfall products averaged over the APN aquifer outcrop area. The spatial resolution of the products used to produce this histogram is 0.25° X 0.25°.

Within the study area most of the rain falls from May through October, while the dry periods occur from November through April, with December as the driest month. Average annual precipitation for the period of study (2000-2017) is 557 mm which mostly occurs as thunderstorms (Table 4). The year2004 was the year with highest precipitation (1012.3 mm/year) and 2011 was the driest year form the selected period (336.7 mm/year).

Table 4. Average monthly precipitation (mm/month) for the APN aquifer outcrop area.

YEAR	Jan	Feb	Mar	Apr	May	Jun	Jul	Aug	Sep	Oct	Nov	Dec	Annual P (mm)
2000	5.0	44.6	8.2	13.1	58.4	126.1	8.1	3.1	62.3	126.7	80.0	18.5	554.1
2001	35.5	22.4	35.5	1.6	53.9	23.4	50.0	21.8	148.7	2.2	43.5	14.7	453.3
2002	0.0	0.2	12.8	41.4	44.4	31.1	130.8	5.1	47.5	161.5	25.1	5.6	505.5
2003	9.9	26.4	11.7	19.6	37.1	87.6	163.0	49.4	156.0	83.2	10.1	0.0	653.8
2004	31.1	23.3	122.1	244.8	34.9	120.1	42.9	63.2	91.1	98.2	138.1	2.5	1012.3
2005	31.8	50.9	38.4	1.0	69.3	9.8	44.4	51.8	15.6	143.8	0.0	1.4	458.1
2006	1.5	1.2	0.4	24.8	74.1	25.5	22.1	45.7	107.3	10.5	0.0	17.5	330.8
2007	69.0	0.5	58.9	58.2	203.7	145.5	222.2	20.5	141.4	4.3	22.3	8.9	955.4
2008	2.1	4.9	9.7	23.1	100.4	24.9	33.9	208.0	45.9	0.6	0.2	3.9	457.6
2009	8.2	10.9	17.8	34.1	38.1	32.0	18.5	8.4	125.3	26.3	12.3	21.0	352.8
2010	46.4	52.1	16.6	77.2	160.5	53.4	148.9	13.2	130.2	0.1	1.0	0.2	700.1
2011	7.1	3.3	12.6	6.1	11.2	25.6	41.4	49.2	41.7	71.2	28.6	38.8	336.7
2012	9.9	59.3	51.7	23.6	153.7	3.6	37.5	13.5	55.4	6.1	1.0	0.9	416.2
2013	25.8	4.5	0.0	6.3	59.2	68.5	39.9	24.1	114.4	97.0	34.2	17.0	491.0
2014	1.9	11.4	10.0	9.4	80.5	48.6	9.6	28.8	75.8	11.5	86.5	6.8	380.6
2015	22.6	23.5	68.7	48.8	150.1	75.6	13.4	19.6	16.1	206.2	48.3	8.7	701.6
2016	19.8	17.0	58.1	57.7	81.2	36.8	12.6	150.6	157.1	0.6	91.8	62.6	745.7
2017	7.0	38.2	21.2	45.7	47.0	48.3	16.7	42.7	188.2	17.6	4.6	43.7	521.1
AVG	18.6	21.9	30.8	40.9	81.0	54.8	58.6	45.5	95.6	59.3	34.9	15.2	**557.0**

Three rain gages from Texas were used to validate the precipitation data obtained from remote sensing images (Figure 8), and the correlation of the data sources varies between 0.51 and 0.75. While there are several rain gages in the area of interest (Figure 8), there are some zones without rain gages or, in the case of having data for the period between 2000 and 2017, there are gaps for days or even months. Due to the limitations described before, it was more convenient to use the satellite data available.

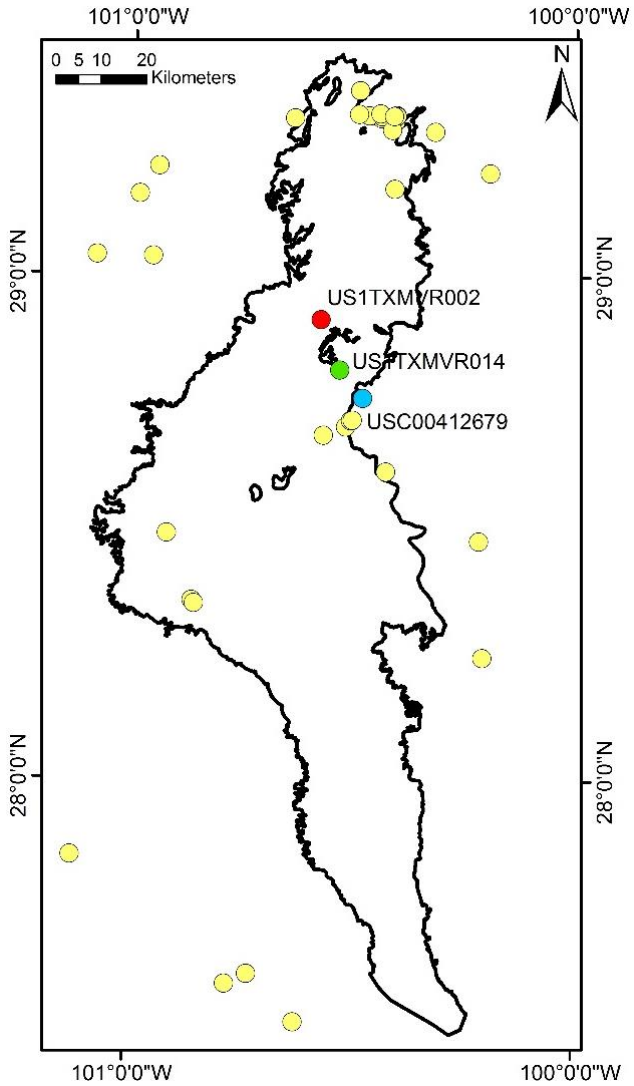

Figure 8. Available rain gages in the APN aquifer and surrounding areas (yellow dots). The stations used in the linear fitting (red, blue, green).

A data comparison was performed using the satellite data and the three rain gage stations with the least gaps available, which are located near the Rio Grande/Rio Bravo (Figure 8). It is noteworthy that the linear regression performed between the rain gages and the satellite data produced higher slopes for station USC00412679, mainly because this is the station with most of the data available for the period 2000-2017 (Figure 9). Also, statistical measurements were performed showing that the highest values of Pearson correlation and Nash-Sutcliffe efficiency, as well as the lowest root mean square error are indicators of high correlation between the rain gage station USC00412679 and the data obtained from TRMM satellite images (Table 5).

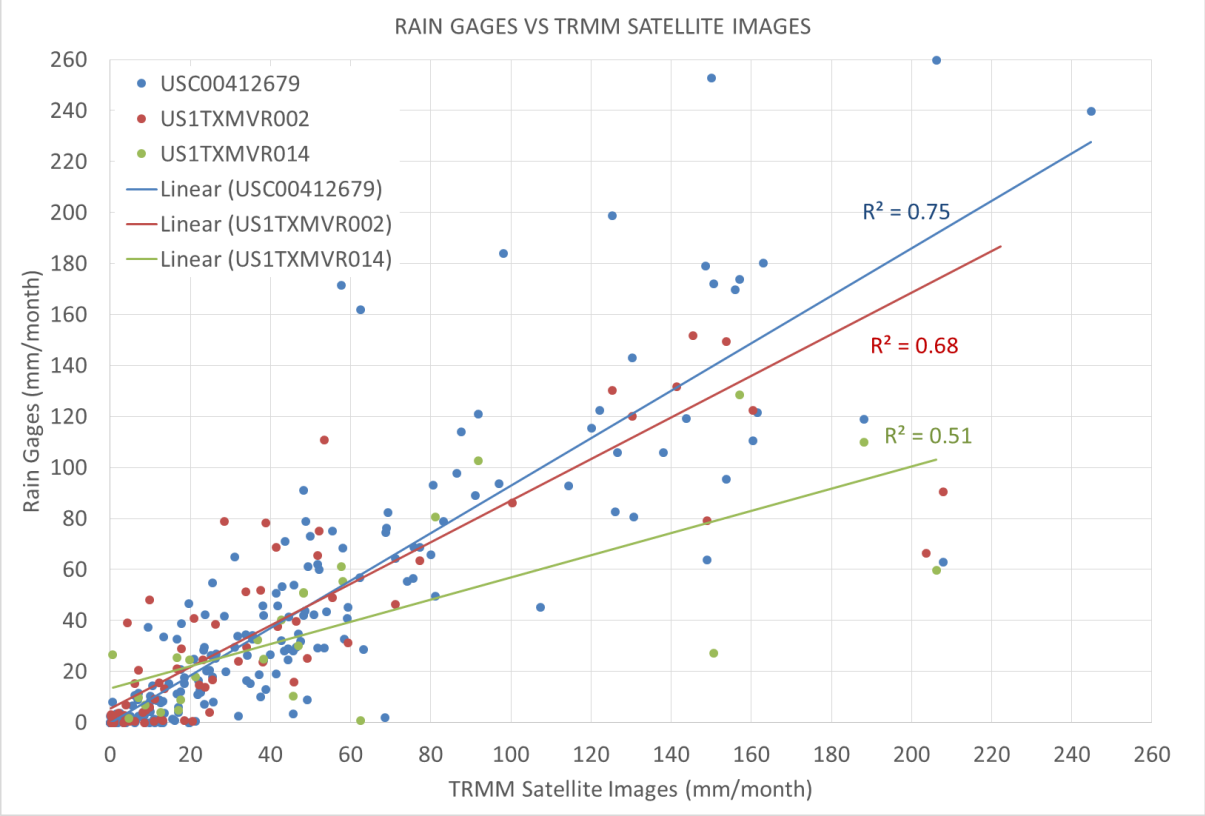

Figure 9. Linear fitting between rain gages and TRMM precipitation data.

Table 5. Results of comparison between satellite data and rain gages data.

PERFORMANCE MEASURE	US1TXMVR014	US1TXMVR002	USC00412679
Squared Pearson Correlation (R^2)	0.51	0.68	0.75
Root mean squared error (RMSE)	44.05	32.47	26.51
Nash-Sutcliffe efficiency (NSE)	0.64	-0.65	0.74

Visual MODFLOW does not allow to include precipitation directly in the numerical model, instead accepting the recharge. To do so, it was necessary to obtain the natural recharge in the area from the monthly precipitation values obtained at the beginning of this section; this value has not been physically measured but it was calculated using the Soil Conservation Service (SCS) curve number (CN) method, also known as SCS-CN (NRCS, 2004) and the precipitation values in the area. According to Stewart et al. (2011), a recommended curve number (CN) for semiarid regions ranges from 68.21 to 92.64. An intermediate value of 80 was used to perform the calculations of potential of maximum retention (Equation 1) and initial abstraction (Equation 2) to obtain the amount of water that infiltrates during a rainfall event

$$S = \frac{25400}{CN} - 254 \qquad \text{Equation 1}$$

where S is the potential of maximum retention after runoff starts (mm) and CN is the Curve Number

$$I_a = 0.2S \qquad \text{Equation 2}$$

where I_a is the initial abstraction (mm).

If the amount of water during a rainfall event was greater than the initial abstraction, it was assumed that the remaining water ran off and only the amount of water that equals I_a infiltrated. When the water during a rainfall event was lower than I_a, all the water infiltrated into the ground as natural recharge and there was no runoff.

The comparison of runoff versus recharge calculated with the SCS-CN method for the APN aquifer is shown on Figure 10.

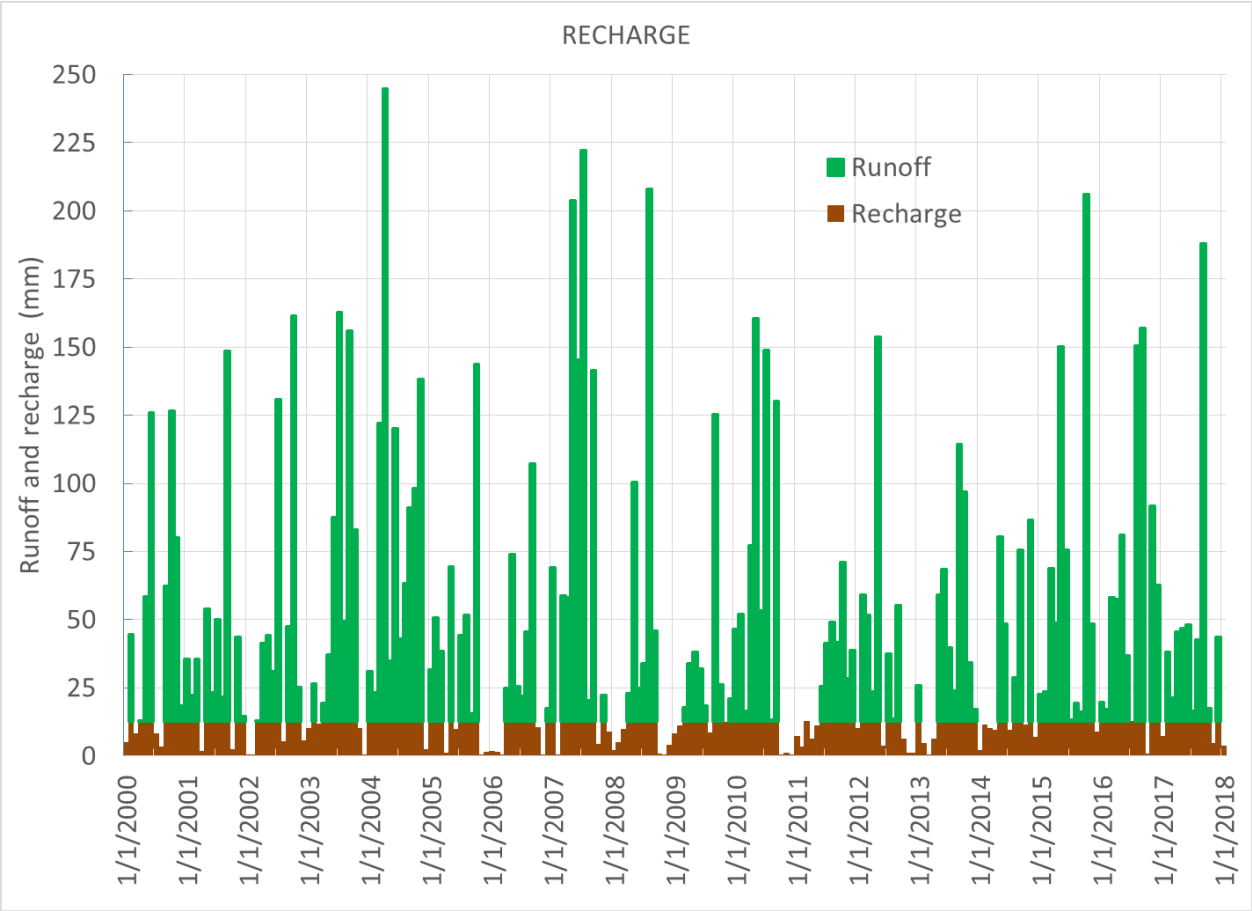

Figure 10. Comparison of monthly runoff and recharge. The values were obtained using monthly precipitation and the SCS-CN method.

A txt file was generated to input the recharge data into VMF with categories of “start day”, “end day” and “recharge” (Calculated with the SCS-CN method) on a monthly basis. The monthly recharge value was assumed to be representative for the entire APN aquifer area.

3.6 River Gages

The information was obtained from the International Water Boundary Commission webpage (IBWC) for four river gages (Figure 11), where discharge and stage were measured every fifteen minutes on real time. Only data for the last month previous to the data retrieval on each station were available. Furthermore, it was possible to download historical daily average discharge in m^3/s for the period 2000-2016. For 2017, values from 2002 (which were the most similar year in precipitation to 2017) were duplicated to complete the datasets.

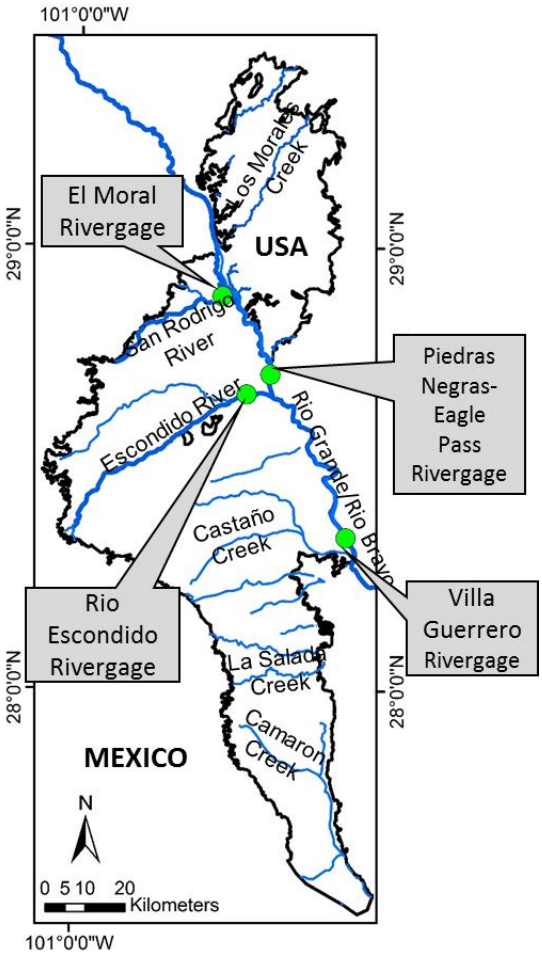

Figure 11. Location of available river gages and stream channels within the study area near the Rio Grande/Rio Bravo system.

The VMF river package accepts river stage as a specified head boundary but does not accept river discharge. Manning's equation (Equation 3) was used to calculate the stage along the channels from discharge interpolated between stations:

$$Q = \left(\frac{1.00}{n}\right) AR^{2/3}\sqrt{S} \qquad (SI) \qquad \text{Equation 3}$$

where Q is discharge, n is roughness coefficient, A is the flow area, R is the wetting perimeter and S is the channel slope.

A trapezoidal channel shape was chosen for the application of Manning's equation since this approximated the channel shape in most places the best (Figure 12). Equation 4 was used to calculate the stage (*a*)

$$Q = \left(\frac{1.00}{n}\right)\left(\frac{L+b}{2} * a\right)(C_1 + C_2 + b)^{2/3}\sqrt{S} \qquad (SI) \qquad \text{Equation 4}$$

where the channel bottom width (b) was assumed as constant and the bank zones (C_1, C_2, distance from bottom of the river to the water level on the river edge) as well as the channel surface width (L, distance from one shore to the next) changed depending on the stage (*a*, water elevation) calculated.

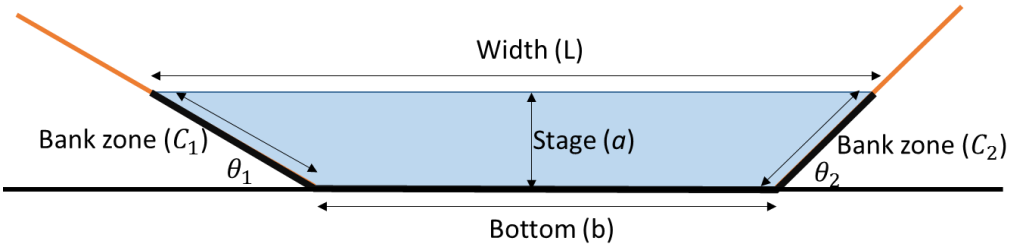

Figure 12. Simplified cross section used for river dimension estimations.

The values of roughness coefficient (n) and slope (S) for every river gage were calibrated using the datasets where stage and discharge were measured every fifteen

minutes. Next, the width of the channels (L) used in the calibration parameters of Manning's equation were obtained from river cross sections extracted from Google earth software in the river gages locations as seen in Figure 13. Then, the values of roughness coefficient (n), slope (S) and river bottom width (b) were substituted into Equation 4 to calculate stage (a) in a daily basis for the historic data.

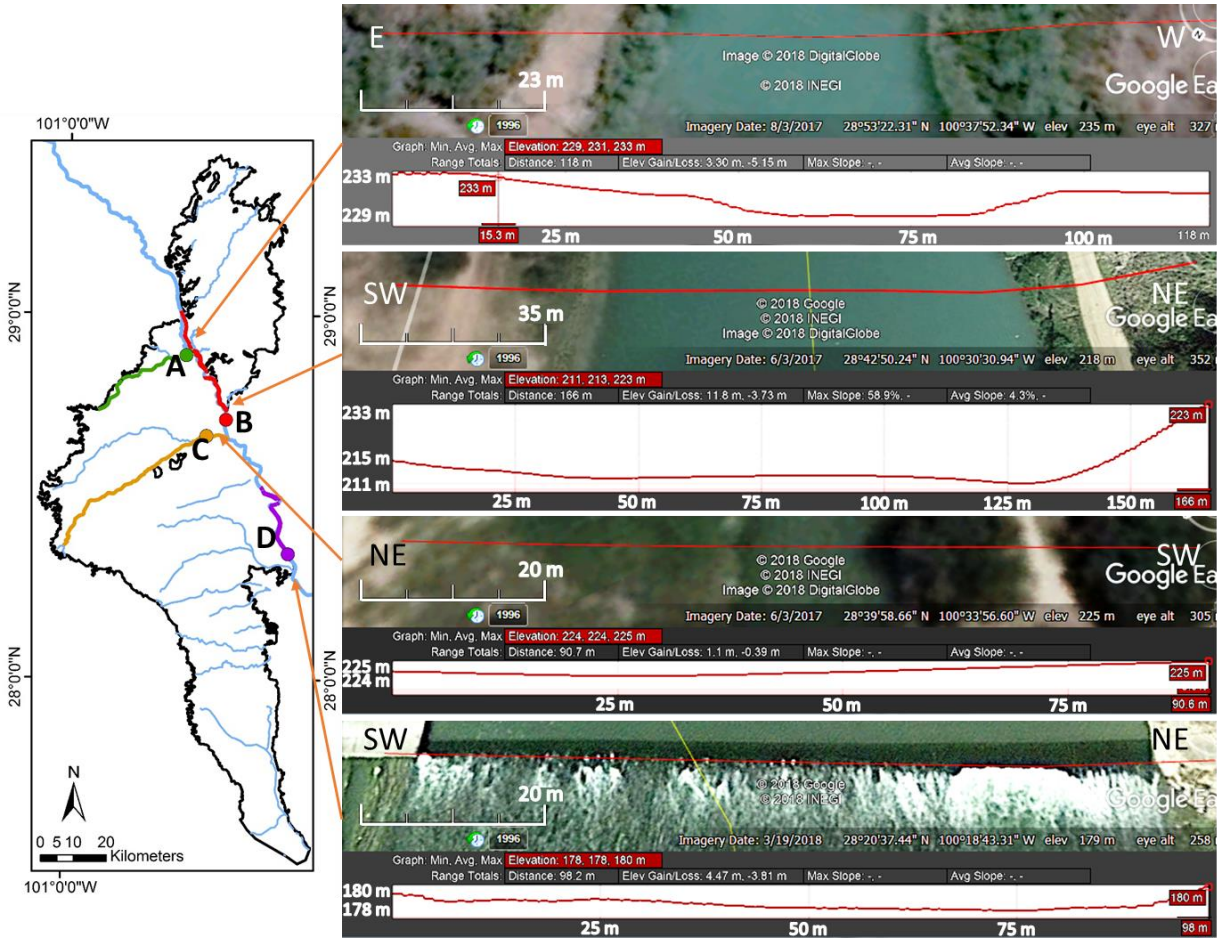

Figure 13. River cross sections. (A) El Moral, (B) Piedras Negras-Eagle Pass, (C) Rio Escondido, (D) El Indio-Villa Guerrero river gages. The different color indicates the segment that every river gage covered in the numerical model.

Rating curves were generated with the observed discharge versus the calculated stage (Figure 14). The high stage outliers were observed in between July 5, 2010 and July 7, 2010 and correspond to a storm event recorded by the rain gages during July 5, 2010 when the reported rainfall reached a maximum of 157 mm in one day.

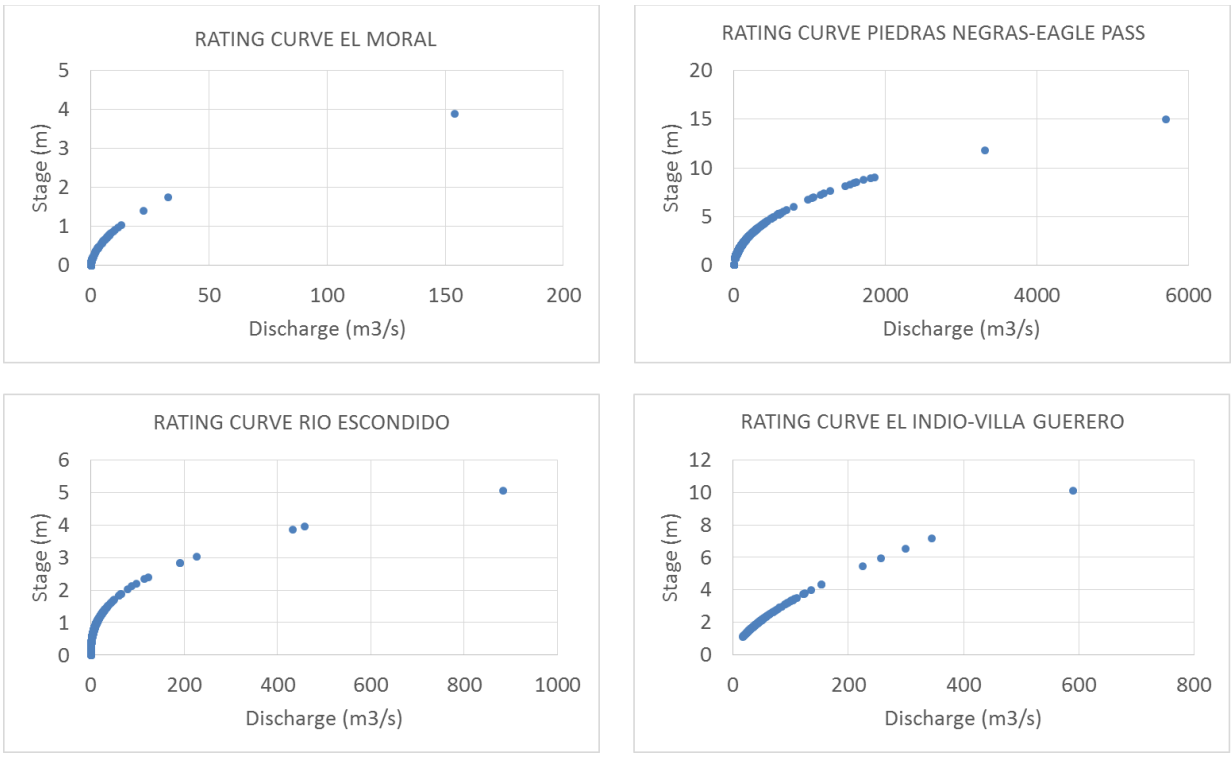

Figure 14. Rating curves for the available river gages. Datasets downloaded from IBWC (2018).

The data input into VMF was calculated by taking a monthly representative value for each river gage for the period 2000-2017. To choose the most representative monthly values, a statistical analysis was performed (Table 6). The data distribution were not normal due to a small number of very high river discharge which caused high

skewness values; in that case the recommendation was taking the median instead of the average discharge and stage values per month.

Table 6. Statistical analysis for river gages discharge in m3/s over the period 2000-2017. The daily discharge data was obtained from the IBWC website (IBWC, 2018) .

RIVER GAGE	VILLA GUERRERO	PIEDRAS NEGRAS-EAGLE PASS	EL MORAL	RIO ESCONDIDO
Mean	70.31	64.44	5.45	2.4
Standard Error	2.02	2.16	0.69	0.19
Median	43.4	40.4	0.34	0.83
Mode	28.1	0.46	0	0.06
Standard Deviation	134.07	142.99	45.85	15.18
Sample Variance	17974.82	20446.46	2102.46	230.43
Kurtosis	276.49	640.29	679.52	2076.26
Skewness	13.81	19.99	23.41	40.98
Range	3729.6	5699.78	1670	883
Minimum	10.4	0.22	0	0
Maximum	3740	5700	1670	883
Sum	308169	282452.7	23911.56	14929.49
Count	4383	4383	4383	6210
Confidence Interval (95.0%)	3.97	4.23	1.36	0.38

It is important to mention that one of the primary settings on VMF is the establishment of a grid, which will be used to perform all the required calculations and the generation of the numerical model. In this stage, it was necessary to define the cells of this grid that would include the rivers in future calculations. Furthermore, it was necessary to establish the cells where the rivers were located to prepare the txt file for the data input. The fields needed to log the information into the software were the following: row and column obtained from the grid (instead of x and y coordinates), layer where the river will be located (layer 1 or the upper layer of the model), start time and

stop time (in a monthly basis), stage, the bottom elevation of the river and conductance, which was calculated previously for each cell using the Equation 5:

$$\boldsymbol{Conductance} = \frac{\boldsymbol{L*W*K}}{\boldsymbol{T}} \qquad \text{Equation 5}$$

where L is the length of the river per cell (previously measured manually), W is the width of the river (obtained from google earth cross sections), K in this case is the riverbed hydraulic conductivity, which was assumed to be 0.2 m/d for silty sediments and T which is the riverbed thickness and was assumed to be 0.2 m due to the absence of data about dimensions of the river. Due to the lack of more detailed data, the same monthly river stage was used for the entire segment of the river, and not only for the river gage location (Figure 13).

3.7 Potentiometric Surface and initial conditions

The potentiometric surface for the model was generated from well information retrieved on September 1999 in the region between Allende, Nava and Piedras Negras in Mexico; US EPA provided 86 wells with water level observations used to simulate the initial conditions. This information had to be cleaned because there were several points with anomalous water depths; these wells were excluded from the generation of the interpolated map. The availability of well water levels in USA was very limited for the period 1999-2000. Only one observation well was found within the area of interest with available data during 2000. This information was downloaded from the TWDB webpage. Additionally, the water well information was used to generate an interpolation map with the potentiometric surface on the APN aquifer on January 1, 2000, which is assumed to be the initial condition, necessary to input in VMF. (Figure 15).

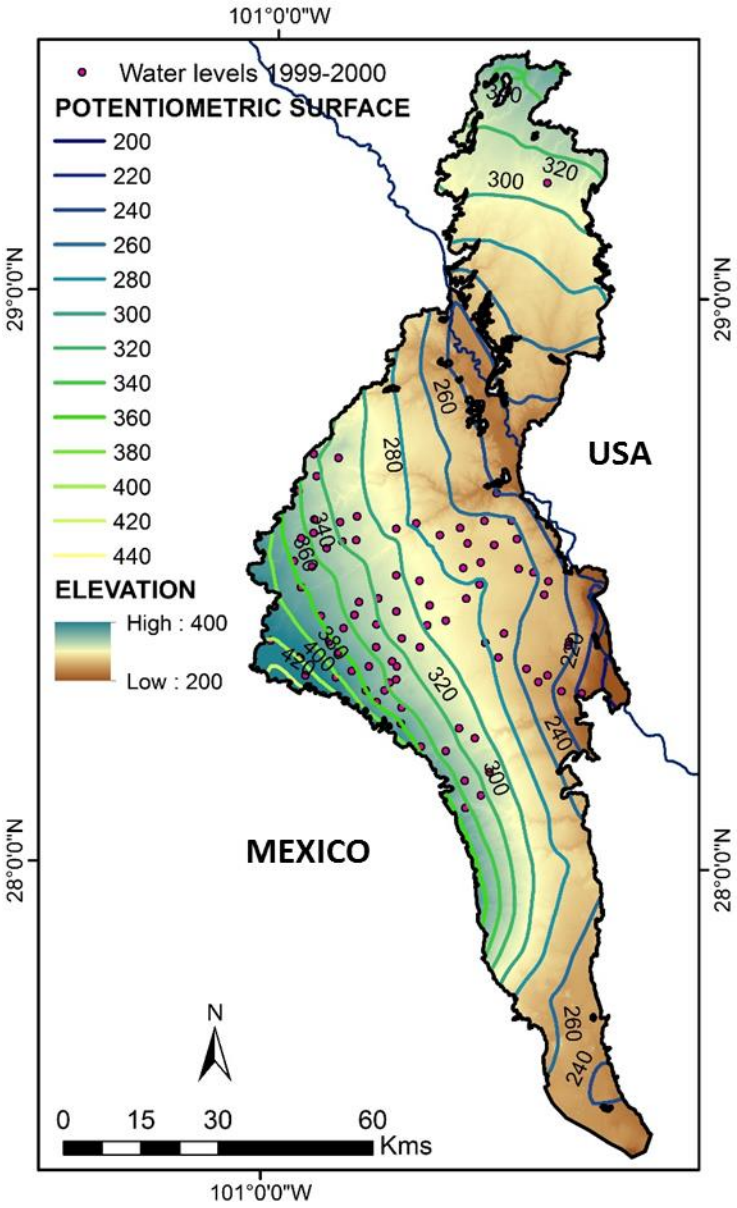

Figure 15. Potentiometric surface measured within wells screened in the APN aquifer during 1999-2000 and location of the water levels available in the study area.

3.8 Observation Wells

The observation wells were obtained from a database provided by private companies on Mexico as well as one observation well located on Texas available at the TWDB webpage for a total of 222 observation wells screened within the APN aquifer.

The water level observations recorded in Mexico were mostly from the years of 2006, 2008, 2011 and 2014, while the observation well located in Texas (USA) had twelve available water level measurements from 2000 to 2006. Furthermore, 170 observation wells have one or two water level measurements, and the remaining 52 have three or more water level measurements mostly on the years of 2008 and 2014 (Figure 16). These water levels were used during the calibration process, which is widely explained on section 4.2.

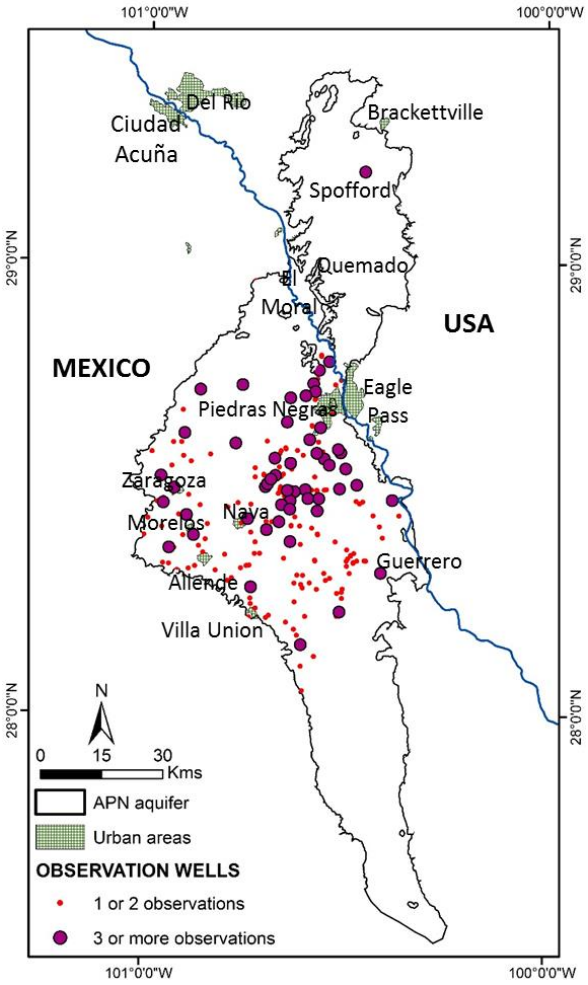

Figure 16. Observation wells distribution in the APN aquifer. The observation wells were used for calibration purposes, the water level measurements were taken from 2006 to 2014.

3.9 Pumping Wells

The water well information was obtained from REPDA, Lesser and associates, and Mexican private companies for the wells located in Mexico; the well information for the USA was downloaded from the TWDB website. Most of the pumping wells are located in Mexico (704 wells out of 799 wells), with 95 pumping wells located in USA.

Several pumping wells were reported as active but without available pumping rates. In this case a pumping rate of 50 m^3/d was assigned if the pumping rate was absent. Nine wells located in Mexico had reported pumping rates on anomalous amounts (greater than 5000 m^3/d); therefore, the pumping rate assigned was 3000 m^3/d (Figure 17). Most of the wells had low pumping rates (92% of the wells) and only 8% had rates over 750 m^3/d; however, the wells with the higher pumping rates are located in the Mexico side of the APN aquifer. Due to the lack of information about well screening, it was assumed that the entire well had screen casing.

The pumping schedules were arranged based on the comments section which were included by some institutions who managed the well information. These entities in charge of managing the wells explained the periods that the wells worked and included the data as a comment in the well; if there was no information available, the assumption was that the well was constantly pumping water at the assigned rate in their database.

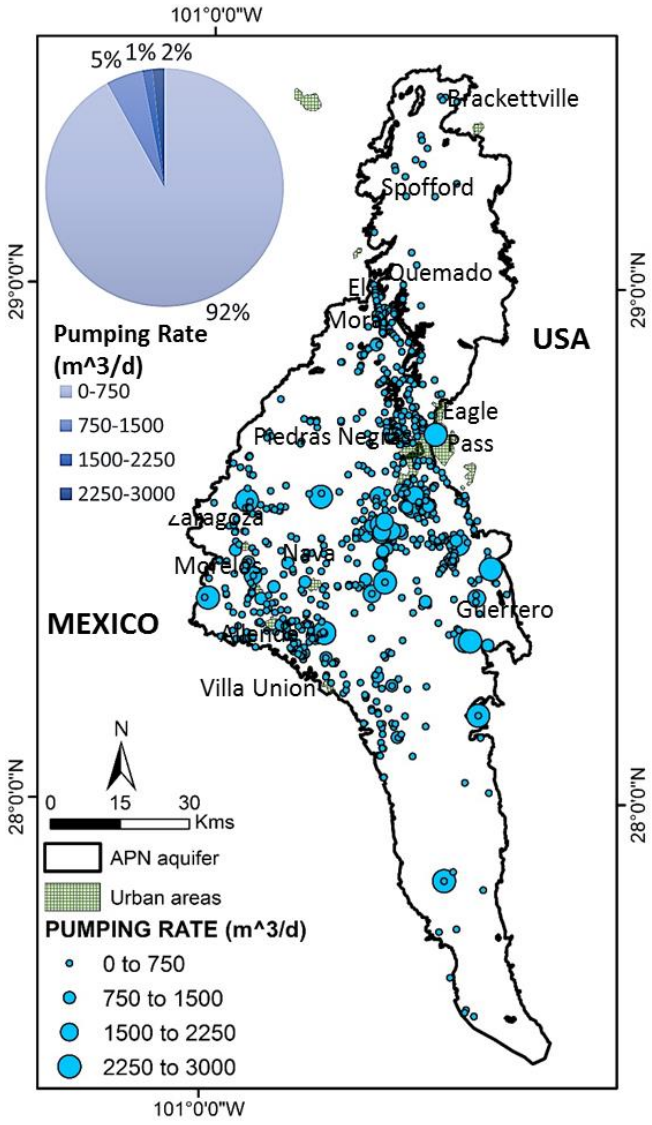

Figure 17. Available pumping wells in APN aquifer with extraction rates. According to the pie graph, most of the wells have rates below 750 m^3/d, and the greater pumping rates are from wells located on the Mexico side of the APN Aquifer.

3.10 Layer definition

One of the assumptions was that the aquifer was unconfined with only one layer of sediments which was homogenous and isotropic. To simulate the water flow below the hyporheic zone, it was necessary to divide the aquifer in two layers (Figure 18) to evaluate water flows moving across the border, and in and out of the Rio Grande/Rio

Bravo and variations of flow directions due to the effect of pumping wells in the surrounding areas of the river.

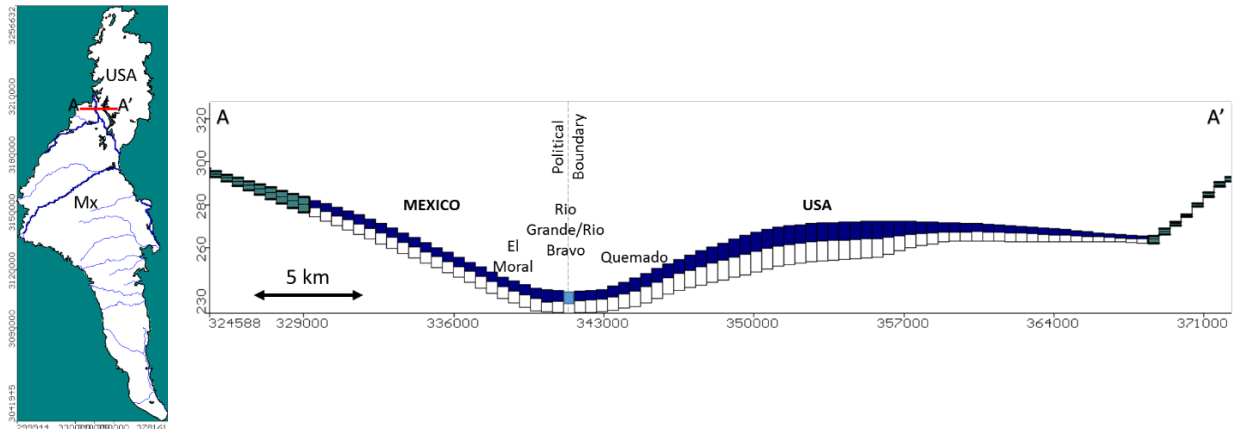

Figure 18. Cross section of the APN aquifer (Layer one in blue color, layer 2 on white color, inactive area as green cells).

The upper layer was adjusted to show the rivers only in the surface and not cutting through the aquifer, to represent the surface water interaction around the river, and restricting the lower layer exclusively to groundwater interactions below the Rio Grande/Rio Bravo system.

3.11 Hydraulic conductivity

Taken from previous studies made by Boghici (2002), the horizontal hydraulic conductivity (Kx) used to run the model ranges from 160 m/d to 430 m/d near the Quemado valley, on the Rio Grande/Rio Bravo. The Kx value used in the surrounding region of the Rio Grande/Rio Bravo was 160 m/d and the same value was also assigned to the surrounding areas of Rio Escondido and San Rodrigo Rivers.

Castillo Aguiñaga (2000) divided the aquifer in two layers with different K values obtained from pumping tests performed in 1996, wherein ranges of K were calculated

for the upper layer of 65 m/d to 128 m/d and 7 m/d to 91 m/d for the lower layer; in this study, the lowest values of 64 m/s for layer 1 and 7 m/s for layer 2 were selected as recommended by Hill and Tiedeman (2008), who found that the estimated hydraulic conductivities obtained from numerical models are often smaller than the measurements obtained from pumping tests because usually the packing material used on the casing has a higher hydraulic conductivity than the surrounding media. In the APN aquifer, a combination of the values from the previously mentioned authors was used as seen in Figure 19.

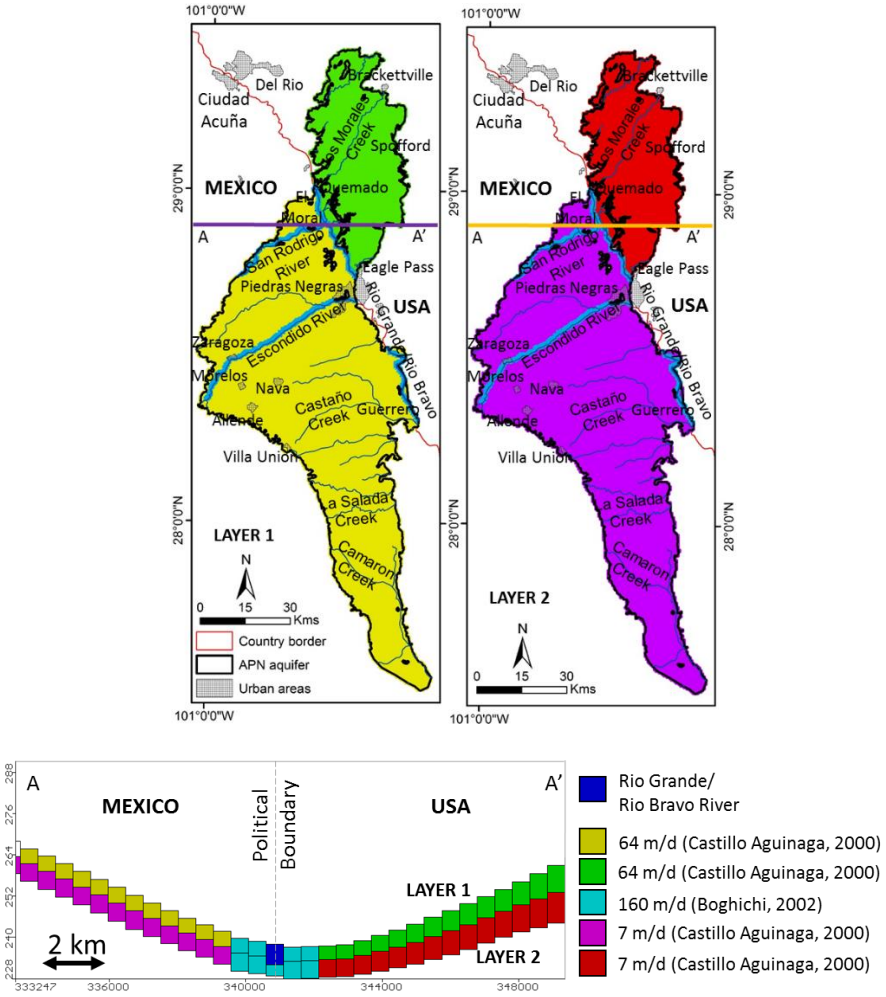

Figure 19. Hydraulic conductivity (Kx) areas in APN aquifer layers 1 and 2.

The hydraulic conductivity for VMF has to be defined in X, Y and Z direction; for this aquifer Kx = Ky = Kz*0.1 as recommended by Todd (1980) for alluvial deposits.

3.12 Specific yield (Sy), specific storage (Ss), total porosity and effective porosity

Boghici (2002) recommended a specific yield of 0.22, which is an average value typical of unconsolidated sandy materials like the APN aquifer. The specific storage for unconsolidated materials ranges from $4.9*10^{-4}$ m^{-1} to 10^{-3} m^{-1} according to Domenico and Mifflin (1965). CONAGUA (2014) reports a value of 0.001 m^{-} in the flat plains of the APN aquifer, which was the specific storage (Ss) selected for the numerical model. This falls on the upper end of the range given by Domenico and Mifflin for unconsolidated deposits, which is the assumption of lithology for the APN Aquifer.

Taking into account the value for specific yield of 0.22 in unconsolidated sands, the expected total porosity would be 0.25 (Heath, 1983). For the value of effective porosity, the same value of 0.25 assigned to total porosity was set in the model; this assumption of both porosities being equal is a common practice on numerical modeling for sandy aquifers (Zheng and Bennett, 2002)

3.13 Water Budget Areas

Three water budget areas were defined as seen in Figure 20. One area was defined for the Texas side (USA), one was defined for the Coahuila side (Mexico), and one for the Rio Grande/Rio Bravo with the aim of evaluating the water amount exchanges between the river and both regions of the aquifer.

Furthermore, to simulate pre-development conditions, a time step of 0.1 days near the start of the transient model simulation was included to evaluate the amounts of water flowing in and out of the aquifer. The pumping wells were set to start after the 0.1

days to make sure they would not have any influence on the pre development conditions.

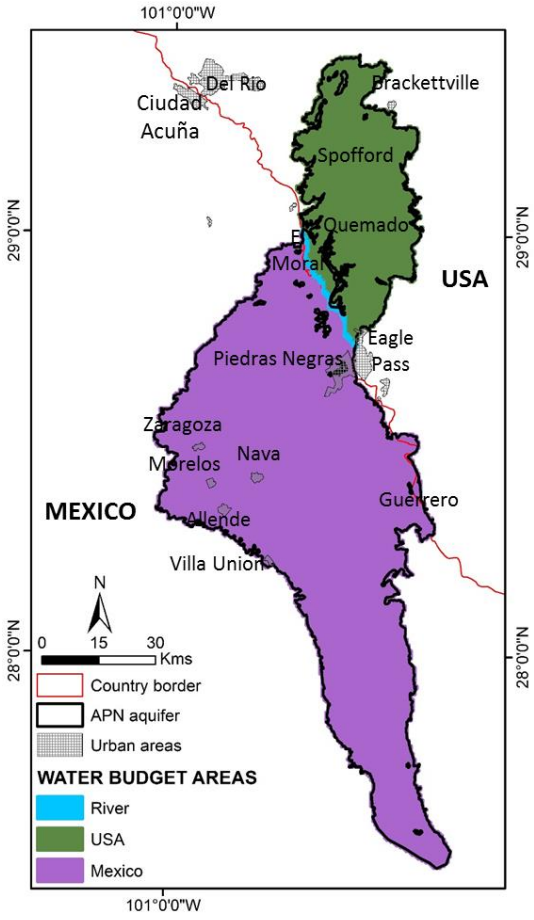

Figure 20. Water budget areas defined for the APN aquifer. Three areas were defined to evaluate the amounts of water flowing from and to the Rio Grande/Rio bravo, Mexico and USA.

4. GROUNDWATER MODEL OF ALLENDE-PIEDRAS NEGRAS AQUIFER

4.1 Numerical model

To achieve a better understanding of the APN aquifer as a groundwater system, a numerical model was created to represent the aquifer development. This model was the focus of this research and also is the foundation of further groundwater modeling projects in the surrounding areas of the USA – Mexico border. The model was developed using Visual MODFLOW classic interface, a software distributed by Waterloo Hydrogeologic.

The transient flow option was selected to run the model creating a time dependent solution. In this mode the model runs for several data inputs at different times, the software generates smaller portions of time known as time steps, which in the case of the APN numerical model is every 28-31 days depending on the month for a total of 216 time steps. The model was set to calculate for 17 years or 6575 days. On every time step, the recharge, ET, pumping conditions are different, and the software simulates changes of head for every time step under varying conditions.

The selection of the solver to run the numerical model was based on the comparisons of the accumulated mass balance at the end of the simulation as suggested by Kumar (2015). The Preconditioned conjugate-gradient (PCG) solver calculated an accumulated discrepancy of -4.93% compared to a discrepancy of -3.67% obtained after using the solver for Visual MODFLOW (WHS). The WHS solver showed a lower cumulative discrepancy and was selected to run the numerical model.

4.2 Calibration

One initial PEST calibration (Parameter Estimation Simulation) was performed using one observation well from Texas. Every time that a parameter is calibrated, the model is ran again to proceed to the next calibration parameter. During this first PEST calibration, Kx was designated as the primary calibration parameter. Recharge and specific storage were designated as secondary calibration parameters. The most influential parameter over the calculated water table in order of fitting the observation well was the recharge, which was modified with a multiplier of 0.66 (calculated with PEST). The next parameter that caused significant changes in the water table was the specific storage (Ss), which was set at a value of 0.001 before starting the calibration. After the calibration with PEST, the value obtained for storage was 0.0015 which gave more accurate water levels when compared to the measurements from the observation wells.

The hydraulic conductivity (Kx) was set with an initial value of 250 m/d over the whole area but, after a PEST calibration, Kx decreased substantially to approximately 7 m/d. A sensitivity analysis was done with similar values to the obtained after the PEST calibration, and the calculated heads did not have important variations unless hydraulic conductivity values spanning several magnitudes of difference were used; these Kx values were not applied because they were out of normal ranges for gravels and sands (1-1000 m/d from Bouwer (1978)). Finally, the hydraulic conductivity values were set as explained in section 3.11, choosing the lowest hydraulic conductivities reported by Boghici (2002) and Castillo Aguiñaga (2000).

The results from model calibration with observed water levels in wells versus calculated water levels in wells are described in Figure 21; the calibration times selected were the time steps when the observations were measured in the field or the closest time step with available water levels from observation wells. The heads reported for the 222 observation wells were compared to the calculated water levels for each time step (month), obtaining at a 95% confidence interval a standard error of the estimate from 0.358 to 0.384 m, a root mean squared ranging from 5.354 to 5.754 m and a correlation coefficient of 0.99 which are good indicators of an efficient calibration process.

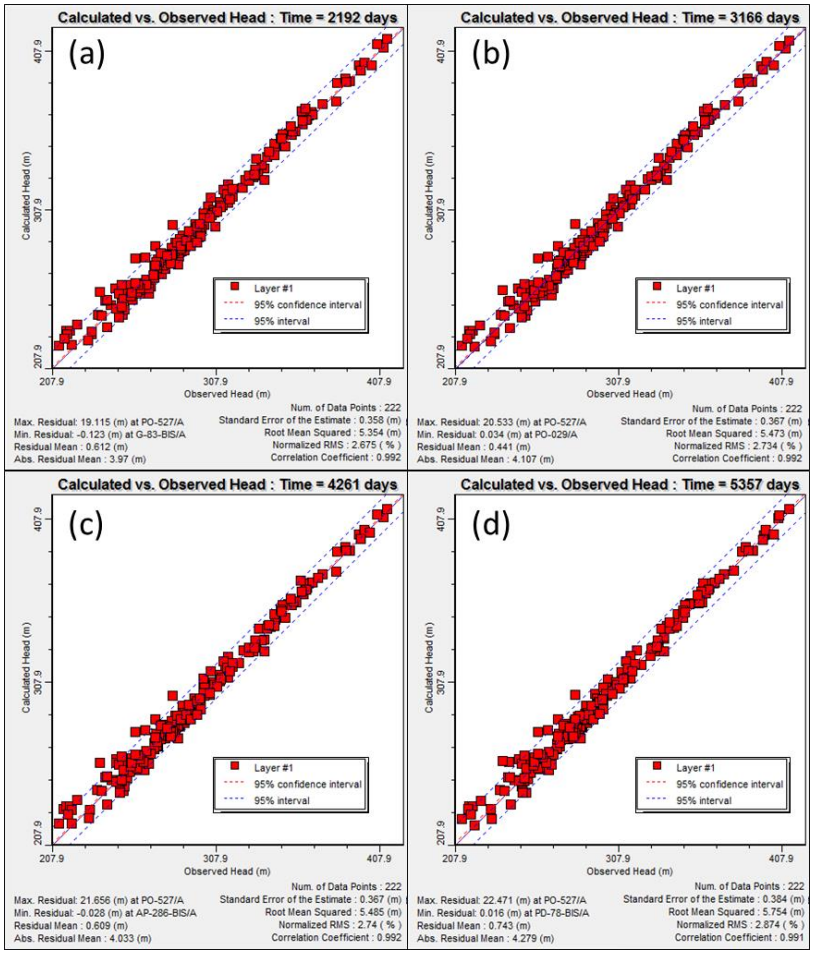

Figure 21. Model calibration correlation graphs for the years with available water levels. (a)2006, (b)2008, (c)2011, (d)2014.

4.3 Description of conceptual model

Visual MODFLOW Classic Interface was used to generate a numerical groundwater flow model to evaluate flow patterns in the APN aquifer, while focusing in the Rio Grande/Rio Bravo system and surrounding areas. The dimensions of the study area is 218 km long, 76 km wide and covers the entire APN aquifer. The grid size was set to 500x500 m with 436 rows and 152 columns as seen in Figure 22.

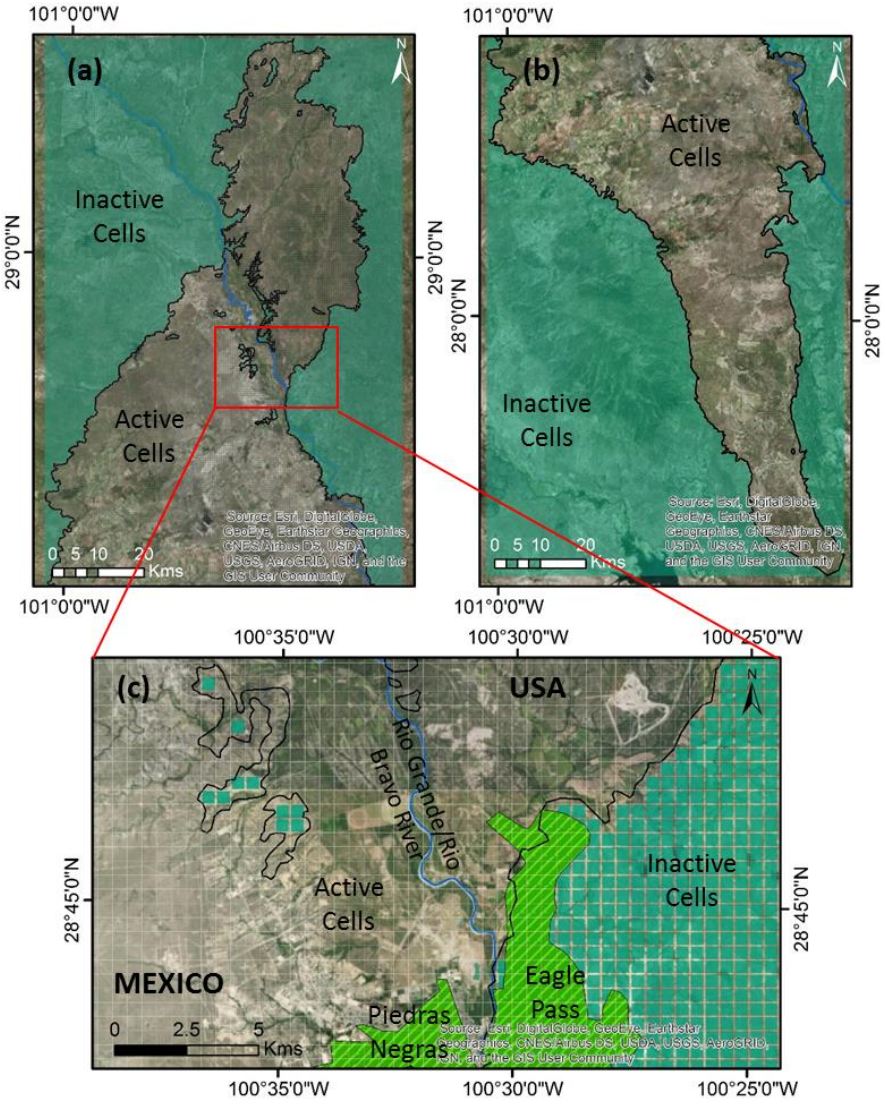

Figure 22. View of the APN aquifer grid (a)Northern region, (b)Southern region, (c) detailed view.

The aquifer thickness varies from 1 to 40 m and was divided in two layers with the aim of properly representing the river location described in section 3.10 and the hydraulic parameters described in section 3.11. The main sources of recharge to the APN aquifer comes from precipitation and runoff captured by streams and the infiltration from rivers with perennial flow; however, there were areas in the aquifer where the water level increases over time even during dry periods (low recharge) and without the influence of perennial rivers and streams. These increments could be an indicator of cross-formational flow from the Cretaceous formations underlying the APN aquifer as suggested by Boghici (2002) and Grupo Modelo (2011). This particular observation will be deeply discussed on Section 5.

The discharge points within the APN aquifer are the pumping wells used in irrigation and public supply, ET and most of the rivers. The Rio Grande/Rio Bravo is mostly a gaining river in the APN aquifer, which means that the aquifer discharges water into the river in the region near Quemado, Texas and El Moral, Coahuila. However, in the area located to the north of Piedras Negras, Coahuila, and Eagle Pass, Texas, the direction of flow is reversed and the Rio Grande/Rio Bravo recharges the aquifer. This reversal occurs mostly due to the high density of pumping wells between Piedras Negras and Villa Union (Coahuila), which contributes to the water table depletion in the area and a consequent water infiltration from the Rio Grande/Rio Bravo. Another loss of water in the APN aquifer is caused by evapotranspiration, which is expected due to the arid to semiarid climate conditions in the area. This process reduces the potential water volumes infiltrating into the aquifer. The Figure 23 shows the conceptual model of the APN aquifer including the Texas and Coahuila sides.

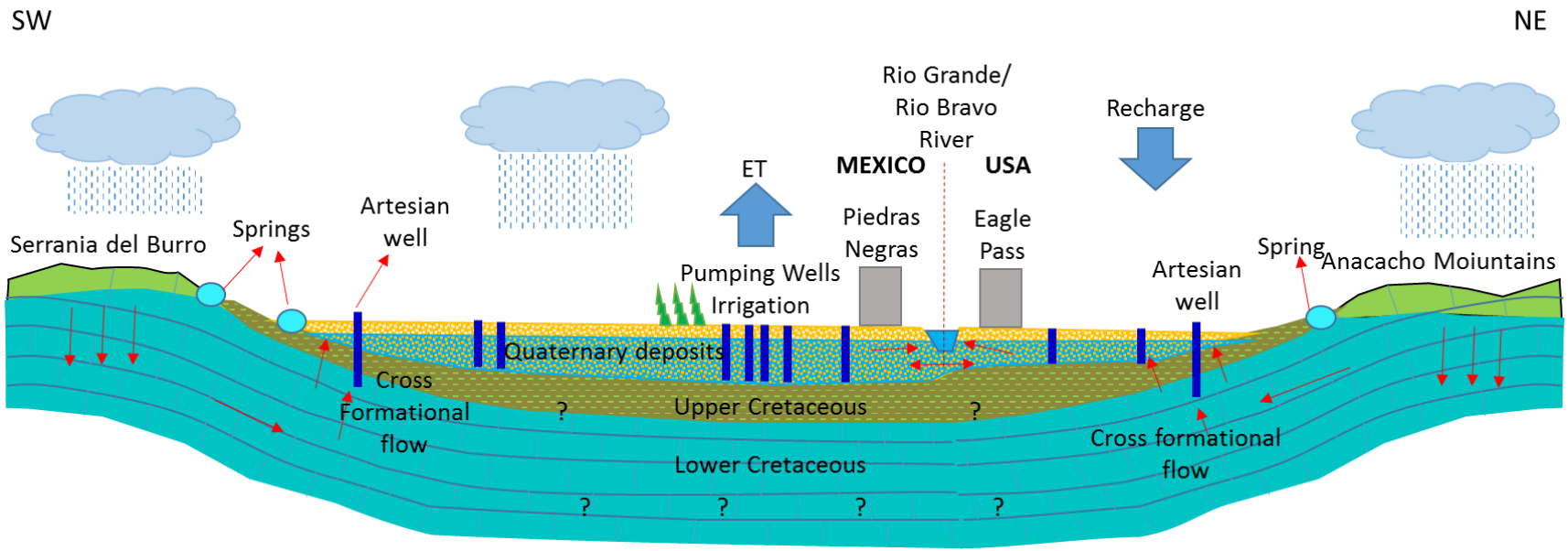

Figure 23. Hydrogeological conceptual model of the APN aquifer.

5. RESULTS AND DISCUSSION

One of the major findings according to the model of the APN aquifer during the period between 2000 and 2017 was the depletion of the water availability over time. The second major finding is that the water convergence zone is expected to be found below the hyporheic zone of the Rio Grande/Rio Bravo under predevelopment conditions; but that the water convergence zone has shifted under the influence of pumping from wells located near the riparian zones on both sides of the border. Third, this condition has also driven water loss from the river to the aquifer showing variations in the calculations of the water budget, where most of the groundwater discharged into the Rio Grande/Rio Bravo comes from Mexico instead of being an equal proportion from each country. Also the annual volume of surface water from the Rio Grande/Rio Bravo that enters the aquifer is greater on the USA portion of the APN aquifer.

5.1 Potentiometric surfaces and water level evolution

The pre-development potentiometric surface was generated from water table readings taken in September 1999 by Comision Nacional del Agua (CNA) and by US EPA, and then the water levels were interpolated using the Kriging method. Due to the lack of detailed water levels around 2000 for the Mexico side, the obtained potentiometric surface for 1999 was assumed to simulate the initial conditions of the area. Most of the well data available covers Mexico and only one observation well was located in the USA.

The pre-development potentiometric surface follows the topographic slope, and the water flows from the high terrains in Serrania del Burro and Lomerio Peyotes to the flat

lands between El Moral, Piedras Negras, and Guerrero and later into the Rio Grande/ Rio Bravo valley following a general trend from the Southwest to the Northeast in the Mexico side. On the US side, the water flows downslope from the Anacacho Mountains into the Rio Bravo Rio Grande/ Rio Bravo valley in a North-South direction (Figure 24). The emulation of the water flow patterns to the topography in the APN aquifer is an indicator of an unconfined aquifer type.

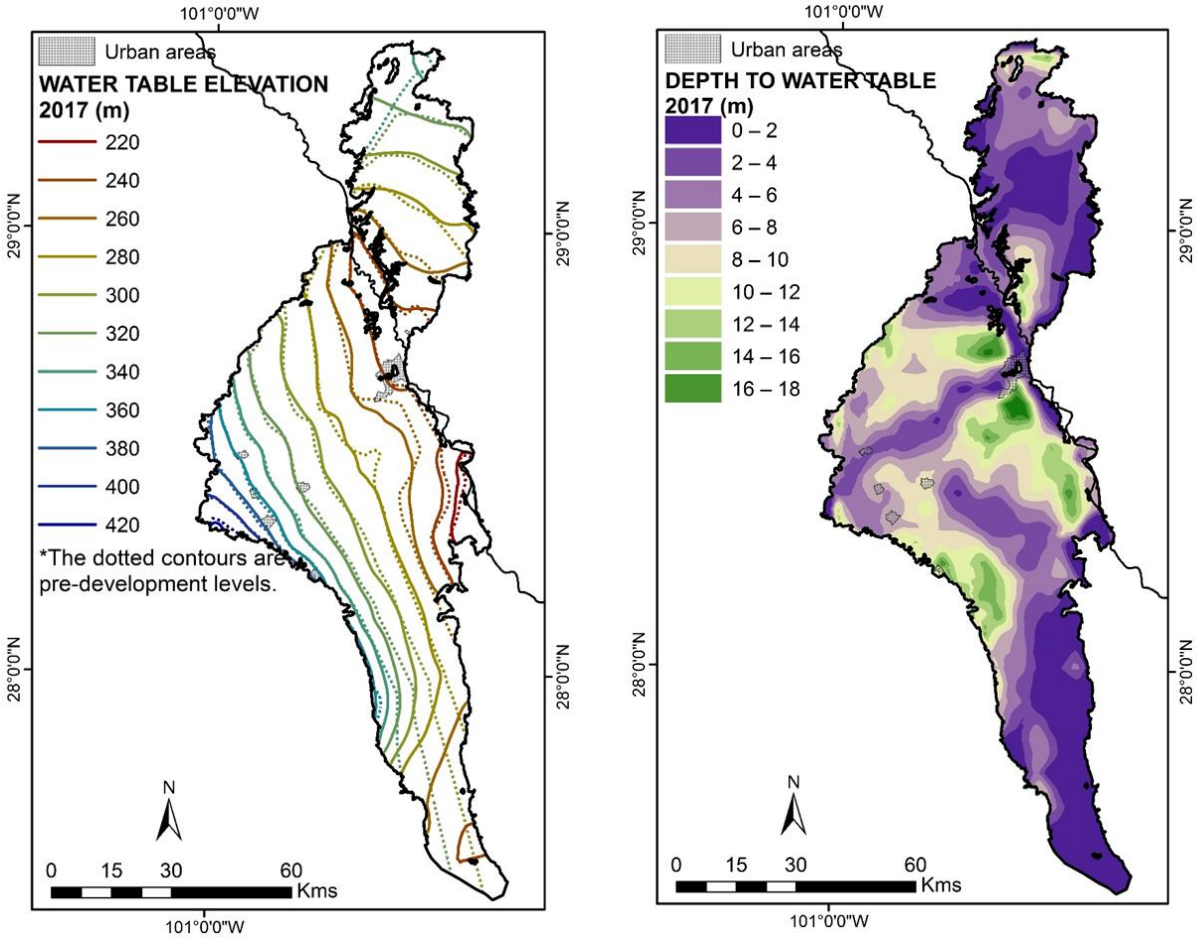

Figure 24. Potentiometric surface and water table depth on December 2017. The dotted contours on the Water Table Elevation map represent pre development levels, while the continuous contours represent the water table at the end of the simulation on December 2017.

The potentiometric surface shows a change of the water levels when compared with the pre-development conditions; with respect of the terrain, this change resembles a reversal on the water flows as shown in Figure 24. This change in water levels is related to the higher outflow in the APN aquifer, which cannot be recovered by the inflow entrances; this depletion has been estimated for the entire aquifer in 0.76 m for 17 years. Additionally, the depth to the water table reflects the areas where the pumping has been substantial in the area between Piedras Negras and Villa Union in the Mexico side, and a consequent local depletion is observed as seen in Figure 24.

After comparing the accumulated average drawdown at the end of each year from 2000 to 2017, the water levels are generally decreasing with an averaged water table depletion of 0.76 m in 17 years, and approximately 0.04 m per year; however, due to a high spatial variability of the water table depletion, there are maximum drawdowns of 17.24 m. There are some local regions where the water table recovered mainly due to cessation of pumping and water infiltration from streams, such as the region between the cities of Allende and Piedras Negras. The area located at the south of Piedras Negras has suffered a strong local depletion of 14.8 m due to the great amount of water wells operating in the area (Figure 25).

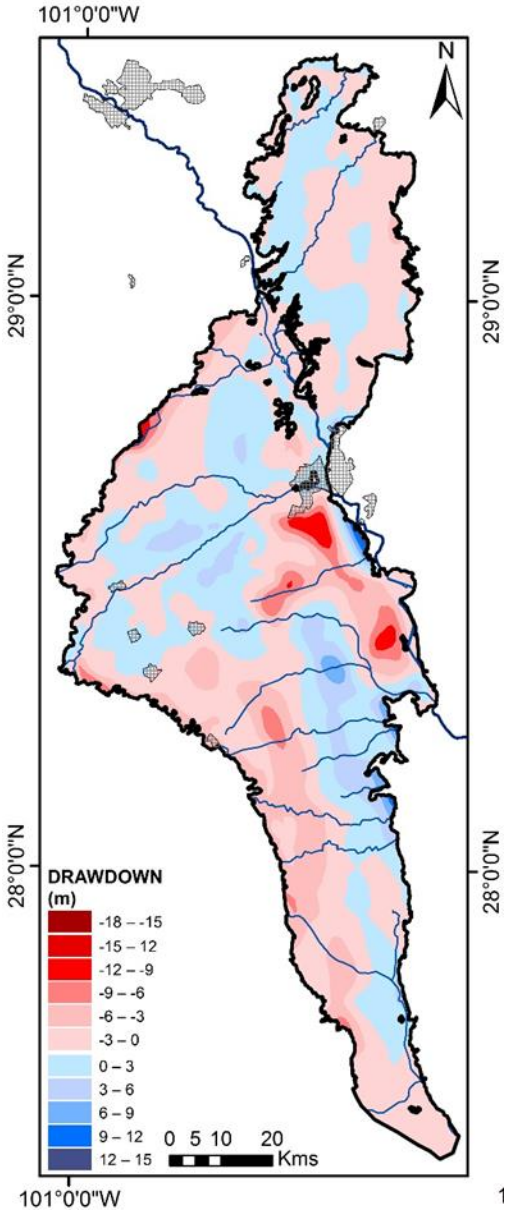

Figure 25. Total modeled drawdown for December 2017.

The fastest drawdown rate was calculated on 2011, with a depletions of 0.063 m per year because the rainfall was limited over the first six months of 2011 (Figure 7). The depletion was minimal on 2010, with only 0.015 m at the end of the year due to extraordinary rainfall events during April, June and July 2010. The predominant trend of the water table has been a regional reduction over time as seen in Figure 26.

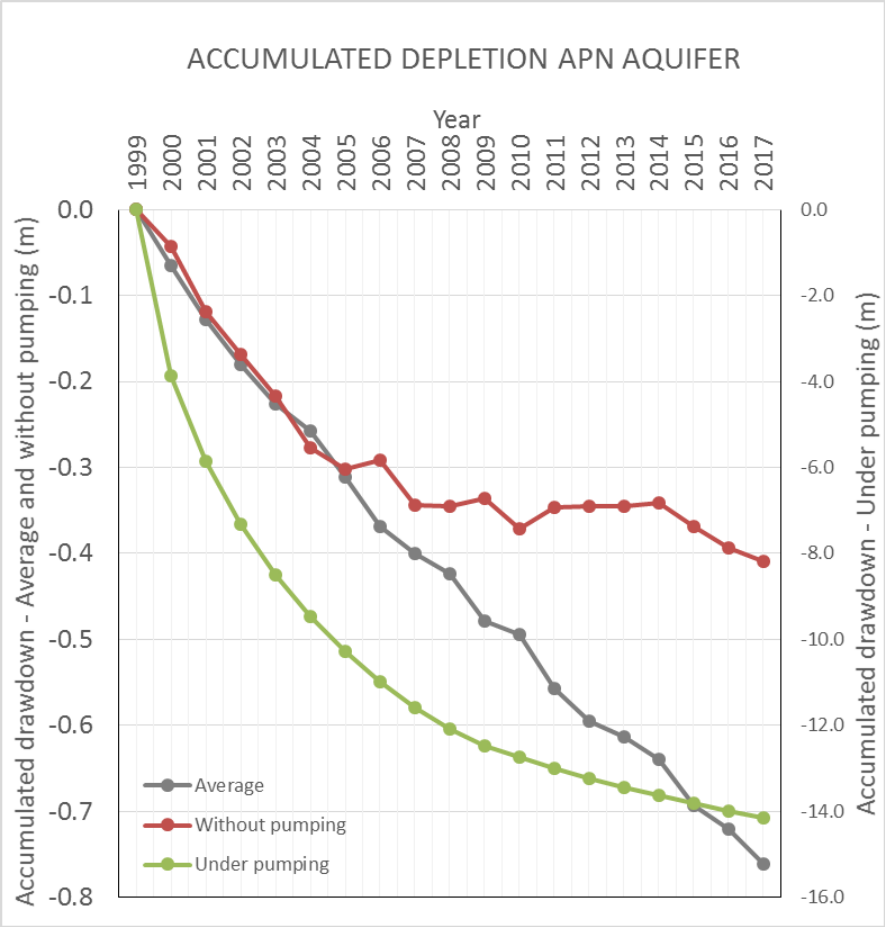

Figure 26. Accumulated average depletion per year. The average for the entire aquifer was plotted together with the drawdown of a region without pumping wells and a region with significant drawdown due to extreme pumping.

The plot includes also an accumulated drawdown form an area located at the north of Eagle Pass, where there are no pumping wells nearby, and the accumulated drawdown reached 0.4 m in 17 years. On the other side, an area located on the south of Piedras Negras was selected, where there is a high density of pumping wells, and the accumulated drawdown reached 14.2 m in the total period simulation of 17 years. It is also noticeable the curved trend of the drawdown for the southern Piedras Negras region, which could be a result of the strong influence of the pumping regimes over the water table.

5.2 Groundwater and surface water interactions

Due to the important spatial variability of the water table, the monthly water table levels for the APN aquifer were extracted from the numerical model by selecting an area where there were no pumping wells that could affect the water table calculations, the area selected is located on the north of Eagle Pass (USA); this was made with the aim of performing comparisons with parameters such as precipitation and river stage. The monthly water table level was detrended by differencing from one linear model fitting, and three nonlinear model fittings (polynomials of 2nd and 4th order) as seen in Figure 27. The structures of the polynomial fittings were chosen by observations of the best fitting equations using the software Excel, calculating the predicted value and detrending by subtracting the predicted value from the observed value; this process was repeated with one polynomial fitting of 4th order and two polynomial fittings of 2nd order (Figure 27).

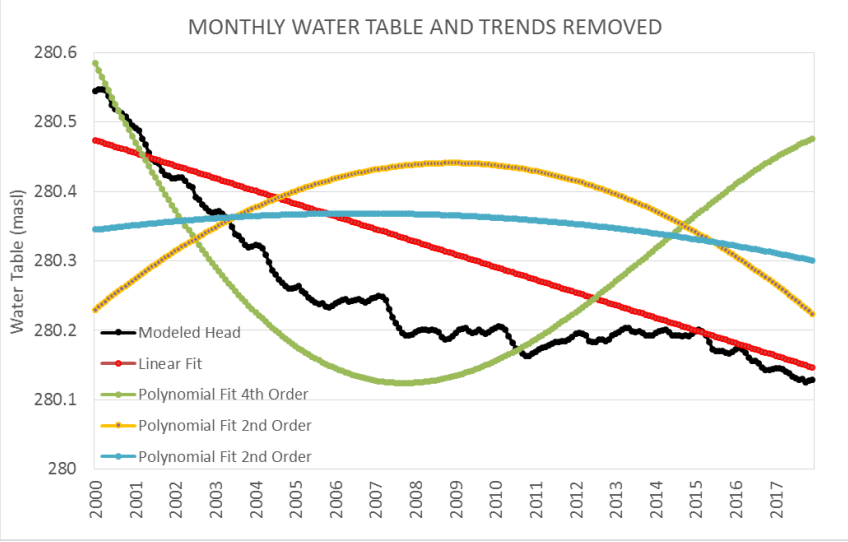

Figure 27. Monthly water level table and trends removed (Linear trend, red line; polynomial trend 4th order, green line; Polynomial fits 2nd order, yellow and blue lines)

After detrending the water table dataset, the water table was normalized and plotted together with the normalized monthly precipitation and normalized river stage datasets to evaluate possible relationships among them (Figure 28)

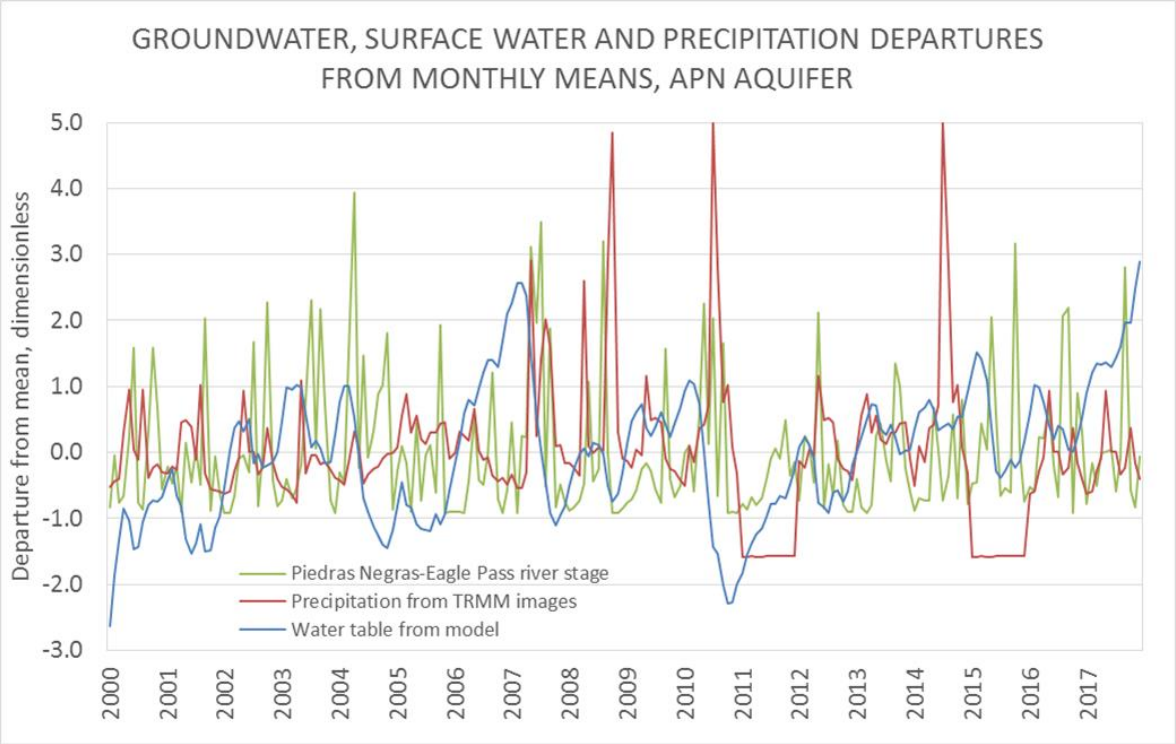

Figure 28. Normalized precipitation, river stage (Rio Grande/Rio Bravo) and detrended – normalized water table in the APN aquifer.

While there is not an evident correlation of the data according to Figure 28, an increase in the water table is related to a rise in river stage on 2003, 2004, 2007, 2008 and 2009. During the years of 2007, 2008 and 2010 the water table increment seems to be related to precipitation when high precipitation events occurred repeatedly for several months such as 2007 and 2010, where there were three consecutive rainy months. When an exceptional storm event had place, but the consecutive months did

not have repeated rainfall events, the water table was not affected as seen in years 2002 and 2015. A correlation test was performed for the water table, precipitation and the river gage to determine the strongest and the weakest correlations between the variables (Table 7).

Table 7. Correlation coefficients for normalized water table, precipitation and river stage datasets.

	Normalized Water Table	Normalized Precipitation	Normalized River Stage
Normalized Water Table	1	-	-
Normalized Precipitation	0.027	1	-
Normalized River Stage	-0.069	0.115	1

.

In general, weak to negligible correlations were found between the water table versus precipitation, the water table versus the river stage, and the river stage versus precipitation. The lack of correlation between synoptically occurring rain and water level fluctuations does not necessarily mean there is no relationship. Delays between rainfall events and water table changes would be expected to lower the correlation strength. In the case of precipitation, the spatial variability of rainfall amounts makes difficult to establish a relationship with the river stage. In order of evaluating this lag time within the occurrence of a rainy month and the implications over the water table and the river levels, cross correlation analysis were performed. The plots for cross correlation were generated using the software R and de code is included in Appendix A.

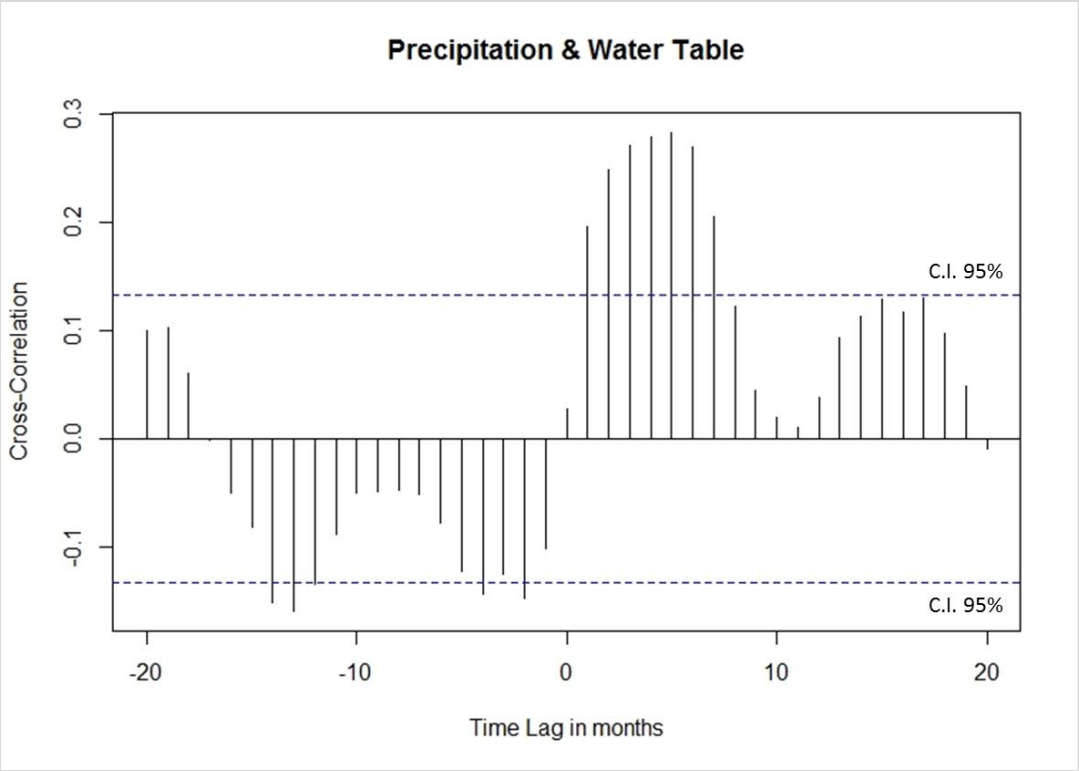

Figure 29. Cross correlation between precipitation and water table level at different time lags. The positive cross correlation means that, if precipitation increases, the water table will increase too. The positive time lag means that the increment in the water table will occur mostly on the first five months after the rainy season.

The cross correlation diagram for precipitation and water table shows a positive relationship with a positive time lag (Figure 29), which is an indicator that the precipitation does not affect immediately the water table but starts reaching it after one month of occurring the precipitation, with a dominant cross correlation at six months. One of the reasons would be that the water from precipitation takes a significant time, even months to reach the water table in the unsaturated zone (Larocque et al., 1998), which could be known by analyzing the residence time through isotope analysis.

A strong positive relationship between the water table and the river stage, with a negative time lag from five months to one month in the cross correlation plot (Figure

30), indicates that the river stage increases and as a consequence the water table increases. This response could be related to the saturation of the riparian zones due to the river action, which result in a groundwater recharge in the nearest areas of the Rio Grande/ Rio Bravo. In this case, this behavior is typical of a losing river, which would be consistent with the findings on the surrounding areas of Piedras Negras and Eagle Pass, where the extensive pumping has affected the water table but mostly the river levels in this region of the APN Aquifer; this change on the flowpaths of the aquifer and the river will be explained in detail on section 5.5.

However, an important negative cross correlation between the water table and the river stage with a positive time lag is also noticeable in figure 30; this trend suggests that the head in the aquifer decreases because the water flows downslope from the aquifer and later the river stage increases because the groundwater reaches the river with a time span of three months, which would be a characteristic feature of a gaining river. This finding also corroborates the suggestion made by Boghici (2002) where several streams as well as the Rio Grande/Rio Bravo were gaining rivers.

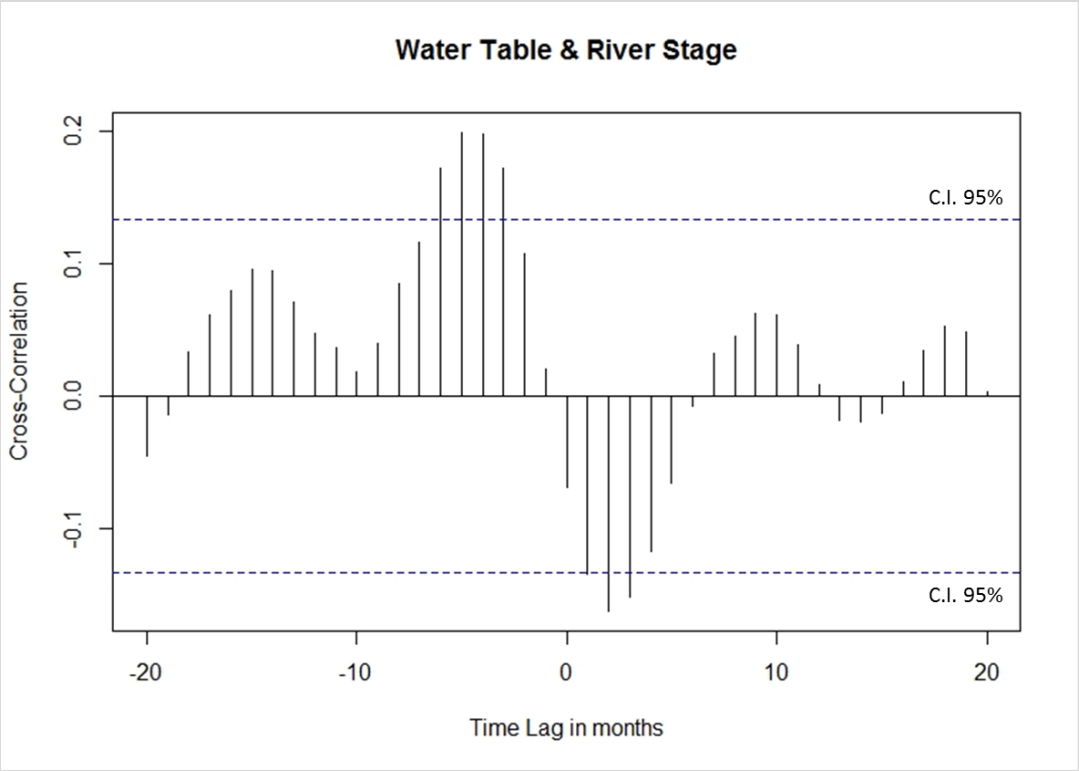

Figure 30. Cross correlation between Piedras Negras-Eagle Pass river gage and water table.

A limitation on the comparisons performed above is time scale, which has been set in months for the entire numerical modeling; therefore, it could be expected that the cross-correlation would be significant and more consistent if the time scale is modified to days. The lack of information from observation wells with long term data, time resolution, and proper location near the Rio Grande/Rio Bravo makes difficult to perform a robust analysis of the water table and its relationships with corresponding variables, such as precipitation and river gages.

5.3 Drought impact

The United States drought monitor was used to identify the worst droughts from 2000 to 2017 and evaluate the water table response on the driest periods reported by

robust monitors. The US drought monitor is obtained from a compilation of several drought indexes indicators taken from different models, such as the standardized precipitation index and the palmer drought severity index amongst others. It is generated by the National Drought Mitigation Center (NDMC), the U.S. Department of Agriculture (USDA) and the National Oceanic and Atmospheric Association (NOAA) (Svoboda et al., 2002). The detailed drought monitor outputs for Texas were used to identify the driest months for the Southeast Texas, which is the area where the APN aquifer is located. Figure 31 shows the selected months with highest droughts reported.

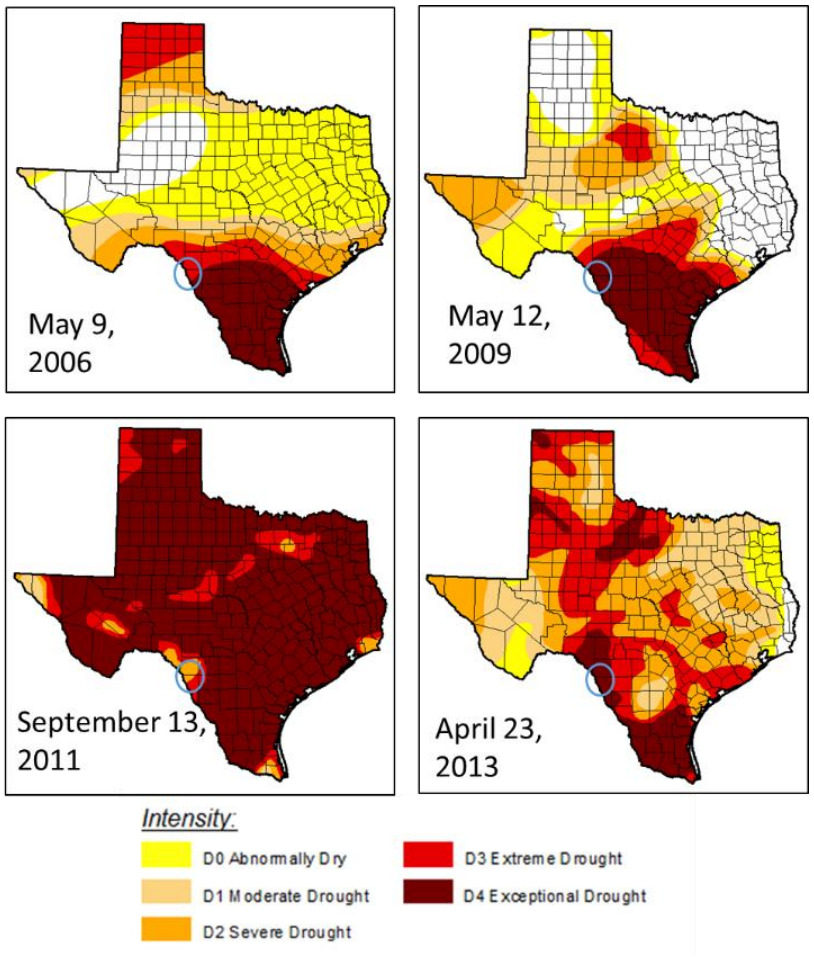

Figure 31. Drought monitors for selected extreme droughts in South Texas (Modified from Svoboda et. al, 2002). The APN aquifer is marked in blue.

According to the drought monitor, Maverick and Kinney counties were not under any drought anomaly on December 2000 and also was one of the periods were the active pumping wells in the APN aquifer were minimal. Depth to the water tables were compared for the periods of December 2000 and September 2011 to evaluate the effects of exceptional droughts over the water table for the APN aquifer (Figure 32).

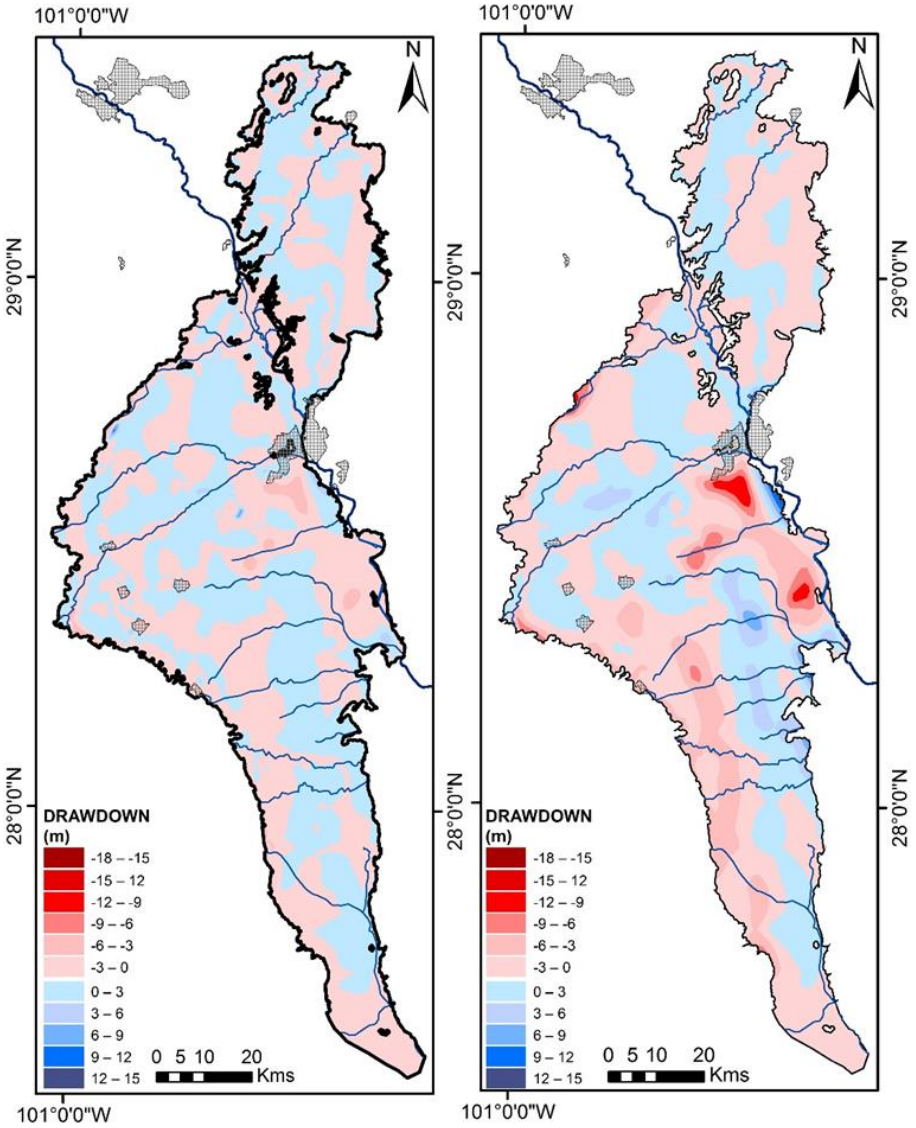

Figure 32. Selected periods for water table depth during a typical wet month versus a dry month (December 2000 on the left and September 2011 on the right).

Most of the water table depth changes were observed at a local scale, where the excessive pumping has caused the depletion of the water table between the regions of Piedras Negras and Guerrero reaching depths close to 20 m. The depletion seen at the on the region between Allende and La Union is probably a consequence of less recharge instead of water extraction, because the wells located in the area are minimal; however, another cause would be the cross formational flow moving from the upper Quarternary rocks into the older Cretaceous rocks. For now, there is not enough information to determine the cause of the depletion in the southwest of the aquifer. The drawdown history was also reported by CONAGUA (2014) as a response of a severe drought that started on 2008 but worsened on 2011.

5.4 Cross formational flow

A comparison of the periods with the lowest recharge rates and lower river stages was performed to select the driest months during the modeled period. The heads for the periods selected (January 2002 and November 2012) were subtracted from the initial heads to locate areas where even after critical dry periods, the water table increases. This recovery of the water table is not a result of natural surficial or anthropogenic phenomena as rivers or injection wells. Regions near the Anacacho Mountains, Serrania Del Burro and Lomerio Peyotes showed this local water table increase which could be an indicator of cross formational flow. The region between Guerrero and Villa Union also shows extreme water level increases on 2012 which cannot be associated to the influence of Castaño Creek due to its low water discharge (2 m^3/s). The areas where this phenomena occurred were marked in Figure 33.

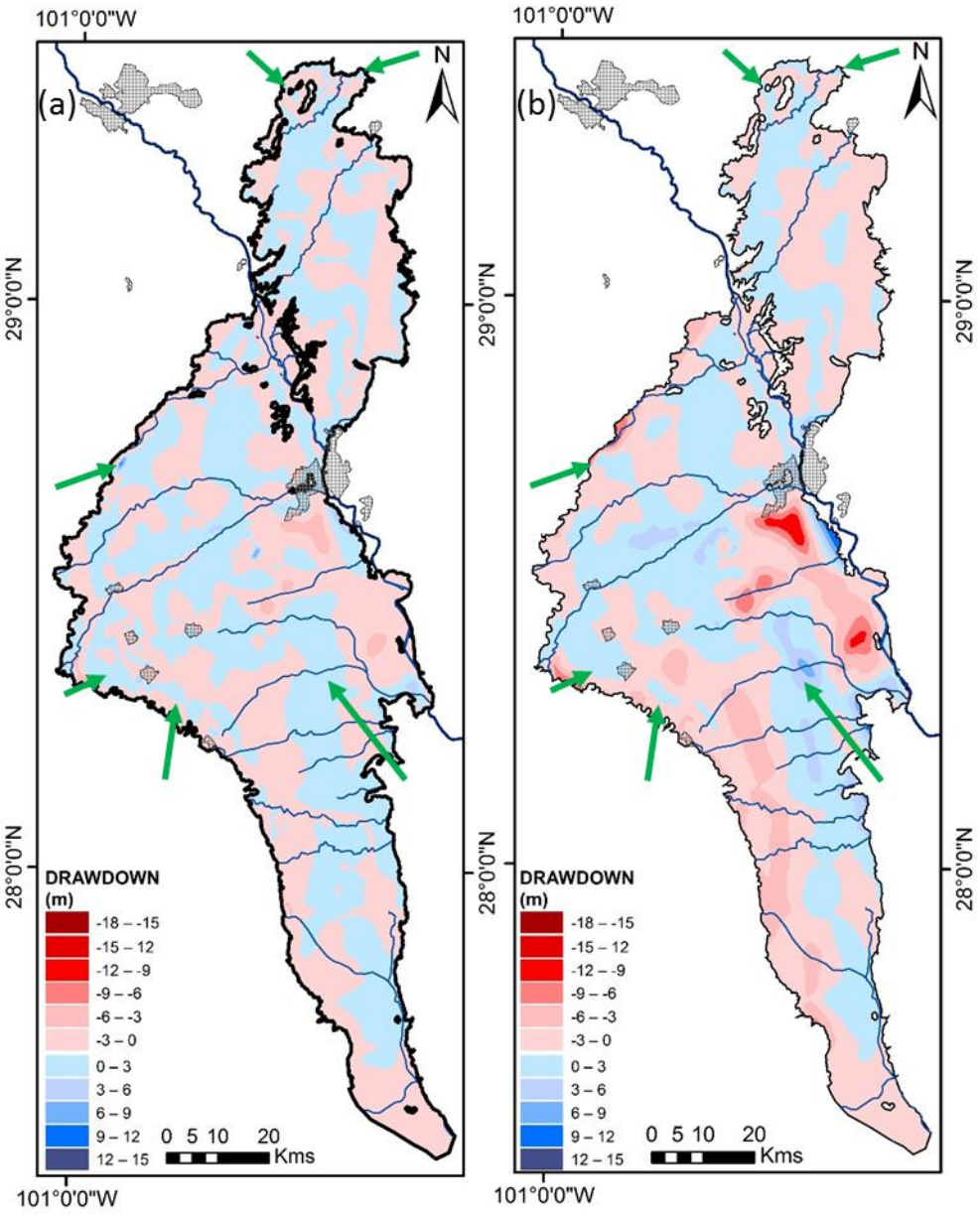

Figure 33. Severe drawdowns (a)January 2002, (b)November 2012. The green arrows mark the areas where the water levels increased in spite of the severe droughts experienced.

Batzner (1976) suggests that cross formational flow from the Edwards-Trinity aquifer is recharging the APN aquifer near the Lomerios Peyotes area and, according to previous studies developed by Castillo Aguiñaga (2000), Boghici (2002), Lesser-Illades et al. (2008) and TWRI (Ghosh, 2018) the areas identified with carbonate-type

groundwater were delimited between Guerrero and Villa Union (Coahuila), the surrounding areas of Lomerio Peyotes, and the Northern central portion of the APN aquifer. The high carbonate content in groundwater is an indicator that the water had interaction with the underlying limestones causing carbonate and calcium dissolution.

The locations with high carbonate content in water identified by Boghici (2002) as type 1 on Figure 34, match with most of the areas marked on Figure 33 as cross formational flow from the underlying aquifers in the area, such as the Edwards Aquifer, which is the predominant aquifer in the surrounding perimeter of the APN aquifer. The same trend is described for the APN aquifer portion located in Mexico by Castillo Aguiñaga (2000) as zones 1 and 2 in Figure 35.

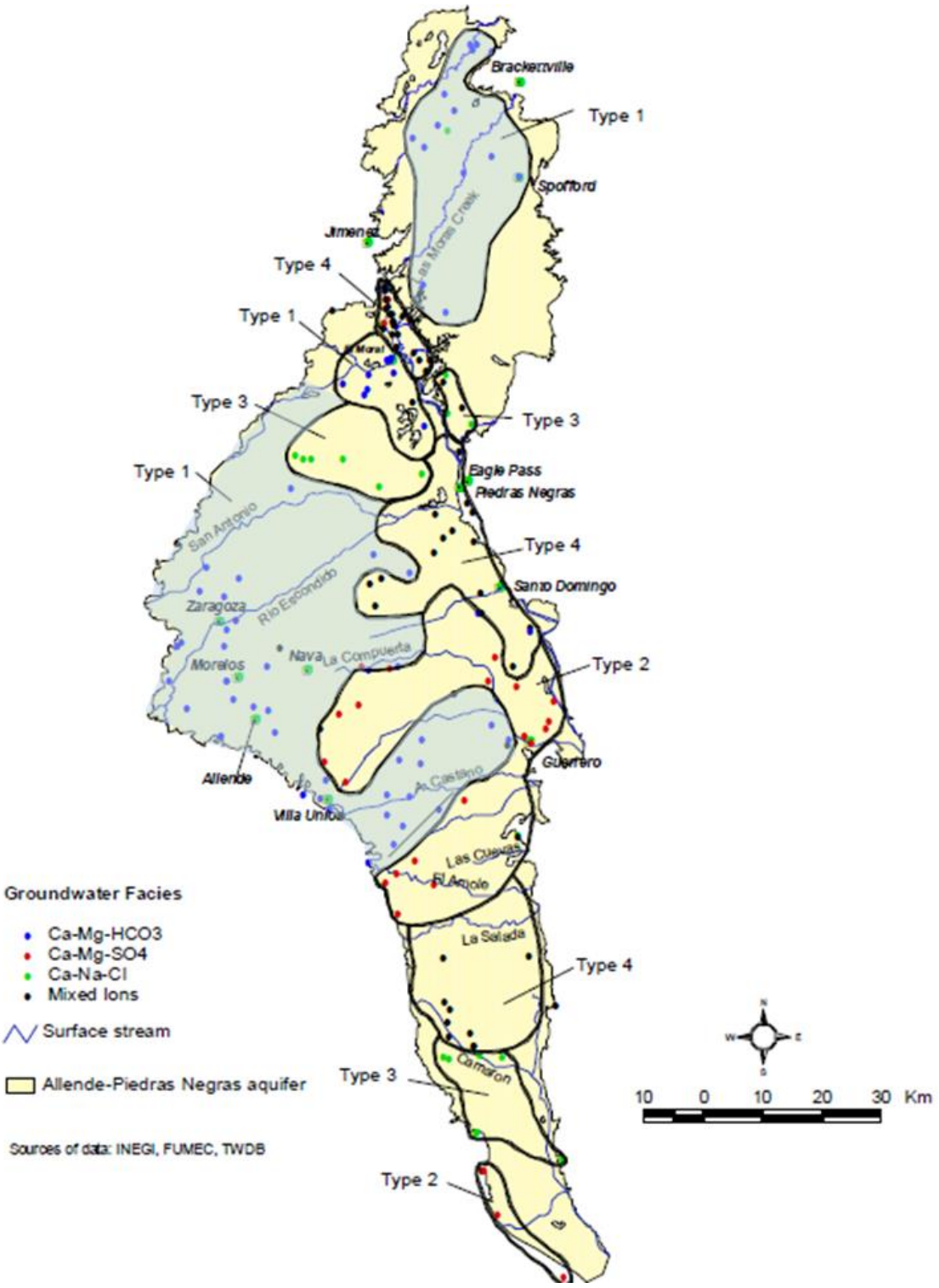

Figure 34. Hydrochemical facies distribution in the APN aquifer (Modified from Boghici, 2002). The type 1 locations are areas where groundwater has a high content in carbonates.

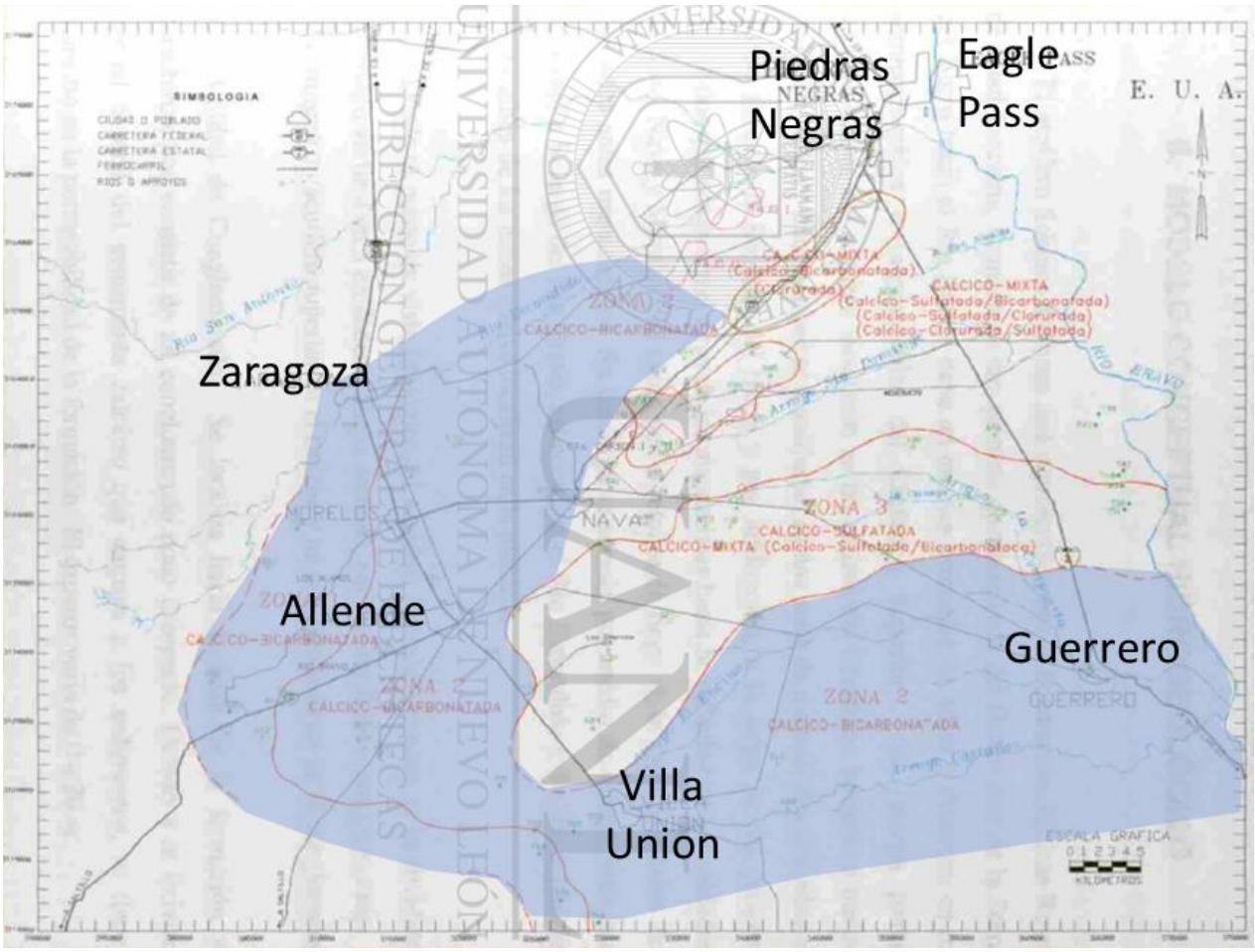

Figure 35. Hydrogeochemical zoning (Modified from Castillo-Aguinaga, 2000). The blue areas show high carbonate content in groundwater.

5.5 Water flow across Rio Grande/Rio Bravo system

Under pre-development conditions, the groundwater convergence zone would be located on the Rio Grande/Rio Bravo or under its hyporheic zone as explained by Williams (1993) (Figure 36). Under pumping conditions, the dynamics between the river and the aquifer show alteration as suggested by Hantush (1959), which explains the effects of pumping wells on the riparian areas and develops a numerical method to

calculate the effective distance between a stream and a well where there would not be influence in the water levels of a stream.

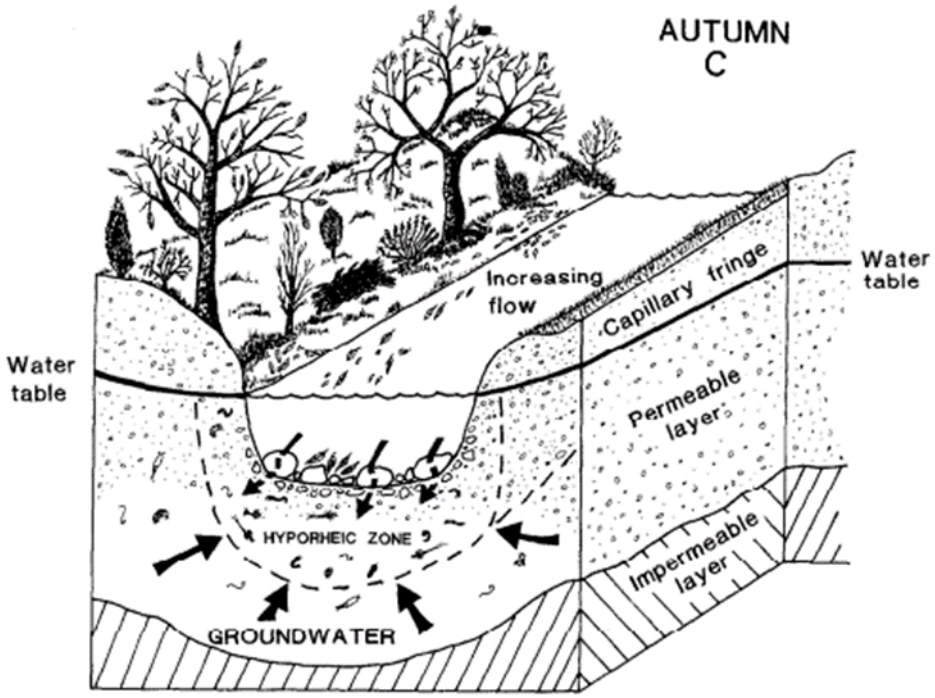

Figure 36. Descriptive scheme of the hyporheic zone and the surrounding groundwater area. The arrows indicate the direction of the water flow. Reprinted with permission from RightsLink Permissions Springer Nature Customer Service Centre GmbH: Springer Nature, Hydrobiologia 251, Nutrient and flow vector dynamics at the hyporheic/groundwater interface and their effects on the interstitial fauna, D.Dudley Williams (1993).

The groundwater flow directions in the APN aquifer follow the slope terrain and converge in the Rio Grande/Rio Bravo. The groundwater in the Texas side of the aquifer flows from the Anacacho Mountains to the southwest and the groundwater in Coahuila flows from the highlands of Serrania del Burro and Lomerio Peyotes to the northeast towards the Rio Grande/Rio Bravo (Figure 37 (a)).

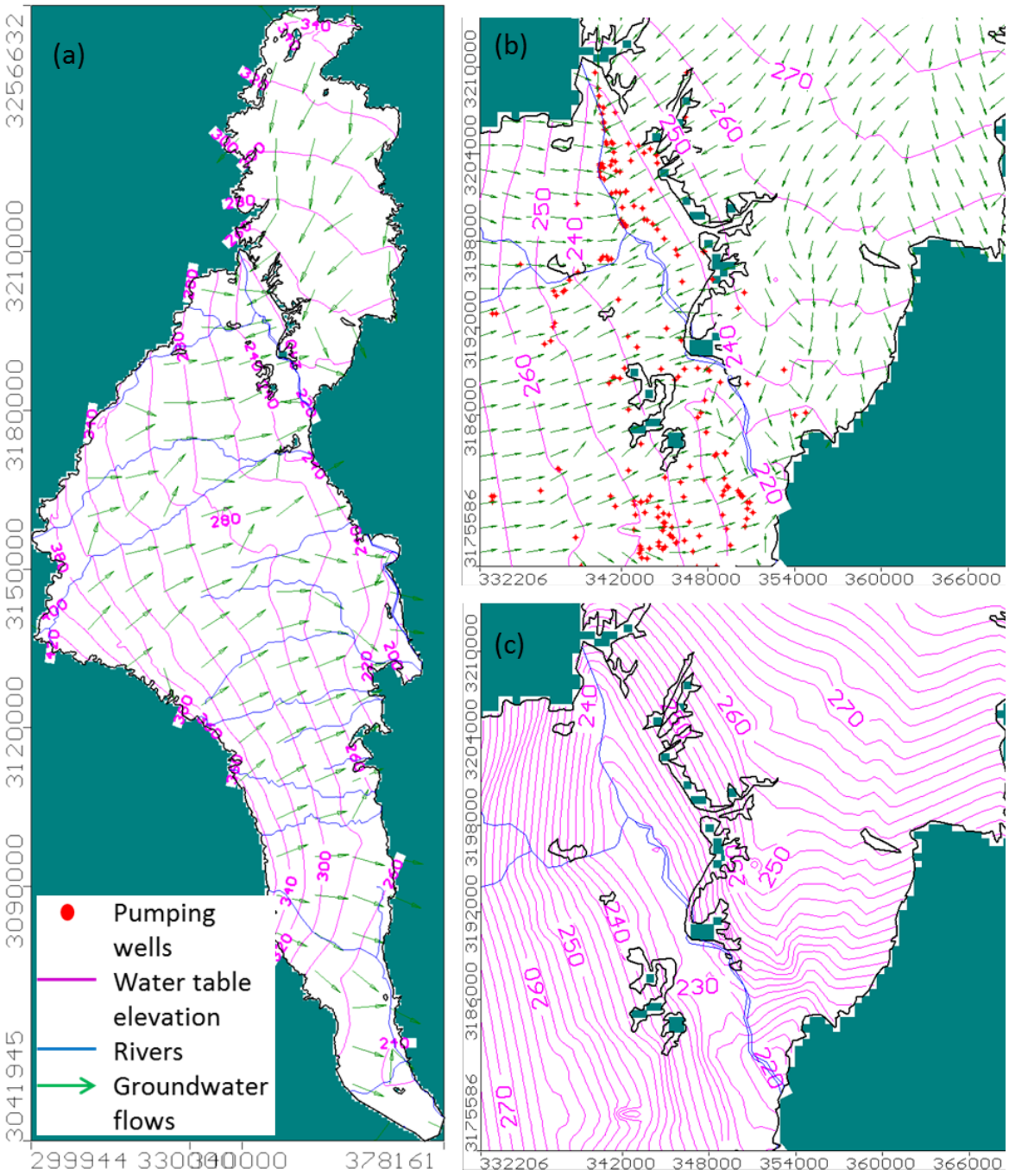

Figure 37. APN aquifer water table elevation and water flows. Plain view. (a)Whole APN aquifer. (b) Detail of Rio Grande/Rio Bravo and surrounding pumping wells. (c)Detail of water table around Rio Grande/Rio Bravo.

After a detailed evaluation of the Rio Grande/Rio Bravo riparian zones, the groundwater flows into the Rio Grande/Rio Bravo and under predevelopment conditions, the river can be classified as a gaining river, specifically in the regions at the north of Quemado, Texas and El Moral, Coahuila (Figure 37 (b) and (c), Figure 38, cross section A-A'). Contrastingly, the river becomes losing river in the southern region near Guerrero, Coahuila, where the river recharges the aquifer during dry seasons as seen in Figures 37 (b and c) and 38 (Cross section B-B'). However, according to the model, the predominant behavior is a gaining river because the water table contour lines are pointing upstream in most of the Rio Grande/Rio Bravo course.

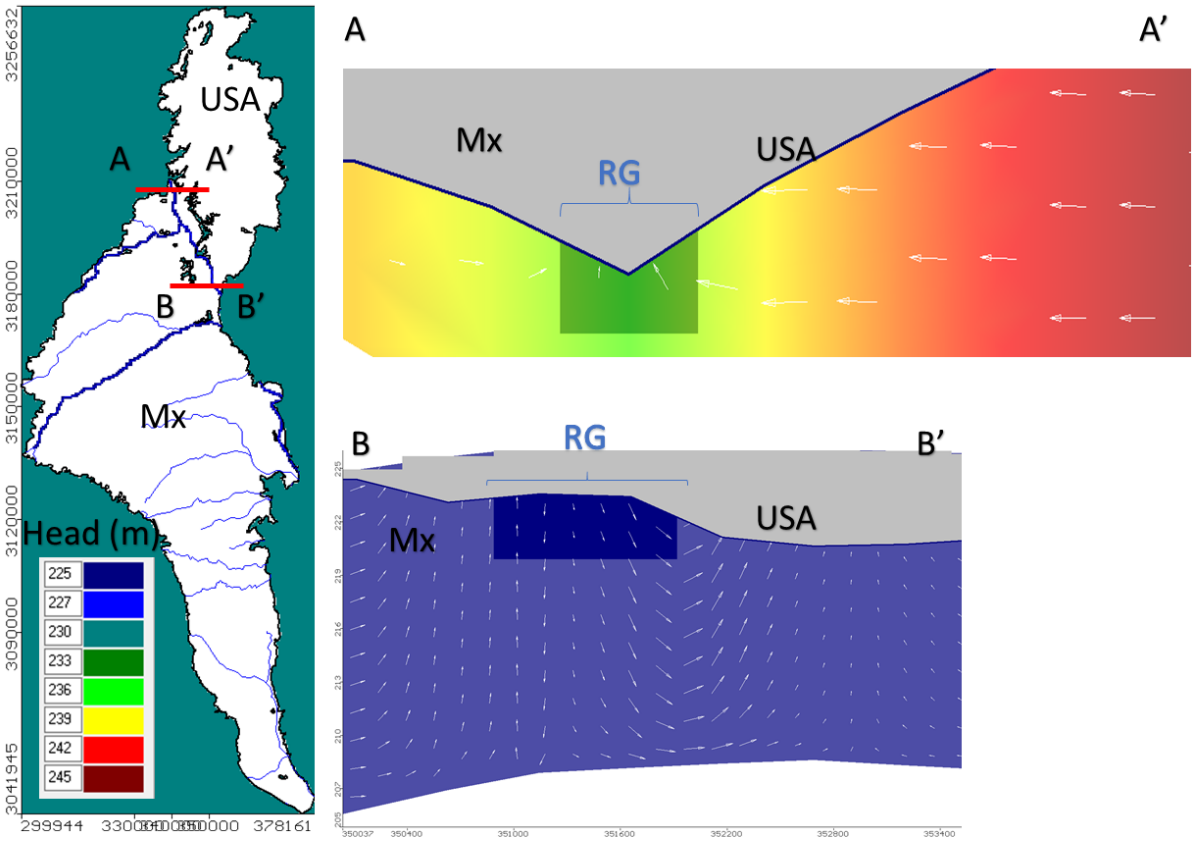

Figure 38. Cross sections along the Rio Grande/Rio Bravo near El Moral, Coahuila and Quemado, Texas (A-A') and Piedras Negras (Coahuila) and Eagle Pass, Texas (B-B'). Pre-development conditions.

a local effect of the pumping wells over the river flows is noticeable, as well as the groundwater flow modification where the groundwater converges at one side of the hyporheic zone but not below the hyporheic zone as seen under pre-development conditions. Depending on the closeness of the pumping wells to the river and location, the groundwater convergence zone will switch to either country depending on the well location, or even disappear completely to flow predominantly to the area where the pumping wells have higher influence. In Figure 39 (cross section C-C') the groundwater flow switches to the Texas side due to the water extraction in South Quemado, and sometimes groundwater discharges into the Rio Grande/Rio Bravo and afterwards the water returns to the aquifer. This phenomena of water discharge and later infiltration back into the aquifer was named flow-through by Hoehn (1998)

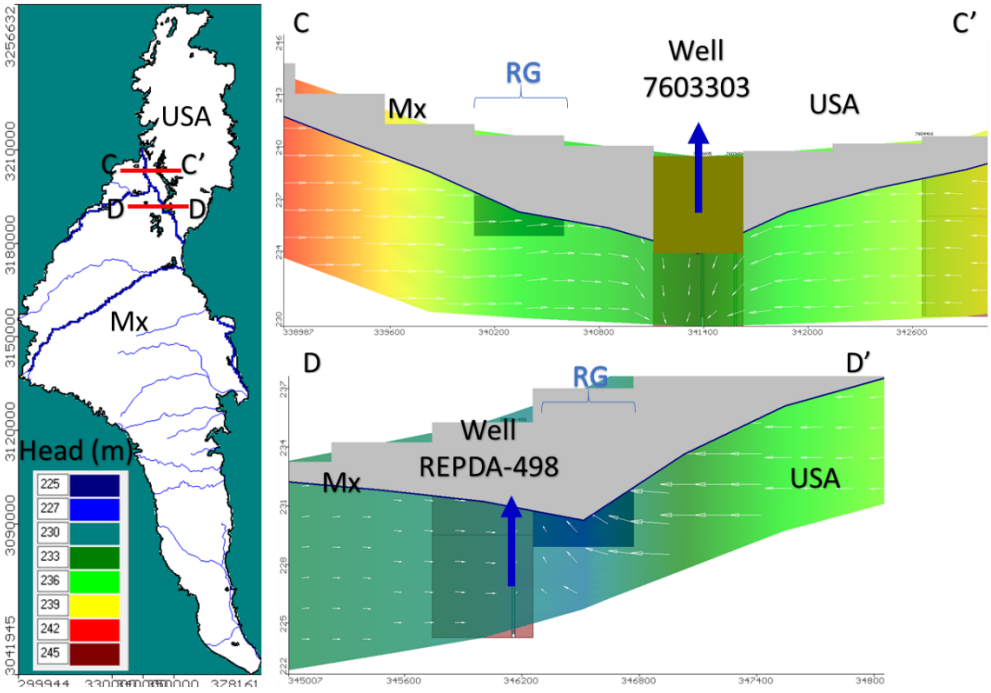

Figure 39. Cross sections along the Rio Grande/Rio Bravo near El Moral, Coahuila and Quemado, Texas (C-C') and Piedras Negras (Coahuila) and Eagle Pass, Texas (D-D'). Post development conditions.

In the area located at the north of Piedras Negras, Coahuila, the density of pumping wells in Mexico is higher and as a result, switching of the groundwater convergence zone occurs to Mexico as well as flow-through from the east to the west as seen in Figure 39 (Cross section D-D').

After identifying the areas where the convergence zone moved away from the riverbed, it was possible to establish a buffer zone around the river of 2000 m, where most of the wells located into the delimited area are affecting the water flow patterns and causing the switching of the water convergence zone between countries (Figure 40). The red regions were flow patterns located in Mexico under pre-development conditions, but during pumping, the flow patterns suffered inversion from Mexico into the USA aquifer portion; and the green regions showed a shifting of water flow patterns from the USA into Mexico. It is important to mention that if pumping regimes were modified or new water wells were developed in the riparian zones, the buffer zone would also be modified.

The main implication of this alteration in the water flow patterns is that this type of aquifer where the river acts as a political border have little transboundary flow, unless the extraction of groundwater affects the baseflow of the river and even induces a change in the hydraulic heads, which modify the system into a transboundary groundwater flow (Rivera, 2015).

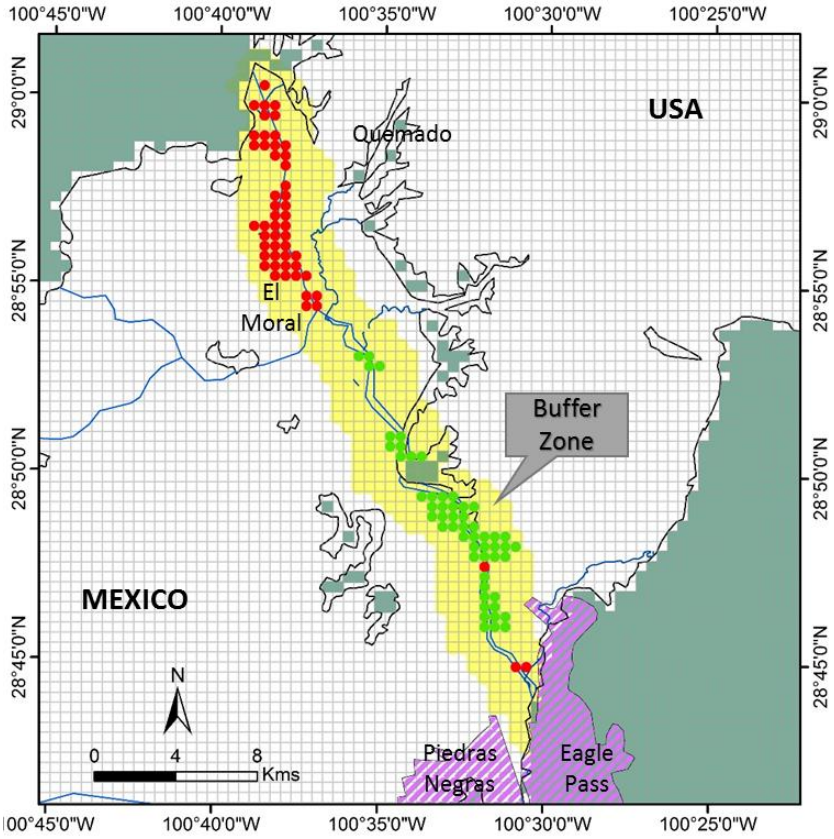

Figure 40. Buffer zone around the Rio Grande/Rio Bravo.

5.6 Water budget

A water budget was generated for the areas previously shown in Figure 20 with the aim of obtaining the total water discharges into the Rio Grande/Rio Bravo from the aquifer in Mexico and the USA separately as well as the recharge from the Rio Grande/Rio Bravo into both sections from the APN aquifer. The estimated water budget under pre-development conditions was estimated as shown on Figure 41.

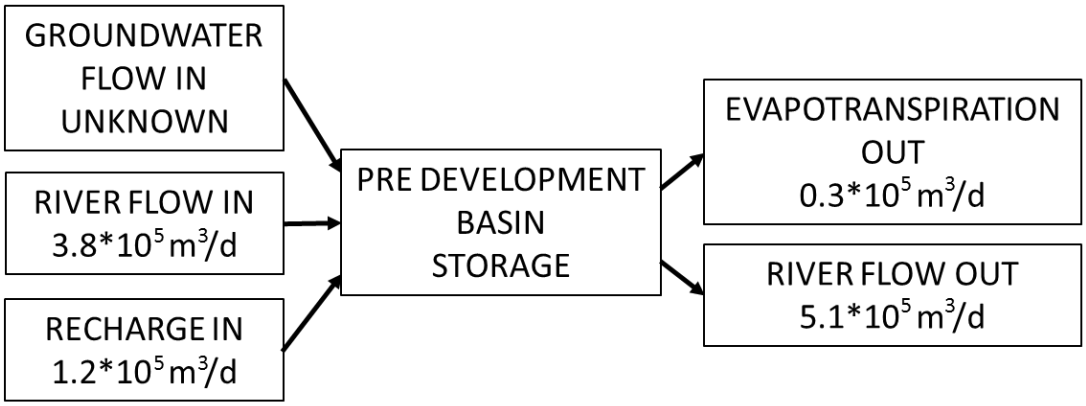

Figure 41. Water budget for the APN aquifer under pre-development conditions.

The APN aquifer recharge is mainly controlled by the rainfall infiltration, but due to the limited rainfall events and the arid to semiarid climate, important amounts of water are flowing out due to evapotranspiration. Also, even when a water exchange between the Rio Grande/Rio Bravo and the riparian zones was observed form the water budget analysis, the river is an important outflow of the APN aquifer. Figure 42 shows the total amounts of water flowing in and out of the APN aquifer for the 17-year numerical model, a detailed volume report can be seen in Appendix B. The data was obtained from the accumulated mass balance calculation from VMF.

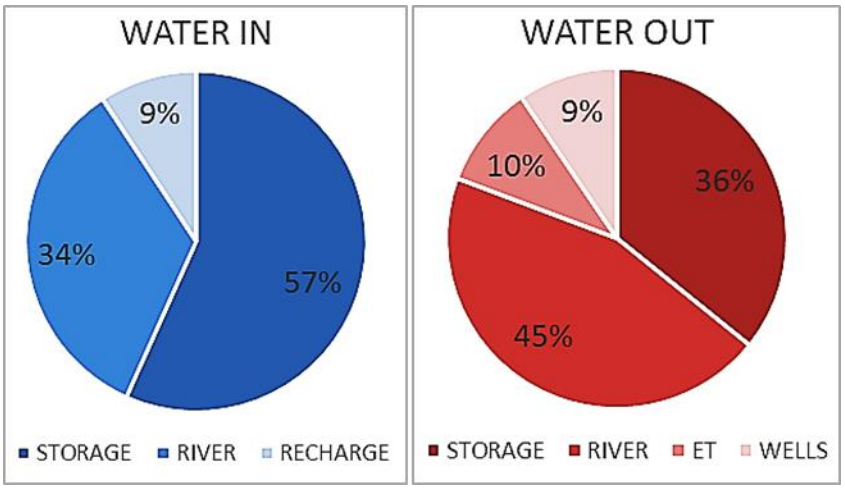

Figure 42. Accumulated mass balance for the period 2000-2017.

The negative discrepancy was obtained from the mass balance, which is an indicator that the outflow was higher in the APN aquifer depleting the groundwater already stored into the aquifer. The inflow sources as recharge through rainfall and the river infiltration are not enough to recover the water pumped from the aquifer, and due to the arid to semi-arid climate present in the zone, the short and weak rainfall events tend to evaporate faster than infiltrate into the soil.

Under pre-development conditions the recharge and the discharge of the APN aquifer should be equal; but under development conditions, activities as water pumping and land use change affect the amount of water entering and leaving the system; in this case the storage becomes a source of water when the recharge patterns have been compromised (Alley et al., 1999). It is common to observe a change in storage at the beginning of pumping in any aquifer because the system responds to the water withdrawal, and this change will cease when the system reaches a new equilibrium and the inflows equal the outflows again (Alley et al., 1999).

After a comparison of the inflows and outflows form the APN aquifer per year, the storage from inflow and outflow are different during the entire simulation. The implication of this discrepancy is that the aquifer has not reached equilibrium and, instead, part of the water moving out of the aquifer through the rivers, ET and wells is coming from the storage (Figure 43).

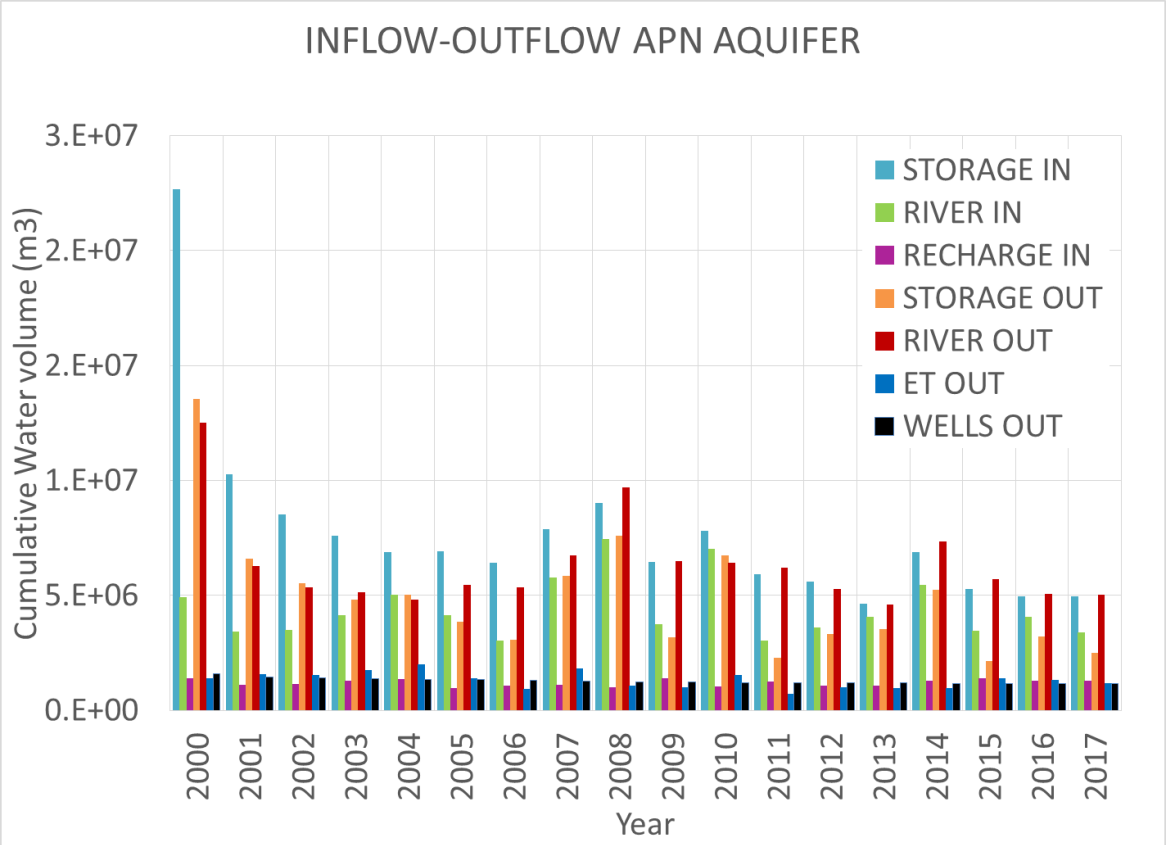

Figure 43. Annual detailed inflow-outflow volumes for the period 2000-2017.

Also, the total amounts of inflow and outflow in the APN aquifer indicate that there is a small negative difference because the outflows are higher than the inflows. According to Figure 44, during most of the years the outflows were greater, with negative differences of up t0 10.92% for 2008. There were years where the inflows and

outflows differences were slightly positive (2004, 2005 and 2010), and the differences ranged from 0.03% to 0.41%.

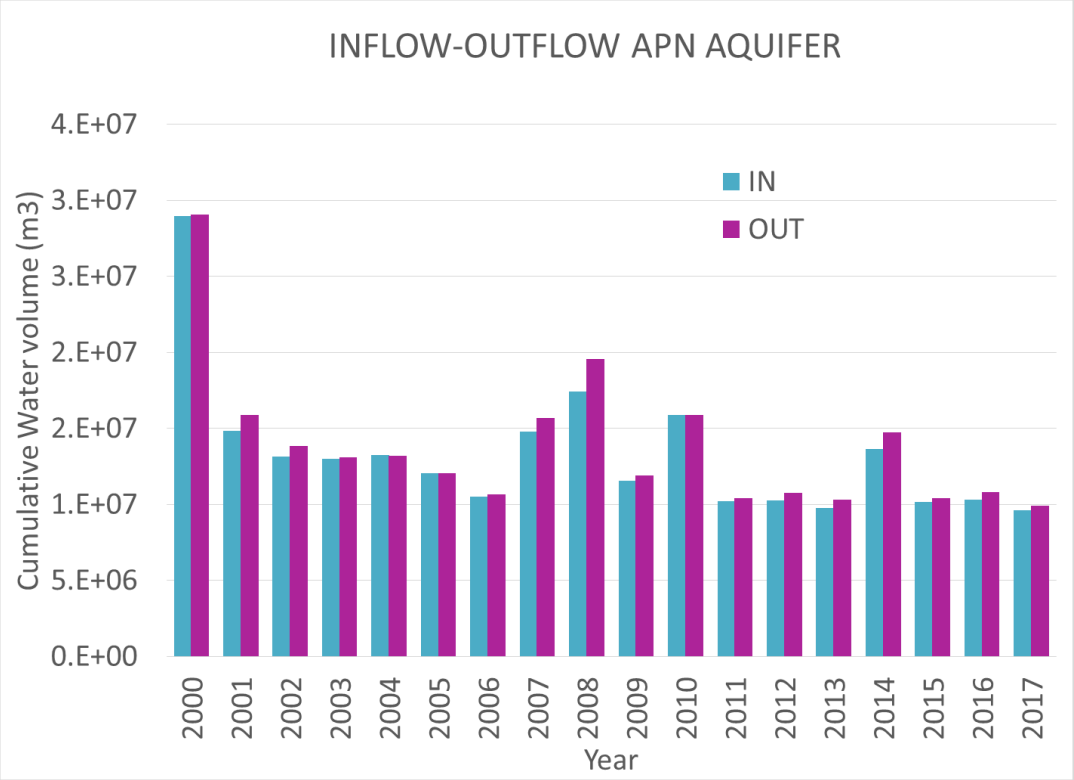

Figure 44. Annual total inflow-outflow volumes for the period 2000-2017.

The river is an important source of water infiltration into the APN aquifer, and as seen in section 4.5, some areas of the Rio Grande/Rio Bravo would work as infiltration points and different regions will function as discharge points. The Rio Grande/Rio Bravo is a discharge zone for the APN aquifer, which under pre- development conditions has the same groundwater amount coming from the USA and Mexico portions, but under the influence of pumping wells on the riparian zones, the relationship of groundwater discharged into the Rio Grande/Rio Bravo is modified. According to Figure 45 and Table 8, most of the water discharged into the Rio Grande/Rio Bravo comes from

Mexico with a 55.5%, and a remaining 44.5% coming from the USA. 51.1% of the water infiltrated from the Rio Grande/Rio Bravo gets in to the USA portion of the APN aquifer, and 48.9% infiltrates into the Mexico portion.

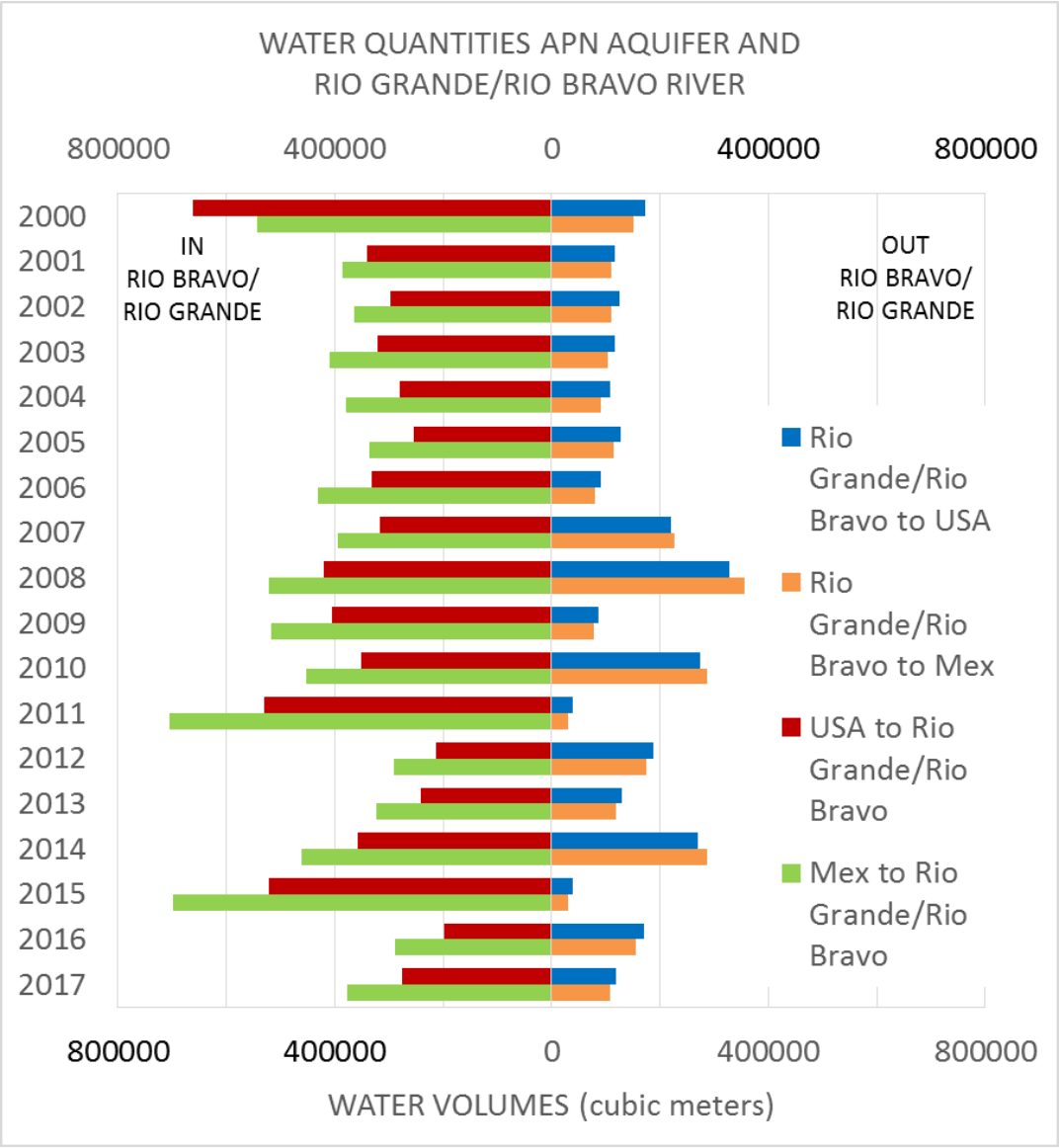

Figure 45. Annual inflow-outflow volumes for the Rio Bravo/Rio Grande.

Table 8. Inflows and outflows of groundwater for the Rio Grande/Rio Bravo (in m^3/year).

	IN			OUT		
Year	Mex to RG	USA to RG	Total RG	RG to Mex	RG to USA	Total RG
2000	544197	662724	1206921	151473	173343	324816
2001	385090	339995	725085	109613	116961	226575
2002	364370	298214	662584	109753	124105	233858
2003	410231	320664	730895	103417	117402	220819
2004	379656	280598	660254	91117	107083	198200
2005	336856	254588	591444	114101	127904	242005
2006	431401	332539	763940	78955	91629	170584
2007	395310	316154	711464	226430	220340	446770
2008	521849	420480	942329	355569	328682	684251
2009	518054	404295	922349	77574	87375	164949
2010	453684	351696	805380	286024	274237	560261
2011	704433	530649	1235082	30721	38775	69496
2012	291746	214279	506026	174084	186862	360946
2013	324039	240470	564509	118044	130040	248084
2014	460766	357633	818399	287398	270573	557971
2015	698718	521846	1220564	30600	37953	68552
2016	288124	198134	486258	155727	171063	326790
2017	378333	275339	653672	107068	117895	224962
TOTAL	7886856	6320297	14207153	2607668	2722220	5329888

6. CONCLUSIONS AND FUTURE WORK

6.1 Conclusions

The following conclusions are drawn from this study:

1) The numerical model for the APN Aquifer was generated for the period 2000-2017 with the software Visual MODFLOW. One of the main observations of this model was that an average drawdown of 0.76 m was quantified for the simulation of 17 years. Even when the trend in depletion lessen after 2011, the aquifer has not recovered the previous water levels.
2) Under pre-development conditions, the water flow paths from the aquifer converged into the Rio Grande/Rio Bravo, but after pumping from wells perforated in areas of the aquifer adjacent to the river, the flow convergence zone shifted to the area where the wells had greater pumping rates. This modification of the baseflow of the river and the change of hydraulic heads permits classifying the APN aquifer as a transboundary groundwater flow system (Rivera, 2015).
3) The comparisons of periods with severe droughts allowed to identify areas with cross formational flow, where there is a vertical flow from underlying aquifers. An important feature of this finding is that in these areas the water table has not suffered depletion and, instead, it showed recovery. These areas are related to the high contents of ion bicarbonates in the water wells reported on these regions, which supports the hypothesis that the cross-

formational flow comes from the underlying limestone aquifers such as Austin Chalk and Edwards aquifer.

4) In addition, it was possible to create a buffer of 2000 m around the river where the water flows from one country to another, and shifts of the water convergence zone occurred depending on pumping regimes and variations of the river discharge. This shifting was a consequence of the pumping water increase in the surrounding areas of the river. The flow convergence zone located below the Rio Grande/Rio Bravo under predevelopment conditions shifted mainly to the Mexico region crossing the border due to the closeness of the wells from Texas to the Rio Grande/Rio Bravo. This flow change is dominated by the pumping rates on the wells located around the river.
5) The wells located more than 2 km from the river did not show effects on water flows across or below the Rio Grande/Rio Bravo system. However, increase in the pumping rates or drilling of new wells in the surrounding areas of the Rio Grande/Rio Bravo could potentially increase the buffer previously outlined.
6) According to the water budget the amounts of water extracted from the aquifer surpassed the inflows, also the storage has not reached equilibrium which puts the APN aquifer under a stress situation because the water extracted naturally or artificially is not enough to recover the aquifer in a long term basis.
7) 55.5% of the groundwater entering into the Rio Grande/Rio Bravo comes from the Mexico side of the APN aquifer, and the remaining 44.5% coming from

the USA side. However, the amount that infiltrates from the Rio Grande/Rio Bravo into the USA portion of the APN aquifer is greater with a 51.1% of the water infiltrated, and the remaining 48.9% infiltrates into the Mexico portion.

6.2 Future work

Part of the future work for the area will be focused in developing a detailed hydrogeological model, trying to replace several of the assumptions by real data and higher temporal resolutions for some of the parameters used to develop the model.

The precipitation used in the model was extracted from satellite data in a monthly basis and an average value was calculated for the entire APN aquifer. In order of increasing the accuracy of the numerical model, data in a daily basis from field gages or remote sensors could be used as well as incorporating spatial variability of precipitation in the area instead of assuming the same value for the entire APN aquifer.

Also, the available rain gages were not used because there were gaps in the data and only one rain gage had a complete record of information for the period studied. An interpolation of the missing data using genetic programming or neural network could help to fill the gaps and prepare the rain gage information to be useful in a numerical model generated on a daily basis.

Refining the grid in the APN aquifer, specifically in the transect between El Moral-Quemado and Piedras Negras-Eagle pass would allow a detailed analysis of the pathways for water flow near the political boundary between Mexico and the USA. Also, an accurate water budget can be generated from this refined numerical model which would support the water flows moving between the aquifer zones as well as the

interactions between the Rio Grande/Rio Bravo and the surrounding zones of the aquifer.

An accurate calculation for recharge taking in account the land use would also improve the quality of the numerical model. However, while Visual MODFLOW is not a good tool to integrate surface water phenomena, the land use responses to recharge can be modeled using specialized watershed software such as SWAT, and include into the groundwater model as recharge.

REFERENCES

AGUILAR, I. 2013. *Metodologia para desarrollar balances de aguas subterraneas: Caso estudio Acuifero Allende-Piedras Negras, Coahuila.* Especializacion en Hidraulica Urbana, Universidad Nacional Automnoma de Mexico.

ALLEY, W. M., REILLY, T. E. & FRANKE, O. L. 1999. *Sustainability of ground-water resources*, US Department of the Interior, US Geological Survey.

ASHWORTH, J. B. & HOPKINS, J. 1995. Aquifers of Texas. Austin, Texas: Texas Water Development Board.

BARKER, R. A., BUSH, P. W. & BAKER, E. T. 1994. Geologic history and hydrogeologic setting of the Edwards-Trinity aquifer system, west-central Texas. U.S. Geological Survey.

BARNES, V. 1974. *Geologic Atlas of Texas: San Antonio sheet*, 1:250000. University of Texas at Austin, Bureau of Economic Geology.

BARNES, V. 1977. *Geologic Atlas of Texas: Del Rio Sheet*, 1:250000. University of Texas at Austin, Bureau of Economic Geology.

BATZNER, J. C. 1976. *The Hydrogeology of Lomerio de Peyotes, Coahuila, Mexico.* University of New Orleans.

BENNETT, R. & SAYRE, A. N. 1962. Geology and ground-water resources of Kinney County, Texas. Texas Water Commission.

BOGHICI, R. 2002. Transboundary Aquifers of the Del Rio/Ciudad Acuña – Laredo/Nuevo Laredo Region. Texas Water Development Board.

BOGHICI, R. 2011. Changes in Water Levels in Texas, 1995 to 2005. Texas Water Development Board.

BOUWER, H. 1978. Groundwater hydrology.

CASTILLO AGUIÑAGA, J. A. 2000. *Características geohidrológicas y estado actual de explotación del acuífero Sabinas-Reynosa en la región noreste del estado de Coahuila.* Universidad Autónoma de Nuevo León.

CENSUS. 2010. *CENSUS* [Online]. United States Census Bureau. Available: https://www.census.gov/ [Accessed May 2018].

CLARK, A. K. & SMALL, T. A. 1997. Geologic framework of the Edwards Aquifer and upper confining unit, and hydrogeologic characteristics of the Edwards Aquifer, south-central Uvalde County, Texas. *Water-Resources Investigations Report.* Austin, TX: U.S. Geological Survey.

COLORADO-RIO GRANDE 1944. Treaty between the United States of Americaand Mexico relating to the utilization of the waters of the Coloradoand Tijuana Rivers, and of the Rio Grande (Rio Bravo) from Fort Quitman, Texas, to the Gulf of Mexico. February 3rd, 3 UNTS**,** 314.

CONAGUA 2006. Estudio de Actualización de Mediciones Piezométricas para la Disponibilidad del Agua Subterránea en el Acuífero Bajo Río Bravo, Tamaulipas.: Moro Ingenieria S.C.

CONAGUA 2014. Determinacion de la Disponibilidad de Agua en el Acuifero Allende-Piedras Negras, Estado de Coahuila. Mexico, DF: Subdireccion General Tecnica, CONAGUA.

CONAGUA 2015a. Actualizacion de la Disponibilidad Media Anual de Agua en el Acuifero Presa La Amistad (0522), Estado de Coahuila. Mexico, DF: Subdireccion General Tecnica, CONAGUA.

CONAGUA 2015b. Actualizacion de la Disponibilidad Media Anual de Agua en el Acuifero Serrania del Burro (0526), Estado de Coahuila. Mexico, DF: Subdireccion General Tecnica, CONAGUA.

CONAGUA 2015c. Actualizacion de la Disponibilidad Media Anual de Agua en el Acuifero Valle de Juarez (0833), Estado de Chihuahua. Mexico, DF: Subdireccion General Tecnica, CONAGUA.

CONAGUA 2015d. Actualizacion de la Disponibilidad Media Anual de Agua en el Acuifero Valle del Peso (0861), Estado de Chihuahua. Mexico, DF: Subdireccion General Tecnica, CONAGUA.

CONAGUA 2015e. Actualizacion de la Disponibilidad Media Anual de Agua Subterranea, Acuifero 2801 Bajo Rio Bravo, Estado de Tamaulipas. Mexico, DF: Subdireccion General Tecnica, CONAGUA.

COUTAGNE, A. 1954. Quelques considérations sur le pouvoir évaporant de l'atmosphère, le déficit d'écoulement effectif et le déficit d'écoulement maximum. *La Houille Blanche***,** 360-374.

DEUSSEN, A. 1914. Geology and underground waters of the southeastern part of the Texas coastal plain. Govt. print. off.

DOF 2011. ACUERDO por el que se dan a conocer los estudios técnicos de aguas nacionales subterráneas del acuífero Allende-Piedras Negras, clave 0501, Estado de Coahuila. *Diario Oficial de la Federacion*.

DOF 2013. DECRETO por el que se establece como zona reglamentada aquella que ocupa el acuífero denominado Allende-Piedras Negras, ubicado en el Estado de Coahuila. *Diario Oficial de la Federacion*.

DOMENICO, P. A. & MIFFLIN, M. D. 1965. Water from low-permeability sediments and land subsidence. *Water Resources Research,* 1**,** 563-576.

ESTAVILLO, G. C. & AGUAYO, C. J. E. 1985. Ambientes Sedimentarios Recientes en Laguna Madre México. *Boletín de la Sociedad Geológica Mexicana,* 46**,** 29-64.

FALLIN, T. 1990. Hydrogeology of the Terlingua Area,Texas. Texas Water Development Board.

GHOSH, O. 2018. Hydrochemical conectivity of the Allende-Piedras Negras transboundary aquifer (unpublished report). Texas Water Resources Institute.

GROAT, C. G. 1972. Presidio Bolson, Trans-Pecos Texas and Adjacent Mexico: Geology of a Desert Basin Aquifer System. *Bureau of Economic Geology. The University of Texas at Austin.,* 76.

GRUPO MODELO 2003. Estudio para determinar la potencialidad del acuífero del área entre Zaragoza y las Albercas, Coahuila. *Lesser y Asociados*.

GRUPO MODELO 2011. Actualización del estudio geohidrológico del acuífero ubicado en los alrededores de la Compañía Cervecera de Coahuila.: Lesser and Associates.

HAMLIN, H. S. 1988. Depositional and ground-water flow systems of the Carrizo-Upper Wilcox, south Texas. *The University of Texas at Austin, Bureau of Economic Geology,* Report of Investigations No. 175**,** 1-61.

HANTUSH, M. S. 1959. Analysis of data from pumping wells near a river. *Journal of Geophysical Research,* 64**,** 1921-1932.

HEATH, R. C. 1983. *Basic ground-water hydrology*, US Geological Survey.

HERRERA-MONREAL, J., SANTIAGO-CARRASCO, B., CABALLERO-MARTÍNEZ, I., RAMÍREZ-GUTIÉRREZ, G. & GONZÁLEZ, R. 2003. *Carta Geológico-Minera Río Bravo*, 1:250000.

HILL, M. C. & TIEDEMAN, C. R. 2008. EFFECTIVE GROUNDWATER MODEL CALIBRATION: With Analysis Of Data, Sensitivities, Predictions, and Uncertainty. *Ground Water,* 46.

HILL, R. T. 1891. Notes on the Geology of the Southwest. *American Geologist,* 7**,** 254-55.

HOEHN, E. 1998. Solute exchange between river water and groundwater in headwater environments. *International Association of Hydrological Sciences, Publication***,** 165-172.

HUFFMAN, G. J. & BOLVIN, D. T. 2013. TRMM and other data precipitation data set documentation. *NASA, Greenbelt, USA,* 28.

IBWC. 2018. *Rio Grande Water Flows* [Online]. International Water and Boundary Commission. Available: https://www.ibwc.gov/Water_Data/rio_grande_WF.html#Stream [Accessed February 2018].

INEGI. 2010. *Censo de Población y Vivienda 2010* [Online]. Instituto Nacional de Estadistica y Geografia. Available: http://www.inegi.org.mx/est/contenidos/proyectos/ccpv/cpv2010/iter_2010.aspx [Accessed].

KINNEY COUNTY GROUNDWATER CONSERVATION DISTRICT 2013. Groundwater Management Plan - 2013. Texas Water Development Board.

KUMAR, C. P. 2015. *Groundwater Assessment and Modelling*.

LAROCQUE, M., MANGIN, A., RAZACK, M. & BANTON, O. 1998. Contribution of correlation and spectral analyses to the regional study of a large karst aquifer (Charente, France). *Journal of Hydrology,* 205**,** 217-231.

LESSER-ILLADES, J. M., GONZÁLEZ-POSADAS, D., LESSER-CARRILLO, L. E. & ARCOS, V. M. C. 2008. El agua subterránea en el acuífero Allende-Piedras Negras, Coahuila, México.

LOAEZA-GARCÍA, J., ZÁRATE-BARRADAS, R., ARREDONDO-MENDOZA, J. & FLORES-CASTILLO, C. 2004. *Carta Geológico-Minera Linares*, 1:250000.

LÓPEZ-RAMOS, J. 1979. *Geología de México, Tomo 2: México, DF.* Tesis Rezendis, 454 p.

MCDONALD, M. G. & HARBAUGH, A. W. 1988. *A modular three-dimensional finite-difference ground-water flow model*, US Geological Survey Reston, VA.

MILANES MURCIA, M. E. 2017. Proposed International Legal And Institutional Framework For Conjunctive Management Of Surface And Groundwater Along The Us–Mexico Border Region. *Management of Transboundary Water Resources under Scarcity: A Multidisciplinary Approach.* World Scientific.

MONTIEL ESCOBAR, J., AMEZCUA, N., REYES, R., MALDONADO, L., ARANDA-OSORIO, J. & SANTIAGO, C. 2005. *Carta geológico-minera, Estado de Coahuila*, Escala 1:500000.

NRCS, U. 2004. National Engineering Handbook: Part 630—Hydrology. *USDA Soil Conservation Service: Washington, DC, USA*.

OLIVERA, B., FUENTE, A. D. L., LLANO, M., BENUMEA, I., SANDOVAL, A. & TERRY, W. 2018. Anuario 2017. Las actividades extractivas en México: minería e hidrocarburos hacia el fin del sexenio. . Fundar, Centro de Análisis e Investigación A.C. .

PAGE, W. R., BERRY, M. E., VANSISTINE, D. P. & SNYDERS, S. R. 2009. *Preliminary Geologic Map of the Laredo, Crystal City-Eagle Pass, San Antonio, and Del Rio 1 x 2 Quadrangles, Texas, and the Nuevo Laredo, Ciudad Acuna, Piedras Negras, and Nueva Rosita 1 x 2 Quadrangles, Mexico*, 1:350000. U.S. Geological Survey.

POTTER, H. History and Evolution of the Rule of Capture. Conference Proceedings, 2004.

RAMIREZ-GUTIERREZ, J., ARANDA-OSORIO, J., VALLE-REYNOSO, O. & ROMO-RAMIREZ, J. 2003. *Carta Geológico-Minera Nuevo Laredo, Coahuila, Nuevo León y Tamaulipas*, 1:250000.

REEVES, R. & SMALL, T. 1973. Ground-water resources of Val Verde County, Texas: Texas Water Development Board. *Board Rept,* 172**,** 152.

RIVERA, A. 2015. Transboundary aquifers along the Canada–USA border: Science, policy and social issues. *Journal of Hydrology: Regional Studies,* 4**,** 623-643.

RODELL, M., HOUSER, P., JAMBOR, U., GOTTSCHALCK, J., MITCHELL, K., MENG, C., ARSENAULT, K., COSGROVE, B., RADAKOVICH, J. & BOSILOVICH, M. 2004. The global land data assimilation system. *Bulletin of the American Meteorological Society,* 85**,** 381-394.

SANCHEZ, R., LOPEZ, V. & ECKSTEIN, G. 2016. Identifying and characterizing transboundary aquifers along the Mexico–US border: An initial assessment. *Journal of Hydrology,* 535**,** 101-119.

SANCHEZ, R., RODRIGUEZ, L. & TORTAJADA, C. 2018. Transboundary aquifers between Chihuahua, Coahuila, Nuevo Leon and Tamaulipas, Mexico, and Texas, USA: Identification and categorization. *Journal of Hydrology: Regional Studies*.

SANTIAGO, C. & ESCALANTE, M. 2006. *Carta Geológico-Minera Torrecillas, Coahuila, Mexico*, 1:50000.

SELLARD, E., ADKINS, W. & PLUMMER, R. 1966. Geology of Texas. Vol. I. Stratigraphy. U. of Tex. *Bull*.

SERVICIO GEOLÓGICO MEXICANO. 2008a. *Carta Geológica-Minera Nueva Rosita G14-1, Coahuila y Nuevo Leon*, 1:250000. Pachuca, Hidalgo.

SERVICIO GEOLÓGICO MEXICANO. 2008b. *Carta Geológica-Minera Piedras Negras H14-11 Coahuila*, 1:250000. Pachuca, Hidalgo.

SHAH, N., NACHABE, M. & ROSS, M. 2007. Extinction depth and evapotranspiration from ground water under selected land covers. *Groundwater,* 45**,** 329-338.

SMITH, C. I. 1970. *Lower cretaceous stratigraphy, northern Coahuila, Mexico*, Bureau of Economic Geology, University of Texas.

SOPHOCLEOUS, M. 2002. Interactions between groundwater and surface water: the state of the science. *Hydrogeology journal,* 10**,** 52-67.

STEWART, D., CANFIELD, E. & HAWKINS, R. 2011. Curve number determination methods and uncertainty in hydrologic soil groups from semiarid watershed data. *Journal of Hydrologic Engineering,* 17**,** 1180-1187.

SVOBODA, M., LECOMTE, D., HAYES, M., HEIM, R., GLEASON, K., ANGEL, J., RIPPEY, B., TINKER, R., PALECKI, M. & STOOKSBURY, D. 2002. The drought monitor. *Bulletin of the American Meteorological Society,* 83**,** 1181-1190.

TERRY, W. 2017. *El crecimiento urbano ante la destrucción de los ecosistemas ribereños: Caso del Río San Rodrigo en Coahuila. México.* [Online]. http://amigosdelriosanrodrigo.org/. Available: http://amigosdelriosanrodrigo.org/ [Accessed June 2018].

TODD, D. K. 1980. *Groundwater hydrology 2ed*, John Wiley.

TROWNBRIDGE, A. 1923. A geologic reconnaissance in the Gulf Coastal Plain of Texas near the Rio Grande.

TWDB 2017a. Conceptual Model Report: Lower Rio Grande Valley Groundwater Transport Model Texas Water Development Board.

TWDB. 2017b. *Water Data Interactive - Groundwater data viewer* [Online]. Texas Water Development Board. Available: https://www2.twdb.texas.gov/apps/WaterDataInteractive/GroundWaterDataViewer# [Accessed August 2017].

U. S. GEOLOGICAL SURVEY. 2007. *Geologic Atlas of Texas* [Online]. Available: https://txpub.usgs.gov/RDM/4HF0HF8HFI9FIHF [Accessed October 2016].

U. S. GEOLOGICAL SURVEY. 2017. *U.S. Geologic Names Lexicon (GEOLEX)* [Online]. Available: https://ngmdb.usgs.gov/Geolex/search [Accessed January 2017].

WILLIAMS, D. D. 1993. Nutrient and flow vector dynamics at the hyporheic/groundwater interface and their effects on the interstitial fauna. *Nutrient Dynamics and Retention in Land/Water Ecotones of Lowland, Temperate Lakes and Rivers.* Springer.

ZHENG, C. & BENNETT, G. D. 2002. *Applied contaminant transport modeling*, Wiley-Interscience New York.

APPENDIX A

R CODE USED FOR CROSS CORRELATION PLOTS

```
setwd("C:/Users/Laura/Documents/00_THESIS/07_Heads/R_ccr") # working directory

# stiles

faw<- read.csv("Heads_month180821.csv",header=TRUE,sep=",")
plot(faw$NormalizeP, type="l",col="red")
lines(faw$NormalizeRGageRG,type="l",col="green")
#x<-faw$NormalizeH2#faw$mm.mth
x<-faw$NormalizeP#faw$Head X is predictor
y<-faw$NormalizeRGageRG#faw$mm.mth Y is response

#auto correlation
acf(x, lag.max = NULL,
    type = c("correlation", "covariance", "partial"),
    plot = TRUE, na.action = na.fail, demean = TRUE)

#cross corelation
ccf(x, y, lag.max = NULL,main="Precipitation & River Stage",xlab="Time Lag in
months",ylab="Cross-Correlation", type = c("correlation", "covariance"),
    plot =TRUE, na.action = na.fail)
```

APPENDIX B

OUTPUT OBTAINED FROM VMF FOR THE MASS BALANCE AT THE END OF THE SIMULATION